

From the Centre of Excellence for Technology and Engineering in Medicine TANDEM
of the University of Lübeck and the Lübeck University of Applied Sciences

Directors: Prof. Dr. Ullrich Wenkebach and Prof. Dr. Hartmut Gehring

Adaptive Regulation of Ventilation Parameters

Dissertation

for fulfilment of Requirements

for the Doctoral Degree of the University of Lübeck

- from the Faculty of Medicine -

Submitted by

Dipl. Ing. Kristel Lopez-Navas, MSc.

from Bogotá, Colombia

Lübeck 2013

First referee: Prof. Dr. med. Hartmut Gehring

Second referee: Prof. Dr. Ing. Alfred Mertins

Date of oral examination: 09.04.2014

Approved for printing. Lübeck, den 09.04.2014

-Promotionskommission der Sektion Medizin-

Abstract

Mechanical ventilation is a life-saving measure in critical and intensive care and in the treatment of patients with chronic respiratory insufficiency. Despite of the great significance of the supportive ventilation for those patients, an insufficient setting of the assistance still causes distress and lung damage to many patients instead of healing them. This still represents an unresolved problem. Adequate setting of ventilatory support can only be achieved through the correct continuous monitoring of the breathing effort of the patient, which is subject to variations, for example due to muscular weakness. Until now, an exact assessment has only been possible through an invasive manoeuvre, which consists of the insertion of a catheter or a tube into the patient's body. But such a procedure is not only uncomfortable for the conscious patients, but it also increments the risks of injury and infection.

The goal of this project was the design, the implementation and the validation of a method for the *non*-invasive and continuous estimation of respiratory effort during spontaneous breathing and support ventilation.

As a first step, the human respiratory mechanics were modelled using the single-compartment model of the respiratory system. With the aid of the modelled system and its equation of motion (EOM), the method was developed to determine the respiratory parameters resistance (R) and compliance (C) and to make a periodic calculation of the breathing effort as the inspiratory Pressure-Time-Product (PTP_{insp}) from the calculated muscular pressure.

The novel method received the name Occlusion+Delta (O+D). Its development integrated the advantages from known procedures like the use of short interruptions of the airway flow (occlusion), established mathematical modelling of the respiratory system and algorithms like multiple linear regression.

The main components of the method are the execution of respiratory occlusions of about 200 ms and the comparison of pairs of cycles. The main assumptions are that both the muscular pressure and the respiratory mechanics in the selected pairs of cycles are constant during regular breathing. The main goal is to eliminate the necessity of invasive techniques, which are normally required to measure the muscular pressure or surrogates of it. Another essential goal of the project was to deliver the results already during the measurement of the respiratory signals. Ultimately the aim would be to integrate the system in existing ventilation machines.

The implementation of the method required the construction of two electronic devices: a shutter to generate short airway occlusions during the expiratory phase of a breath and a measurement box with a flow sensor, pressure sensors and a data acquisition system to get and record the necessary signals. The test phase also required the recalibration of an electromechanical lung simulator (LS4000) and the programming of its control software, as well as the development of dedicated software to record, process, analyse and display the course of the respiratory signals and the results of the method.

The development of the method was accompanied by computer simulations. The provided test data permitted the verification of the correct implementation of the measurement system and the algorithms. In the next step, the electromechanical simulator was used to

produce test data under real conditions. This stage served as the first validation of the estimated variables against the simulated muscular pressure and breathing effort.

After the verification with simulations, a study with 25 healthy volunteers (10 smokers and 15 non-smokers) was executed. The examinations contained three levels of effort: normal, augmented by added dead-space and reduced by 10 mbar of pressure support with a commercial ventilator. These three levels were set with the volunteers, to represent conditions of adequate and insufficient support to patients from the ventilator.

The O+D method was validated in the study with volunteers by comparing its performance and results to those of the simultaneous invasive measurement of transdiaphragmatic pressure (P_{di}), using a double-balloon catheter with the balloons placed in the oesophagus and in the stomach, in combination with multiple linear regression.

The examinations with the volunteers took around one hour each, the short occlusions of the O+D method did not disturb the subjects and delivered the expected signals. This part of the project required deeper analysis to:

1. identify abnormal cycles – for example breaths including swallowing – and artefacts,
2. to automatically and correctly recognise the signals from the occlusions
3. and to identify the corresponding effort level.

In general the estimation of resistance from the O+D method was lower than the results from the invasive method, whereas the differences in compliance from the non-invasive and the invasive method strongly varied. According to these results, the O+D method can contribute to quantify the resistance, but the determination of the compliance is not reliable enough yet. Nevertheless the values of R and C from the O+D method could be used to create successful reconstructions of the muscular pressure of the single cycles.

For the final validation of the method, the values of the inspiratory Pressure-Time-Product (PTP_{insp}) from the invasive measurement of the transdiaphragmatic pressure ($PTP_{P_{di}}$) and from the non-invasive estimation of the muscular pressure (PTP_{O+D}) were compared through linear regression and the Bland-Altman analysis. These revealed ample positive agreement between the PTP_{insp} values from both methods ($PTP_{O+D} = 1.13 * PTP_{P_{di}} - 0.85$, $R^2 = 0.84$; $mean \pm 2SD$ of the differences = -1.78 ± 7.18 mbar*s; $n = 2500$ cycles) with increased variation of the differences during augmented effort.

The main contribution of the method developed here lays in its useful non-invasive and continuous assessment of changes in respiratory effort.

Although the procedure described in this investigation is not completely ready for implementation in commercial devices yet, many of the objectives were reached. Certainly it can be concluded that – based on the novel O+D method – a procedure for commercial devices for assisted ventilation can be implemented. This would bring important advantages: a prompter and a more adequate setting of ventilatory support during the ventilation of patients suffering respiratory insufficiency without invasive catheters or tubes.

Zusammenfassung

Die maschinelle Beatmung ist eine lebenserhaltende Maßnahme, sowohl in der Notfall- und Intensivmedizin als auch für chronisch atmungsinsuffiziente Patienten. Trotz der großen Bedeutung der unterstützenden Beatmung bei diesen Patienten stellt eine unzureichende Einstellung der Assistenz ein ungelöstes Problem dar. Essenziell für die richtige Auswahl der Unterstützung ist eine korrekte Überwachung der Atemleistung der Patienten, welche Schwankungen - beispielhaft durch Ermüdung - unterworfen ist. Dies kann bisher nur durch ein invasives Manöver - dies ist das Einbringen eines Katheters oder einer Sonde in den Patienten - ausreichend exakt eingeschätzt werden. Aber solch eine Prozedur ist nicht nur unangenehm für die bei Bewusstsein behandelten Patienten, sondern sie erhöht auch das Verletzungs- und Infektionsrisiko.

Ziel dieses Projektes war das Design, die Umsetzung und die Validierung einer Methode zur nicht-invasiven kontinuierlichen Schätzung der Atemleistung bei Spontanatmung und unterstützender Beatmung.

Zunächst wurde hierfür die Atemmechanik beim Menschen durch das Ein-Kompartiment-Modell des respiratorischen Systems modelliert. Mit Hilfe des modellierten Systems und dessen Bewegungsgleichung (EOM) wurde die Methode zur Bestimmung der Parameter Resistance (R) und Compliance (C) entwickelt. Der nächste Schritt beinhaltet dann die periodische Kalkulation der für die Inspiration benötigten Atemleistung – pro Atemzug, als das inspiratorische Druck-Zeit-Produkt (PTP_{insp}) aus dem berechneten Muskeldruck.

Die neuartige Methode wurde Occlusion+Delta (O+D) genannt. Ihre Entwicklung integriert die Vorteile aus bekannten Prozeduren wie die Nutzung von kurzen Unterbrechungen des Luftdurchflusses (Okklusionen), etablierte mathematische Modelle des respiratorischen Systems und Algorithmen wie die Multiple Lineare Regression. Die Grundlagen der O+D Methode sind die Durchführung von ca. 200 ms langen expiratorischen Okklusionen und der Vergleich zweier Atemzüge, basierend auf den Annahmen, dass der Muskeldruck bei diesen Atemzügen während regulärer Atmung ähnlich und die Atemmechanik konstant ist. Hierbei ist das übergeordnete Ziel, die Notwendigkeit von invasiven Techniken zu eliminieren, die normalerweise benötigt werden, um den Muskeldruck oder dessen Substitute zu messen.

Ein weiteres wesentliches Ziel der Arbeit ist es, die Ergebnisse bereits während der Messung der respiratorischen Signale zu liefern. Damit verbunden ist die logische Schlussfolgerung, ein solches System in vorhandene Beatmungsgeräte zu integrieren.

Die Umsetzung der Methode erforderte die Herstellung zweier elektronischer Geräte: ein Shutter, um kurze Okklusionen der Atemwege in der Ausatemungsphase eines Atemzuges akkurat zu erzeugen, und ein Messgerät mit Druck- und Durchflusssensoren sowie einem Datenerfassungssystem, um alle notwendigen Signale zu erfassen und zu speichern. Erforderlich für die Testphase waren außerdem die Kalibrierung eines elektromechanischen Lungensimulators (LS4000) und die Programmierung seiner Steuerung, sowie die Entwicklung der Software zur Erfassung, Verarbeitung, Analyse und Darstellung des Verlaufes respiratorischer Signale und der Ergebnisse der Methode.

Die Entwicklung der Methode wurde von Computersimulationen begleitet. Diese lieferten Testdaten und ermöglichten die Verifikation des korrekten Aufbaus des Messsystems und des Algorithmus. Im nächsten Schritt wurde der elektromechanische Lungensimulator dahingehend etabliert, Testdaten unter realen Bedingungen zu erzeugen. Diese Etappe diente der ersten Validierung der geschätzten Variablen gegenüber den bis dahin simulierten Daten für den Muskeldruck und die Atemleistung.

Anschließend wurde eine Studie mit 25 gesunden Probanden (10 Raucher und 15 Nicht-Raucher) durchgeführt. Die Messung enthielt drei Stufen der Atemarbeit: normal, erhöht durch zusätzlichen Totraum und vermindert durch 10 mbar unterstützenden Drucks aus einem kommerziellen Beatmungsgerät. Diese drei Stufen wurden mit den gesunden Probanden festgelegt, um Umstände darzustellen, in denen Patienten angemessene und unangemessene Unterstützung durch das Beatmungsgerät bekommen. Die Validierung der entwickelten O+D Methode in dieser Studie basiert auf dem Vergleich der erhobenen Messdaten mit parallel erhobenen Messungen des transdiaphragmalen Drucks (Pdi) durch invasiv in den Ösophagus und den Magen eingeführte Doppel-Ballon Katheter.

Die Untersuchungen mit den Probanden dauerten jeweils etwa eine Stunde. Die kurzen Okklusionen der O+D Methode haben die Probanden nicht gestört und lieferten die erwarteten Signale. Dieser Teil des Projektes benötigte weiterführende Analysen zur:

1. Identifikation von nicht normalen Atemzügen - beispielhaft Atemzügen mit Schluckbewegungen - und Artefakten,
2. automatischen und korrekten Erkennung der Signale aus den Okklusionen,
3. und die Zuordnung zu den am Beatmungsgerät eingestellten Leistungsstufen.

Im Allgemeinen war die Schätzung der Resistance durch die O+D Methode niedriger als das Ergebnis der invasiven Methode. Bei der Compliance variierten die Differenzen zwischen den Methoden deutlich. Gemäß diesen Ergebnissen kann die O+D Methode einen Beitrag liefern, die Resistance zu quantifizieren, während die Bestimmung der Compliance mit diesem Verfahren noch als unzureichend zu bezeichnen ist. Dennoch konnten die Werte von R und C aus der O+D Methode zu erfolgreichen Rekonstruktionen des Muskeldrucks der einzelnen Atemzüge eingesetzt werden.

Für die endgültige Validierung der Methode wurden die Werte vom inspiratorischen Druck-Zeit-Produkt (PTP_{insp}) aus der invasiven Messung des transdiaphragmalen Drucks (PTP_{Pdi}) und die aus der nicht-invasiven Schätzung des Muskeldrucks (PTP_{O+D}) durch lineare Regression und die Bland-Altman Analyse verglichen. Diese zeigten ausreichende Übereinstimmung zwischen den PTP_{insp} Werten beider Methoden (PTP_{O+D} = 1.13 * PTP_{Pdi} - 0.85, R² = 0.84; Mittelwert ± 2s der Differenzen = -1.78 ± 7.18 mbar * Sek; n = 2500 Atemzüge) mit breiterer Schwankung der Differenzen bei erhöhter Anstrengung.

Der Hauptbeitrag der hier entwickelten Methode liegt an der wertvollen nicht-invasiven kontinuierlichen Schätzung der respiratorischen Anstrengung.

Auch wenn das hier abgebildete Verfahren noch nicht die Reife für eine kommerzielle Einbindung in Beatmungsgeräte hat, sind viele der bearbeiteten Ziele erreicht worden. Es kann sicherlich die Schlussfolgerung gezogen werden, dass - basierend auf dieser neuartigen O+D Methode - ein Verfahren für kommerzielle Geräte zur assistierten Beatmung implementiert werden kann. Damit wären zwei erhebliche Vorteile verbunden: schnellere adäquate Einstellung der Unterstützung während der Beatmung atmungsinsuffizienter Patienten ohne invasive Katheter oder Sonden.

Table of Contents

Abstract	II
Zusammenfassung	IV
1 Introduction	14
1.1 Motivation	14
1.2 Fundamentals.....	14
1.2.1 Physiology	14
1.2.1.1 Ventilation	15
1.2.2 Pathophysiology	15
1.2.3 Lung mechanics.....	16
1.2.3.1 The single compartment model	16
1.2.3.2 The equation of motion	18
1.2.3.3 Work of breathing.....	20
1.2.3.4 Inspiratory Pressure-Time Product.....	20
1.2.4 Mechanical ventilation	21
1.2.4.1 Functional principle and interfaces	21
1.2.4.2 Positive end-expiratory pressure	21
1.2.4.3 Triggered pressure support	22
1.2.4.4 Associated risks	22
1.3 State of the art.....	23
1.3.1 Assessment of respiratory mechanics.....	23
1.3.1.1 Methods to assess respiratory mechanics	23
1.3.1.2 Comparison of existing methods	27
1.3.2 Adaptive ventilation	28
1.3.2.1 Adaptive support ventilation	28
1.3.2.2 Proportional pressure support.....	29
1.4 Definition of the Problem	30
1.4.1 Purpose	30
1.4.2 Methodology.....	30
2 Materials and Methods	34
2.1 Basis methods	34
2.1.1 Expiratory occlusions	34
2.1.2 The Delta-Inst principle.....	34
2.1.3 Multiple linear regression.....	35
2.1.4 Computation of muscular pressure	37
2.1.5 Joining methods.....	37
2.1.6 The Occlusion+Delta method: implementation and considerations.....	40
2.1.6.1 Similarity of cycles	40
2.1.6.2 Selected pairs of cycles.....	41
2.1.6.3 Definition of outliers	41
2.1.6.4 Graphical description.....	42
2.2 Simulated data	43
2.2.1 Computer simulations.....	43
2.2.2 Simulations with the lung simulator LS4000	44
2.2.2.1 The active lung simulator	44
2.2.2.2 Resistance and compliance.....	45
2.2.2.3 Software control	45
2.3 Invasive measurement of transdiaphragmatic pressure	46

2.3.1	The balloon catheter technique.....	47
2.3.2	Filtering artefacts and offset correction.....	48
2.4	Study with volunteers	50
2.4.1	Study design	50
2.4.2	Validation setup.....	51
2.4.3	Methodology.....	54
2.4.4	Safety	56
2.5	Evaluation of results	57
2.5.1	Abnormal signals and outlying estimates.....	57
2.5.2	Statistics.....	58
3	Results.....	60
3.1	Results from the invasive reference method.....	62
3.1.1	Simulations with the lung simulator.....	62
3.1.1.1	Results per simulation case.....	62
3.1.1.2	Analysis of phases per case	62
3.1.2	Results of the study with volunteers.....	62
3.1.2.1	Preparation and pre-processing of data	62
3.1.2.2	Results per subject.....	67
3.1.2.3	Analysis of phases per subject.....	67
3.2	Results from the non-invasive O+D method	68
3.2.1	Simulations with the lung simulator.....	68
3.2.1.1	Results per simulation case.....	68
3.2.1.2	Analysis of phases per case	68
3.2.2	Results of the study with volunteers.....	68
3.2.2.1	Results per subject.....	69
3.2.2.2	Analysis of phases per subject.....	70
3.3	Validation of the non-invasive O+D method	70
3.3.1	Simulations with the lung simulator.....	70
3.3.1.1	Validation results per simulation case.....	70
3.3.1.2	Analysis of phases per case	72
3.3.1.3	Overall analysis of simulation cases.....	73
3.3.2	Results of the study with volunteers.....	74
3.3.2.1	Validation results per subject	74
3.3.2.2	Analysis of phases per subject.....	77
3.3.2.3	Overall analysis of data from volunteers.....	78
3.3.2.4	Overall comparison of phases	79
3.4	Summary of main results.....	80
4	Discussion	83
4.1	Dealing with real data.....	83
4.1.1	Invasive measurement of Pdi.....	83
4.1.1.1	Measurement of gastric pressure	83
4.1.1.2	Disturbances, presumed reactions and cardiac artefacts	84
4.1.1.3	Constant and variable offset	86
4.1.1.4	Abnormal pressure signals	87
4.1.2	Measurement of flow.....	88
4.1.2.1	Real expiratory flow	88
4.1.2.2	Volume compensation and flow offset.....	89
4.1.2.3	Quality of the occlusions	90
4.2	The Occlusion+Delta method: Comparison to the state of the art	90
4.3	Agreement between methods.....	93
4.3.1	Resistance and Compliance.....	93

4.3.2	Agreement of PTPinsp	96
4.3.3	Suitability of the RC model	98
5	Conclusions and Outlook	100
6	Literature	102
7	List of publications	107
Annex A1.	Poster	109
Annex A2.	Letter from the commission of ethics.....	110
Annex B.	Dedicated software.....	111
Annex C.	Dedicated hardware	116
Annex D.	Electronic data	117
Annex E.	Smokers vs. Non-smokers	118
Annex F.	Detailed results of the analysis of phases	119
	Acknowledges.....	122
	Curriculum vitae	123

List of figures

Figure 1-1: Displacement of the diaphragm during breathing	15
Figure 1-2: State of the airways before and after an attack of asthma	16
Figure 1-3: The linear single compartment model of the lung	17
Figure 1-4: Pressure-volume loop and the calculation of compliance	18
Figure 1-5: Equivalent circuit for the RC model of the respiratory system.	19
Figure 1-6: Patients receiving invasive and non-invasive ventilation.....	21
Figure 1-7: Scheme of measured signals in a P0.1 occlusion.	23
Figure 1-8: Determination of R with an inspiratory occlusion.....	24
Figure 1-9: Determination of R with an expiratory occlusion.....	25
Figure 1-10: Scheme of the delta-inst method.	27
Figure 1-11: Flow and volume assistance in PPS.	29
Figure 1-12: Scheme of signals for the O+D method.....	31
Figure 1-13: Overview of methods and data	33
Figure 1-14: Overview of tasks performed for the present investigation.....	33
Figure 2-1: Example of measured Pdi and a possible reconstruction.....	37
Figure 2-2: Signals of a normal and an occluded simulated cycles.....	38
Figure 2-3: Similarity test using the flow-volume relationships	40
Figure 2-4: Summary of steps for the novel method	42
Figure 2-5: Simulink model of a system affected by offset and noise.	43
Figure 2-6: Simulation setup with the active lung simulator.....	44
Figure 2-7: Scheme of the simulation setup.	45
Figure 2-8: User interface of the software to control the simulator.	46
Figure 2-9: Single and double balloon catheters.	47
Figure 2-10: Pressure measurement with two single balloon catheters.....	47
Figure 2-11: Pressure measurement with a double-balloon catheter.....	48
Figure 2-12: Cardiac artefacts in the measured transdiaphragmatic pressure	49
Figure 2-13: Single-sided amplitude spectrum of the measured Pdi.....	49
Figure 2-14: Validation setup	51
Figure 2-15: Evita4 and shutter, front side and back side	52
Figure 2-16: Capnograph and sensors of CO ₂ and SpO ₂	52
Figure 2-17: Sensing system	52
Figure 2-18: Double-balloon catheter.....	53
Figure 2-19: Device for measurement of oesophageal and gastric pressure	53
Figure 2-20: Interface shutter-ventilator.....	53
Figure 2-21: Measurement box	54
Figure 2-22: Setup in the study with volunteers.....	55
Figure 2-23: Two examples of abnormal Pdi	57
Figure 2-24: Examples of disturbances in flow due to swallowing	57
Figure 3-1: Pressure signals for placement of the balloon-catheters.....	63
Figure 3-2: Examples of Pes, Pga and Pdi in the different levels of effort	63
Figure 3-3: Analysis of frequencies of Pdi of three different subjects.....	64
Figure 3-4: Example of original and filtered Pdi.....	64
Figure 3-5: Percentage of cycles with abnormal Pdi per subject	64
Figure 3-6: Example of offset correction in Pdi.	65
Figure 3-7: Offset correction in Pdi from subject 23 and 27.....	65
Figure 3-8: Cycle with high end expiratory volume.....	66
Figure 3-9: End-expiratory volumes in cycles without and with leak.....	66
Figure 3-10: Examples of signals in occluded cycles at 3 levels of respiratory effort.....	69
Figure 3-11: Examples of simulated Pdi and its reconstructions.	70

Figure 3-12: Summary of results for a single simulation case.	71
Figure 3-13: Differences in R and C between methods in the simulated cases.	72
Figure 3-14: Analysis of phases by Bland-Altman of PTP _{insp} per simulation.	72
Figure 3-15: Results of O+D with simulations.....	73
Figure 3-16: Summary of results for single subjects.....	74
Figure 3-17: Differences in mean resistance and compliance between methods.....	76
Figure 3-18: Differences in PTP _{insp} for all 25 volunteers.....	76
Figure 3-19: Analysis of phases by Bland-Altman diagram of two subjects.	77
Figure 3-20: Analysis of phases by Bland-Altman diagram of PTP _{insp} per subject.....	78
Figure 3-21: Analysis of mean R and C of all subjects per phase.....	78
Figure 3-22: Regression and Bland-Altman analysis of PTP _{insp} from all volunteers.....	79
Figure 3-23: Overall mean differences in PTP _{insp} between phases.	80
Figure 3-24: Differences in mean resistance and compliance between methods.....	81
Figure 3-25: Differences in PTP _{insp} for all 25 volunteers.....	82
Figure 3-26: Regression and Bland-Altman analysis of PTP _{insp} from all subjects.	82
Figure 4-1: Observations on the invasively measured pressures.....	84
Figure 4-2: Divergence of areas due to a disturbance in P _{di}	85
Figure 4-3: Presumed reactions of P _{di} in an occluded and an undisturbed cycle	85
Figure 4-4: Effect of a constant P _{di} offset in PTP _{insp} and correction.....	86
Figure 4-5: Changing offset in transdiaphragmatic pressure.....	87
Figure 4-6: Cycles with normal and abnormal P _{di}	88
Figure 4-7: Exponential decrease of expiratory flow and FV-loop.....	89
Figure 4-8: Non-exponential decrease of expiratory flow and FV-loop.	89
Figure 4-9: Offset in the flow signal	89
Figure 4-10: Flow signal from slow valve closure in an old study	90
Figure 4-11: Example of large variation of R and C from real data.....	94
Figure 4-12: Mean R and C per volunteer per phase.....	95
Figure 4-13: Mean R and C per volunteer per phase – Box plots	95
Figure 4-14: Scheme of expected differences in PTP _{insp}	98
Figure 4-15: Example of agreement per phase using PTP _{MLR}	99
Figure B-1: Window for source selection.....	111
Figure B-2: User interface	112
Figure B-3: Example of outputs while the program is running.....	113
Figure B-4: Flow chart of the program for O+D.....	114
Figure B-5: Window for results.....	114
Figure B-6: Window for offline analysis.....	115
Figure C-1: Shutter circuitry	116
Figure E-1: t-test for comparison of R and C of smokers and non-smokers.....	118

List of tables

Table 2-1: Model parameters for simulation with the lung simulator.....	45
Table 2-2: Timing for the examination phases.....	56
Table 3-1: Overview of the chapter Results.....	60
Table 3-2: Abbreviations used in the tables of results.....	60
Table 3-3: Cases simulated for the validation of O+D.....	61
Table 3-4: Demographic data of the participants of the study	61
Table 3-5: R and C from the simulated cases by the control method.....	62
Table 3-6: Characterisation of the balloon catheters	63
Table 3-7: R and C from the volunteers by the invasive method.....	67
Table 3-8: R and C from the simulated cases by the O+D method.....	68
Table 3-9: R and C from the volunteers by the O+D method.	69
Table 3-10: Validation results from simulated cases	71
Table 3-11: Results of measurements with volunteers.....	75
Table 3-12: Sample results of measurements per phase.....	77
Table 3-13: Results of measurements with volunteers.....	81
Table 4-1: Differences between mean resulting and simulated values of R and C.....	93
Table 4-2: Agreement of PTP _{insp} using values of MLR for the reconstruction.....	99

Notation

ALI	Acute lung injury
ARDS	Acute respiratory distress syndrome
ASB	Assisted spontaneous breathing
ASV	Adaptive support ventilation
b	Intercept of the regression line
C	Compliance, Capacitance
C _{curr}	Gliding average of C _{occ}
C _{fit}	Compliance calculated by multiple linear regression
CO ₂	Carbon dioxide
C _{occ}	Compliance calculated by the Occlusion+Delta method
COPD	Chronic obstructive pulmonary disease
CPAP	Continuous positive airway pressure
\bar{d}	Mean difference
DAQ	Data acquisition card
E	Elastance
E _{err}	Similarity factor
EIO	End inspiratory occlusion
EOM	Equation of motion
ePEEP	Extrinsic positive end-expiratory pressure
FA	Flow assistance in PPS mode
FRC	Functional residual capacity
H_0	Null hypothesis
iPEEP	Intrinsic positive end-expiratory pressure, also autoPEEP
l	Length of the tube, litre
LSF	Least squares fitting
m	1) Number of equations 2) Slope of the regression line
MLR	Multiple linear regression
mP _{mus}	Measured muscular pressure
n	1) Number of coefficients 2) Number of samples
nP _{di}	Amount of cycles with normal P _{di}
O+D	Occlusion+Delta method
P	Pressure
p	Significance level
P ₀	Offset pressure
P _{0.1}	Airway occlusion pressure
P _{alv}	Alveolar pressure
P _{ao}	Pressure at the airway opening
PAV	Proportional assist ventilation
P _{aw}	Airway pressure
P _{cmus}	Calculated muscular pressure
P _{di}	Transdiaphragmatic pressure
P _{drive}	Driving pressure
PEEP	Positive end-expiratory pressure
P _{el}	Elastic pressure
P _{es}	Oesophageal pressure
P _{ga}	Gastric pressure
P _L	Transpulmonary pressure

P_{mus}	Muscular pressure
P_{mus_0}	Offset muscular pressure
P_{pl}	Pleural pressure
PPS	Proportional pressure support mode
P_{PPS}	Increase of pressure in PPS mode
P_{re}	Resistive pressure
PSV	Pressure support ventilation
PTP	Pressure-time product
PTP _{insp}	Inspiratory pressure-time product
PTP _{MLR}	PTP _{insp} from the reconstruction of P _{di} using parameters from MLR
PTP _{O+D}	PTP _{insp} from the reconstruction of P _{di} using the novel method
PTP _{P_{di}}	PTP _{insp} from the measured P _{di}
R	Resistance
r	1) Radius of the tube 2) Model output error 3) Correlation coefficient
R^2	coefficient of determination
R _{curr}	Gliding average of R _{occ}
R _{fit}	Resistance calculated by multiple linear regression
R _{int}	Resistance determined with the interrupter technique
R _{occ}	Resistance calculated by the Occlusion+Delta method
S	Sum of the squared errors
sd	Standard deviation of the differences
SD	Standard deviation
SpO ₂	Arterial oxygen saturation
t	1) Time 2) t-value
V	Volume
V'	Flow
V _A	Volume assistance in PPS mode
V _{ee}	End-expiratory volume
V _T	Tidal volume
W	Work
WOB	Work of breathing
Δ	Difference, change
θ	Parameter set
μ	Viscosity of the fluid
μ_x, μ_y	Means of the populations x and y
τ	Time constant

1 Introduction

The interest of adapting mechanical ventilation to the individual patient has continuously increased over the last years, as the technical possibilities advance and the knowledge in the area grows. Although numerous improvements have been reached in different ventilation techniques, adaptation of support is still an unresolved issue for medical personnel and patients. This work deals with the development and validation of a method for continuous non-invasive assessment of respiratory mechanics towards a better adaptation of ventilatory support.

1.1 Motivation

The increasing number of patients being diagnosed with respiratory pathologies like the *chronic obstructive pulmonary disease* (COPD) as well as the necessity for faster weaning from mechanical ventilation have increased the need of ventilatory support for spontaneously breathing patients. In this field, the non-invasive interfaces have also gained significance over invasive techniques [1]. Non-invasive ventilators nowadays are not only used in hospitals and intensive care areas but also in nursing institutions and in home care. In the latter cases particularly, the availability of trained personal as a nurse or a doctor to continuously check the adjustment of the ventilation is limited and inadequate ventilatory settings may then have a negative effect on the patient's state of health. For that reason, adjustment of ventilatory support as response to their individual requirements is advantageous and desired [2]. The ideal is to make it possible that the respirator derives information from the spontaneous breaths of the patient and may, inside the ranges established by the physician, adapt to his/her needs. The core of this work is therefore, the development and validation of a novel method for the non-invasive assessment of respiratory mechanics during spontaneous breathing and ventilatory support.

1.2 Fundamentals

The present section summarizes general concepts needed to understand this work. It contains an overview on the physiology and pathophysiology of the respiratory system, followed by concepts of lung mechanics and mechanical ventilation.

1.2.1 Physiology

The respiratory tract can be divided in the upper respiratory tract comprising the nose, mouth and pharyngeal regions and the lower respiratory tract comprising the trachea, the bronchial tree and the lungs. The bronchial tree is made of two tubes called bronchi which bifurcate numerous times until reaching the terminal bronchioli. Those hold the air sacs called alveoli. There the gas exchange takes place.

According to their way of function, the components of the respiratory system can be classified in *passive and active structures*. The passive structures are the respiratory tract including both upper and lower airways, the surrounding tissues and the thorax. The active part is composed by the respiratory muscles responsible for the inspiration. The mechanical behaviour of the respiratory system is based on the relationships between flows, volumes and pressures acting on those structures. Especially under pathological

conditions or when a mechanical ventilator interacts with the patient, attention must be paid to their relationship patterns.

1.2.1.1 Ventilation

The exchange of air between the atmosphere and the organism is called *ventilation* and is divided in two phases: *inspiration* and *expiration*. In healthy subjects the inspiration starts by contraction of the diaphragm, which has the most functional relevance to create inspiratory force, and partially of the intercostal muscles. The contraction of the diaphragm causes an expansion of the thorax and thus a negative pressure relative to atmospheric, pulling air from the atmosphere into the body. When this negative pressure is compensated, the contraction ends. The expiration during calm breathing is a passive process during which the muscles relax and return to their original form and position. Due to the elastic recoil of muscles, lungs and chest wall tissues a positive pressure is created transporting the air out of the body. Figure 1-1 illustrates the displacement of the diaphragm. Although these sub-processes occur most of the time involuntarily, some voluntary control is also possible, for example to increase or reduce the breathing frequency, take deep breaths, cough, sneeze, speak, sing and clear one's throat. The cycles relevant for this work deal only with quiet breathing.

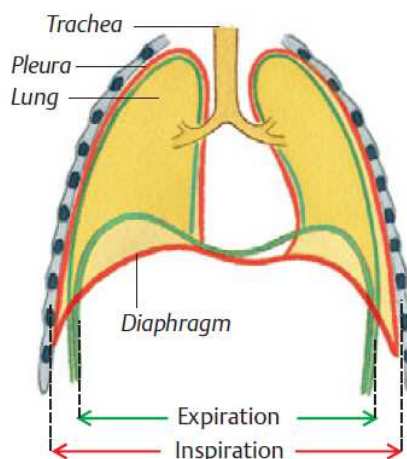


Figure 1-1: Displacement of the diaphragm during breathing [3]
The lungs are covered by a gliding serous membrane called *pleura*.

The ventilation is often characterized by the lung volumes. In this work following lung volumes will be mentioned: a) *tidal volume* (V_T): the normal volume of inspired and expired air during quiet breathing, with common values between 500ml and 1000ml, b) *inspiratory capacity*: the sum of V_T plus the volume that can still be inspired after a quiet inspiration, with common values from 2000ml to 3000ml, c) *residual volume*: the volume of air remaining in the lung even after forcefully expiring; common values are about 1000ml, and d) *functional residual capacity* (FRC): the volume of air contained in the lungs after quiet expiration.

1.2.2 Pathophysiology

Numerous pathologies affect the respiratory system and impede normal breathing. In the worst case a disease or malfunction of the system completely hinders ventilation making the patient depend on external assistance to survive. This is known as *respiratory insufficiency* or *respiratory failure*. When breathing is possible but the required effort is abnormally high, a sensation of breathlessness or *dyspnoea* appears. The effort needed may

increase as response to muscular diseases but also to pathological changes of the structures. Such conditions that cause abnormalities in the mechanical behaviour of the respiratory system can be divided in two groups: *obstructive* and *restrictive* diseases.

Three widespread respiratory diseases are typically obstructive: *asthma*, *bronchitis* and *chronic obstructive pulmonary disease* (COPD). An obstruction of the airways appears due to inflammation and contraction of airway smooth muscle (see Figure 1-2). Another obstructive condition is the *emphysema*. It is characterized by a reduction in the surface area of the blood-gas barrier and a subsequent reduction of the oxygenation.

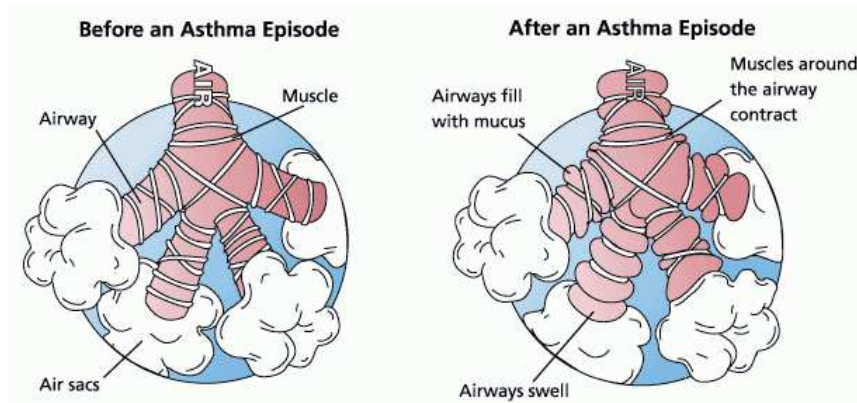


Figure 1-2: State of the airways before and after an attack of asthma [4]

Restrictive diseases are characterized by a reduction of the elasticity of the tissues. The most known restrictive disease is *pulmonary fibrosis*, where an excess of fibrous connective tissue makes the lung stiff and reduces the inspiratory capacity, producing shortness of breath and discomfort.

1.2.3 Lung mechanics

To understand respiratory mechanics, fundamental information from the system can be gained through the measurement of flow, volume and pressure signals. With them one can develop theoretical models and use them to obtain concrete parameters to describe the system. Mathematical models of the respiratory system are defined as “a set of equations that serve both as a precise statement of our assumptions about how the lung works mechanically and as a means of exploring the consequences of this assumptions” [5].

1.2.3.1 The single compartment model

The simplest way of modelling the respiratory system is considering the whole as a single compartment made of a pipe with resistance R and a balloon with elastance E . An alternative analogy is given in [5] and shown in Figure 1-3. This model consists of two “telescopic canisters” connected by a spring with constant E and a pipe with flow resistance R . Whether it is a balloon or a canister, the *elastic pressure* (P_{el}) inside the compartment is linearly related to the volume (V) and the *resistive pressure* (P_{re}), the difference of pressure between the two ends of the pipe, is linearly related to the flow (V').

Both flow and volume are functions of time (t), therefore written as $V(t)$ and $V'(t)$. To satisfy those relations, pressure and volume, or respectively pressure and flow must be connected by constant parameters. The ratio of P_{el} and V is defined as the *elastance* (E) which indicates how difficult it is to inflate the compartment. Its reciprocal value is the *compliance* (C) which indicates how easily the modelled lung is inflated. In the same way,

the ratio of P_{re} and V' is defined as the *resistance* (R). The use of such simple parameters in the model implies great but useful simplification of the reality.

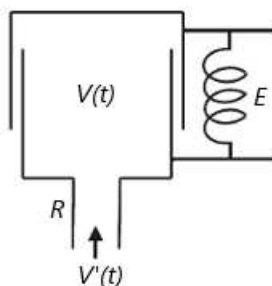


Figure 1-3: The linear single compartment model of the lung [5]
Two telescopic canisters connected by a spring with constant E and a pipe with flow resistance R.

o Resistance

The respiratory resistance (R) represents, as its name says, the resistance that the air must overcome to travel from the atmosphere down to the alveoli and is the ratio between pressure (P) and flow. The respiratory resistance of healthy adults is commonly around 2 to 4 mbar/l/s but it changes with age ranging from around 25 mbar/l/s for newborns, 4 mbar/l/s for children and 1 to 2 mbar/l/s for adults [6].

$$R = \frac{P}{V'} \left[\frac{\text{mbar}}{\text{l/s}} \right] \quad (\text{Eq. 1.1})$$

The resistance of the airway tree is strongly influenced by the dimensions of its branches. This is best explained by the law of Hagen-Poiseuille which shows that the resistance is directly proportional to the length of the tube and the viscosity of the fluid but inversely proportional to the fourth power of the radius of the tube. This last relationship clarifies why small reductions of the airways diameter cause a significant increase of resistance, which can be seen for example during an attack of asthma and after intubation.

$$R = \frac{P}{V'} = \frac{8\mu l}{\pi r^4} \quad (\text{Eq. 1.2})$$

with

μ viscosity of the fluid

l length of the tube

r radius of the tube

o Compliance

The respiratory compliance (C) is a measure of elasticity and corresponds to the ratio of the variations in volume and pressure.

$$C = \frac{V}{P} \left[\frac{\text{ml}}{\text{mbar}} \right] \quad (\text{Eq. 1.3})$$

A usual way to calculate the compliance is to find the slope of the static pressure-volume curve. The plot in Figure 1-4 shows pressure in the horizontal axis and volume in the vertical axis. The slope of the resulting line is C.

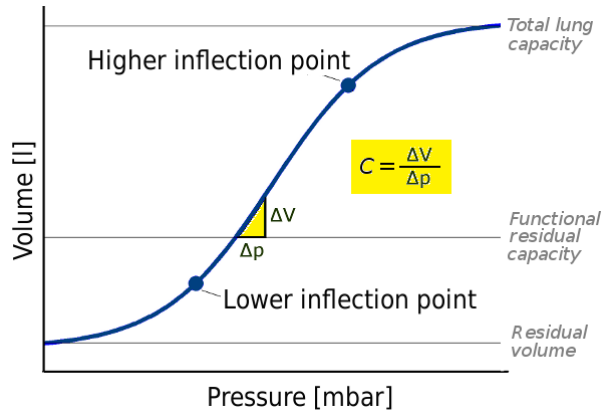


Figure 1-4: Pressure-volume loop and the calculation of compliance as the ratio between the changes in volume (ΔV) and the changes in pressure (ΔP)

In healthy subjects this curve is mostly linear with a constant slope. Its volume limits reduce in conditions like *acute lung injury* (ALI) and *acute respiratory distress syndrome* (ARDS): the lower and upper parts of the curve represent a limitation in the compliance when the lung is reaching its minimum or maximum volume. The inflection points in the curve show the conditions from where collapsed alveoli reopen (lower inflection point) or from where the alveoli are over-expanded and may be damaged (higher inflection point). The compliance of healthy systems is commonly around 100ml/mbar.

1.2.3.2 The equation of motion

Ventilation is allowed by variations in the air of volume in the lung. These variations are produced by negative (muscular) pressures and/or by positive (from mechanical ventilation) pressures. They cause a distending pressure over the lungs called *transpulmonary pressure* (P_L) which determines the lung volume. It is defined as the difference between the pleural pressure (P_{pl}) and the alveolar pressure (P_{alv}).

The measurement of P_{alv} is facilitated by the fact that it equals atmospheric pressure at FRC and when the airways are open. The pleural pressure, on the contrary, can only be directly measured by putting a catheter in the pleural space [7]. For this reason the *oesophageal pressure* (P_{es}), usually measured by placing a catheter in the lower third of the oesophagus, is commonly used as a surrogate for P_{pl} . This is possible due to the physiological proximity between the pleural space and the oesophagus, which behaves passively during calmed breathing and can thus transmit the adjacent pressure.

Similarly the *gastric pressure* (P_{ga}) can be measured with a catheter placed in the stomach. This is particularly useful because by calculating the difference between the oesophageal and gastric pressures the pressure over the diaphragm can be obtained (Eq. 1.4). This is called *transdiaphragmatic pressure* (P_{di}) and it serves as a useful approximation to the muscular pressure (P_{mus}).

$$P_{di} = P_{es} - P_{ga} \quad (\text{Eq. 1.4})$$

The combined effect of muscular pressure and the pressure from the ventilator over the airways (P_{aw}) constitutes the driving pressure (P_{drive}) required to produce air flow and volume changes in the respiratory system.

The mathematical expression for these relationships based on the single compartment model is the equation of motion (EOM)

$$P_{aw} + P_{mus} = V'R + V/C + P_0 \quad (\text{Eq. 1.5})$$

with

P_{aw}	the airway pressure in mbar
P_{mus}	the muscular pressure in mbar
V'	the flow in l/s
R	the resistance of the respiratory system in mbar/l/s
V	the volume in litre
C	the compliance of the respiratory system in l/mbar
P_0	an offset pressure in mbar

It relates the applied driving pressure for flow delivery, composed by the pressure applied by the ventilator on the airways (P_{aw}) and the pressure applied by the muscles (P_{mus}), to the resistive and elastic pressures causing the flow (V') and the volume (V) according to the impedances (resistance and compliance) and an offset pressure P_0 , that usually represents the positive end-expiratory pressure (PEEP). When the muscular effort is approximated by the transdiaphragmatic pressure, the equation turns into

$$P_{aw} + P_{di} = V'R + V/C + P_0 \quad (\text{Eq. 1.6})$$

These relationships can be graphically illustrated by using knowledge from electrical circuits to build an electrical analogue: as the resistance in fluid mechanics relates the driving pressure with the airflow flowing through it, the electrical resistance, also written R , relates the driving potential across the resistive element with the current passing through it; the respiratory compliance is modelled by an electrical element with *capacitance* C , which in fluid mechanics represents the applied pressure necessary to expand or contract a determined volume in an elastic compartment.

Figure 1-5 shows the electrical analogue of the single compartment model with a supplied pressure, zero offset, the flow through the airways, the airway pressure, the muscular pressure and the elements R and C .

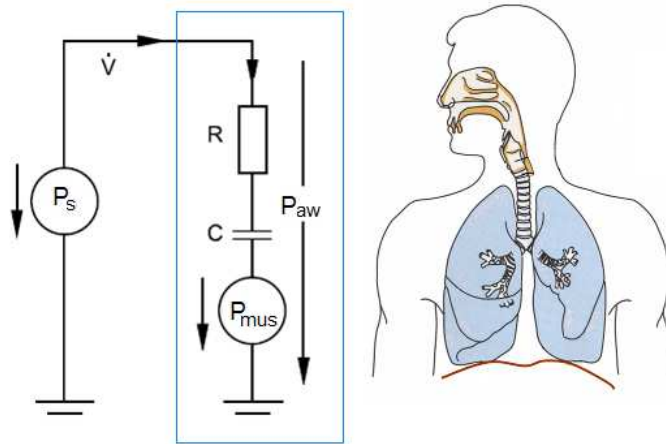


Figure 1-5: Equivalent circuit for the RC model of the respiratory system.
 P_s : supplied pressure. V' : flow. R : resistance. C : compliance.
 P_{aw} : airway pressure. P_{mus} : muscular pressure.

1.2.3.3 Work of breathing

The energetics of breathing belongs to the most important criteria in lung mechanics to assess the activity of the respiratory muscles. Whether the muscles are acting alone in spontaneous breathing or receiving assistance from a ventilator, the forces generated by them can be measured in terms of *work of breathing* (WOB).

In general mechanics work is calculated as the product of force and distance. In fluid mechanics, it is calculated as the product of pressure and volume in joules.

$$W = P \cdot V \quad [J] \quad (\text{Eq. 1.7})$$

During quiet breathing the changes of volume correspond to the tidal volume V_T . The forces causing inflation and deflation of the lungs are generated by the pressure applied at the airway opening (P_{aw}) and by the muscular pressure (P_{mus}). Depending on the origin of the pressure, one talks about work of breathing done by the ventilator and work of breathing done by the patient. The determination of the second one however is difficult because the measurement of muscular pressure is not as easy as the measurement of P_{aw} . This is why one approximates P_{mus} by measuring the transdiaphragmatic pressure P_{di} as a solution.

Positive work means that a given volume change is promoted by the pressure change, while negative work means that the volume change takes place against that pressure change [8]. Particularly the inspiratory work made by the patient is interesting during ventilation, because it reflects the activity of the inspiratory muscles and tells whether the machine is really supporting the respiratory muscles or working against them: a decrease in work of breathing accompanied by volumes and flows inside normal ranges would indicate successful support, whereas an increment of work of breathing with similar conditions may indicate too low mechanical aid.

1.2.3.4 Inspiratory Pressure-Time Product

Work of breathing is not always the best parameter to express energetics of breathing. The best example of this is given by pressure applied to an occluded airway: although pressure exists, the volume does not change indicating no work. An alternative is the *pressure-time product*, which results from integrating the applied pressure over the time of application.

$$PTP = \int P \cdot dt \quad [mbar \cdot s] \quad (\text{Eq. 1.8})$$

Also in this case, special attention is given to the energy used to inhale. This is measured by the *inspiratory pressure-time product* (PTP_{insp}). Its value can be calculated for the patient, by using P_{di} as pressure for the calculation, or for the ventilator, by using P_{aw} . These values also help to understand if the ventilator is supporting the muscles or opposing to them creating an additional workload for the patient. PTP_{insp} is usually calculated as the area under the pressure-time curve during the inspiration. Its value can be also presented as PTP_{insp} per minute, if multiplied by the respiratory rate.

1.2.4 Mechanical ventilation

When the respiratory system is able to generate and apply the forces required for adequate ventilation, spontaneous breathing is possible. If damage or failure of the ventilatory function of the respiratory system impedes the normal processes, the ventilation may be supported by mechanical ventilation.

Mechanical ventilation is used for relatively short time during operations or in the intensive care unit; long term mechanical ventilation is indicated for patients suffering of chronic illnesses and is employed in nursing institutions and in home care. Common medical conditions leading to mechanical ventilation are: Acute lung injury (ALI), COPD, paralysis of the diaphragm, increased work of breathing, hypoxemia¹ and neurological diseases as muscular dystrophy and amyotrophic lateral sclerosis [4].

1.2.4.1 Functional principle and interfaces

Like in spontaneous breathing, during mechanical ventilation the air is transported from the atmosphere into the body and backwards by periodically changing the pressure conditions. The mechanical part, composed by the ventilator, its tubing and an humidification system, is connected to the biological part, the patient. Depending on the mode, the ventilator applies a defined positive pressure during the inspiration to push air into the body. The expiration is passive and results from the elastic recoil of lung and muscles.

Depending on the interface one speaks of *invasive ventilation* and *non-invasive ventilation*. Invasive ventilation requires the insertion of a laryngeal mask or an endotracheal tube. For tracheal intubation the tube is inserted through nose or mouth and is placed into the trachea (Figure 1-6, left) which usually causes pain and coughing. The intubation, as any invasive procedure, means an increased risk of injuries and infection. For the non-invasive ventilation different types of masks are utilized. Depending on the pathology and the patient masks covering nose and mouth (Figure 1-6, right), only nose, the whole face or around the head can be used. The principal disadvantage of the non-invasive ventilation is the presence of leaks.

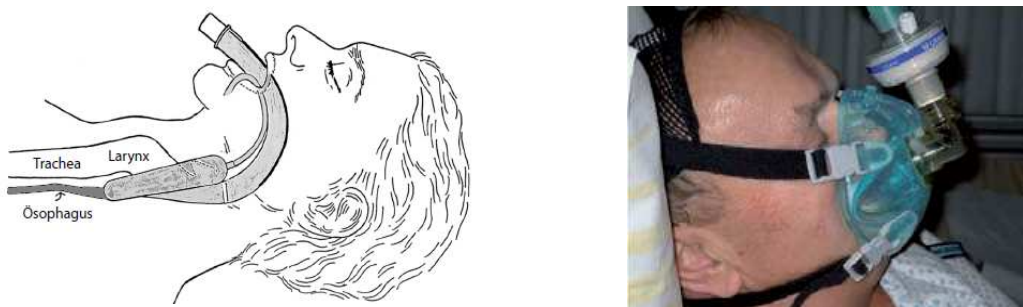


Figure 1-6: Patients receiving invasive and non-invasive ventilation
 Left: ventilation through a laryngeal mask. Figure adapted from [9].
 Right: non invasive ventilation through a nose-mouth mask [10].

1.2.4.2 Positive end-expiratory pressure

The pressure remaining after the end of the respiratory cycle is called *positive end-expiratory pressure* (PEEP). If this pressure is caused by airway obstruction or hindrances

¹ lowered arterial partial pressure of oxygen

to complete expiration, an *intrinsic PEEP* (iPEEP) remains in the lungs. Because the expiration cannot be completed, part of the inhaled air stays in the lung. This is called *air-trapping*. If this occurs one breath after the other, the tidal volume reduces and the gas exchange may be affected.

If set by the ventilator the pressure level is called *extrinsic PEEP* (ePEEP) and is used to augment the residual lung capacity avoiding alveolar collapse and improving oxygenation. Common values of ePEEP go from 0 to 15mbar depending on the patient and pathology [11]. The ventilation mode set to apply a constant pressure is called *continuous positive airway pressure* (CPAP). The only adjustment that it requires is the PEEP level over which the spontaneous breathings take place. CPAP also helps to decrease work of breathing.

1.2.4.3 Triggered pressure support

Some patients are still able to breath, but their inspiratory force is limited and they do not receive enough air. In such cases the ventilator can assist the initial inspiratory effort being triggered by time and/or by the spontaneous efforts of the patient. This is measured as triggers of pressure or flow.

Nowadays, one of the most used modes of ventilatory assistance is the so-called *pressure support ventilation* (PSV). Once triggered, the ventilator applies a preset pressure during a defined time. PSV is used as basis mode in this work, because it is currently well established for non-invasive long ventilation and weaning [11]. In the commercial ventilator Evita4 of Dräger Medical the PSV mode is called *assisted spontaneous breathing* (ASB).

A variation to pressure support ventilation was made towards the adaptation of the assistance, in the mode called *proportional pressure support* (PPS) or *proportional assist ventilation* (PAV). This mode is implemented for instance in the commercial ventilator EvitaXL of Dräger Medical. It bases on separated settings of pressure support intended to compensate the resistive and elastic loads acting on the respiratory system [12], [13]. Basis for the proper setting of the support pressure is therefore the correct determination of resistance and compliance according to the single compartment model. The correct assessment of lung mechanics is however still a challenge. This work may contribute with the development of a method able to estimate lung mechanics in a non-invasive continuous way, that serves for the further improvement and spreading of adaptive modes like PPS. Further details on PPS are given in section 1.3.2.2.

1.2.4.4 Associated risks

Unfortunately mechanical ventilation does not only have benefits for the patients. The most known risk associated to mechanical ventilation is the *barotrauma* which is damage to the tissues caused by high differences of pressure; damages caused by over-distension are called *volutrauma*. Mechanical ventilation may also produce harm with the same characteristics as acute lung injury (ALI) or the acute respiratory distress syndrome (ARDS). This is called *ventilator associated lung injury*. Because the work of diaphragm and other respiratory muscles is limited *muscular atrophy* may also appear. Moreover, the mucociliary motility in the airways may be impaired and the expulsion of secretions may be limited causing pneumonia. Other side effects of mechanical ventilation include decreased stroke volume and cardiac output, fluid retention, decreased venous return from the head with increased intracranial pressure and sleep deprivation [14].

1.3 State of the art

The next step in the development of this work was the revision of established techniques and approaches for the assessment of respiratory mechanics and the adaptation of mechanical ventilatory support. This section presents a summary on these topics.

1.3.1 Assessment of respiratory mechanics

In order to make support ventilation adaptive, continuous evaluation of the respiratory system is necessary. Starting with the mechanics as explained by the RC model (see 1.2.3.1) the aim is to determine non-invasively resistance and compliance, also from patients whose respiratory muscles are active. This section shortly describes existing methods developed to assess respiratory mechanics. All methods to be introduced here are valid for triggered support ventilation and the single compartment model.

1.3.1.1 Methods to assess respiratory mechanics

Some investigations about lung mechanics during spontaneous breathing relevant for this work include:

1. The airway occlusion pressure P0.1 [15], [16], [17]
2. The determination of respiratory resistance after P0.1 [18]
3. The rapid interrupter technique [19], [20], [21], [22], [23], [24], [25], [26]
4. Least squares fitting after high support during support ventilation [27]
5. The Delta-Inst method [28]

A short explanation on these methods follows.

1. The airway occlusion pressure P0.1 [15], [16], [17]

The respiratory muscles of spontaneously breathing patients receiving ventilatory support are able to generate some muscular pressure which cannot be easily measured. Therefore, direct determination of the muscular pressure is not viable in continuous monitoring. A well-known non-invasive alternative is the measurement of the *airway occlusion pressure* P0.1. A sample scheme of the relevant signals is shown in the next figure.

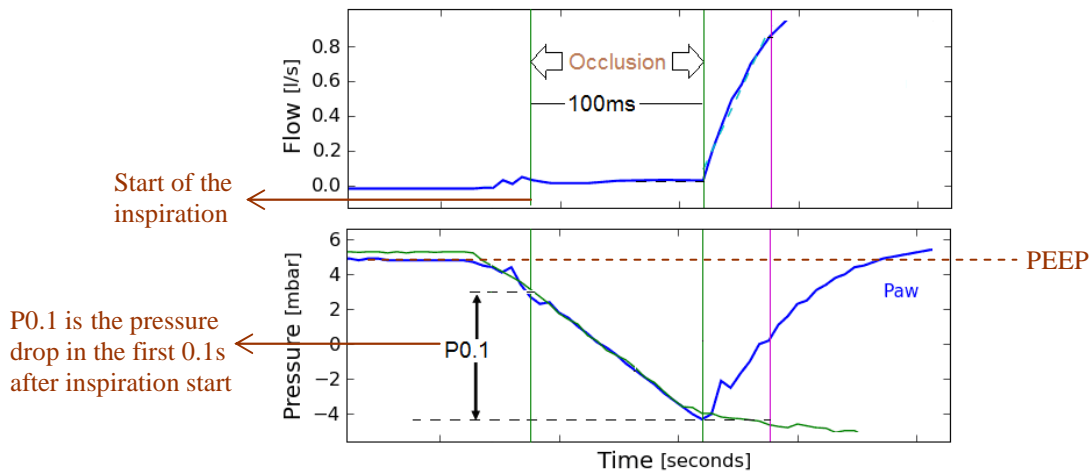


Figure 1-7: Scheme of measured signals in a P0.1 occlusion.
P0.1 is the pressure drop in the first 100ms of the breathing cycle

Directly after the begin of an inspiration, an occlusion is performed by valve closure and the pressure drop after the first 0.1 seconds is measured as an indication of the inspiratory force. This manoeuvre is often used to evaluate the ability of the patient to breath spontaneously during the weaning phase and to titrate high ventilatory assistance [15], [16], [17]. The P0.1 occlusion lasts 100 to 140 ms and is barely perceived by the patients.

2. Determination of respiratory resistance after P0.1 [18]

This method proposed by Ranieri et al. [18] uses the P0.1 occlusion manoeuvre to predict the course of the muscular pressure after the occlusion based on its course during it. With this prediction all variables are available to calculate the resistance at determined time points after the manoeuvre. The existing patient studies have not confirmed yet that the predictions are reliable enough.

3. The rapid interrupter technique [19], [20], [21], [22], [23], [24], [25]

This technique bases on airflow interruptions to estimate respiratory mechanics including resistance, elastance, muscular pressure and respiratory work. During pressure support oesophageal pressure (P_{es}), airway pressure (P_{aw}) and flow (V') are measured. At a defined time a valve shuts the airway and the flow goes to zero while the volume stops increasing. A rapid decrease in P_{aw} is observed and marked as P_A . But since noise and oscillations affect the signal, P_A must be rather be determined by back-extrapolating the decreasing P_{aw} after the start of the interruption.

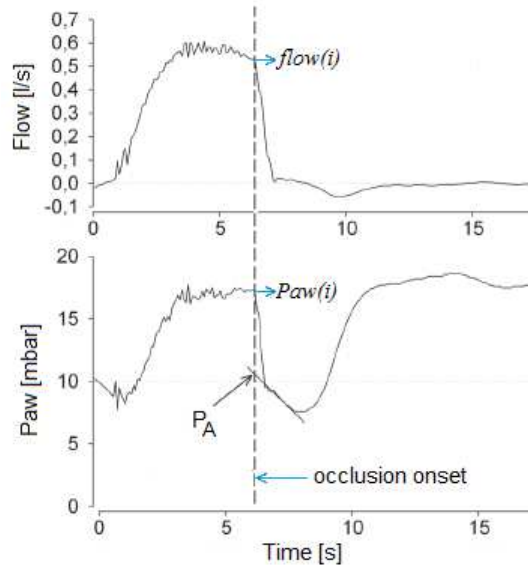


Figure 1-8: Determination of R with an inspiratory occlusion. Based on from [29]

The rapid decrease in P_{aw} is assumed to represent the resistive pressure drop and the resistance (R_{int}) can be calculated as

$$R_{int} = \frac{P_{aw}(i) - P_A}{flow(i)} \quad (\text{Eq. 1.9})$$

with

- $P_{aw}(i)$ the airway pressure just before the interruption
- $flow(i)$ the flow just before the interruption
- P_A the back-extrapolated pressure directly after the interruption

Such interruptions have been used over decades with variations in its duration and in the time or volume measured at its begin. Interruptions lasting only 0.1 seconds suffice to

determine R_{int} [24]. But interruptions lasting several seconds can be used to measure the further decrease of P_{aw} after the start of the manoeuvre, which is due to the sustained effort of the patient. In this case, muscular relaxation is expected to follow and must be confirmed by a plateau in P_{aw} and P_{es} . The difference between the relaxed occlusion plateau of P_{aw} and P_A measures the activity of the respiratory muscles during the preceding inspiration [20].

Bellani et al. [29] plotted the calculated P_{mus} over the time between inspiration begin and interruption to obtain a time course of the inspiratory effort over different breaths at different times and volumes. This assumes that all included interrupted breaths emerge from a constant inspiratory effort. To this respect they state that the technique is conceptually applicable to other forms of assistance with great variability as for example PAV.

In a further implementation designed to determine static and dynamic compliance the interrupter technique makes use of an *end inspiratory occlusion* (EIO) [30]. In this case the flow goes to zero and the volume is sustained while the P_{aw} decreases. A notable drawback of this implementation is the large duration of the occlusions which extend over several seconds resulting in discomfort for the patient and are thus inappropriate for continuous assessment of lung mechanics.

A variation of the rapid interrupter technique is *the shutter method* [26]. It uses a short interruption of flow during a relaxed expiration to calculate R as the ratio between changes of pressure and changes in flow before and after the occlusion as

$$R = \frac{P_1 - P_2}{V'_1} \tag{Eq. 1.10}$$

with

- P_1 the pressure before the interruption
- P_2 the pressure after the interruption
- V'_1 the flow before the interruption

An ideal representation of the required variables is shown in Figure 1-9.

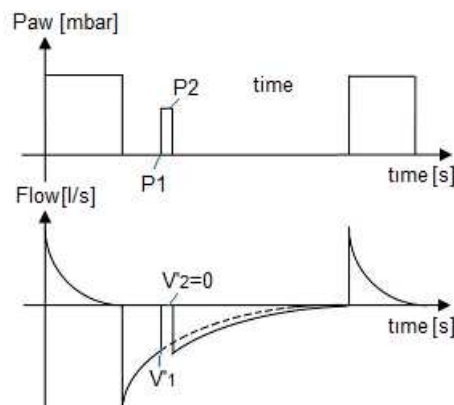


Figure 1-9: Determination of R with an expiratory occlusion.
 P_1 : pressure before the interruption. P_2 : pressure after the interruption.
 V'_1 : flow before the interruption. V'_2 : zero flow.

If muscle relaxation is complete during the expiration the occlusions can be used to obtain C too. In that case the expiratory flow decreases exponentially and following relationships can be established:

$$V(t) = V_0 \cdot e^{-t/\tau} \quad (\text{Eq. 1.11})$$

$$V'(t) = \frac{dV(t)}{dt} = (-1/\tau) \cdot V_0 \cdot e^{-t/\tau} = (-1/\tau) \cdot V(t) \quad (\text{Eq. 1.12})$$

with

$V(t)$	the volume as a function of the time t
V_0	the volume at expiration begin
$V'(t)$	the flow as a function of the time t
τ	the time constant defined as $\tau = R \cdot C$

The time constant τ can be found as the inverted negative slope of the expiratory flow-volume loop. Having τ and R it is possible to calculate C . This approach was initially included in the present work but was lastly discarded because only a few breathing cycles (about 15%) from the recorded real data (see electronic data in the attached CD) indeed showed an exponential decrease of the expiratory flow (see details in 4.1.2.1).

4. Least squares fitting after high support during support ventilation [27]

The use of mathematical models for biological systems permits their characterisation and quantification through mathematical algorithms. The approach of the study published by Iotti et al. [27] was to offer so much ventilatory support to the patient under proportional assist ventilation, that the respiratory muscles relax and the muscular pressure (P_{mus}) tends to zero. Once P_{mus} is eliminated a least squares fitting algorithm (LSF) is used to obtain R and C . In the original study up to 10cmH₂O above the basal level were given to the patients to reach near-relaxation, which was defined as a $P_{0.1}$ pressure lower than 1.5 cmH₂O. However, the basal level or baseline pressure support was defined for each subject individually. Moreover, near-relaxation of the respiratory muscles is not always desired.

5. The Delta-Inst method [28]

This non-invasive method was designed to assess resistance R and elastance E during pressure support. The technique consists of increasing or decreasing the inspiratory pressure support for a single respiratory cycle [28] under the assumption that the respiratory muscular activity of that cycle resembles the activity of the previous one. If so, the variations in the airway opening pressure (P_{ao}) over time between the two breaths would represent the total variations in driving pressure. R and E can thus be derived by using multiple linear regression from the relationships between the variation in P_{ao} (ΔP_{ao}) and the consequent variations in flow ($\Delta V'$) and volume (ΔV).

Figure 1-10 shows sample flow and pressure signals of the application of the Delta-Inst method during pressure ventilation. Further details are given in 2.1.2.

Navajas et al. [28] stated that this method found, in a previous study, values of R and E similar to those obtained from the invasive measurement of oesophageal pressure in patients suffering acute respiratory failure. Their own study included COPD patients and healthy persons with and without additional resistance. They concluded that the Delta-Inst was a simple method for reliably assessing respiratory resistance.

Due to its simple and comprehensible mathematical implementation, this method has also been used to analyze extended models of the respiratory system. For example in [31] the method was used to simulate leakages in non-invasive ventilation using inverse modelling for the resolution of the mathematical models.

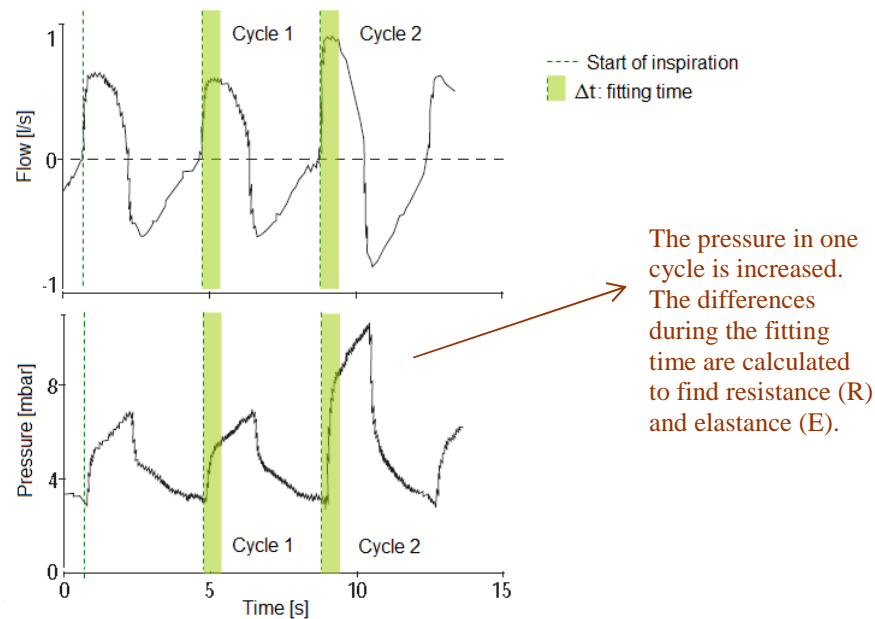


Figure 1-10: Scheme of the delta-inst method. Figure based on [28].
 During ventilation the pressure in a cycle is increased and the differences between cycles during the fitting time are used to find resistance (R) and elastance (E).

1.3.1.2 Comparison of existing methods

The understanding of existing techniques is fundamental for the development of a novel method. This section summarizes the reasons that lead to the development of the method to be explained in 2.1.5.

The occlusion pressure $P_{0.1}$ is common to assess respiratory effort and has had a worthwhile effect on the setting of ventilatory parameters [16]. The use of $P_{0.1}$ to determine respiratory resistance based upon a prediction of P_{mus} intended to draw more information from the manoeuvre, but the assumptions on the time course of P_{mus} could not be confirmed. Similarly, the assumptions on the course of the expiratory flow required by the shutter method were not supported by the real data recorded for this work. A stronger foundation offers the determination of respiratory mechanics by least squares fitting (LSF) after high ventilatory support, but it requires near-relaxation of the respiratory muscles and this may not be desired or convenient for the patient.

Most useful seem to be the rapid interrupter technique and the less known Delta-Inst method. These methods have the advantage that only minimal cooperation is needed and that the required procedures take a very short period of time. Their pros and contras are listed below:

Delta Inst

Pros:

- Does not require maximum relaxation because if the muscular pressure between consecutive cycles can be assumed constant, the variable P_{mus} can be eliminated [28]
- Does not require extra hardware
- Using multiple linear regression (MLR) it is possible to obtain both R and C

- Was previously examined to determine leakages during flow controlled ventilation, to determine R, C and additional simulated parameters, and to reconstruct Pmus [31]
- No occlusion manoeuvre is required

Contras:

- Only one paper including clinical results explains this method and it concludes reliable assessment only for the resistance [28]

Interrupter technique

Pros:

- It is a widespread method with sufficient documentation
- Some members of the team supporting this work had previous experience with it
- Requires only little cooperation

Contras:

- Needs additional hardware to cause the interruptions, whereby an adaptation of the valves of a commercial ventilator is realisable
- It does not deliver a result for E or C. C is obtained only with long interruptions of flow or with a relaxed exhalation with exponentially decreasing flow
- Requires relaxation of the spontaneously breathing patient to reach plateau pressures
- Possible leakages could impede complete flow interruption
- Not standardized: in some cases EIO is applied, in some others the interruption is done during passive expiration, in others during inspiration, with constant flow, at defined volumes and with interruptions that vary from 40ms to 3s.

This comparison was intended to establish which direction was the most appropriate to develop an own method. Other comparisons can be found in [32] and [33].

1.3.2 Adaptive ventilation

Mechanical ventilation can have adverse effects on the lungs and cause damages through the application high shear forces, inadequately high volumes or pressures or sudden changes of them. The risk of lung injury related to over-distension can be reduced by decreasing tidal volumes and inspiratory pressures while maintaining increased PEEP to reduce shear forces and keep the alveoli open. Such precautions are the core of the *protective lung ventilation*. For this, the settings of ventilatory modes have been modernised to avoid high volumes and pressures by defining limits and alarms and to offer different levels of PEEP.

Additionally, some level of adaptation to the patient has been reached by different ventilation modes. Particularly two of them have been designed to adapt the ventilatory settings to the respiratory mechanics of the patient: adaptive support ventilation (ASV) and proportional pressure support (PPS).

1.3.2.1 Adaptive support ventilation

Adaptive support ventilation (ASV) is a closed-loop control mode that may automatically switch its behaviour between resembling pressure controlled ventilation and pressure support, according to the patient status [34]. ASV adjusts pressure support to maintain a target volume. The adaptation is based on calculations done on each breath to find the optimal tidal volume and frequency that minimize the inspiratory workload. According to

[35] central respiratory drive and sternocleidomastoid activity are markedly reduced in ASV, suggesting decreased inspiratory load and improved patient-ventilator interactions. In brief, this mode aims to find the ideal support to reach a target volume. Nevertheless, maintaining the natural variability between cycles has proven to be advantageous in weaning from mechanical ventilation [36].

1.3.2.2 Proportional pressure support

PPS stands for *proportional pressure support* and is also called *proportional assist ventilation* (PAV). This mode is indicated for spontaneously breathing patients and aims to support breathing proportionally to the effort made by the patient. PPS has a special significance in this investigation because although it started as a promising method, the correct determination of lung mechanics represents a challenge in its application. A method for continuous reliable non-invasive estimation of R and C would be advantageous for its further implementation.

In contrast to pressure support ventilation (PSV) (see 1.2.4.3), PPS proposes a delivery of support which is proportional to the inspiratory effort of the patient. This is estimated using the resistance and compliance previously measured during controlled ventilation or obtained by methods like the interrupter technique. The support given in the inspiration is constituted by *volume assist* (VA) and *flow assist* (FA). The volume assist aims to compensate the elastic work required to increment the lung volume due to the lung elasticity; the flow assist aims to compensate the resistive work required to generate flow through the airways.

The resistive support is the necessary increase in pressure P_{PPS} that will compensate the flow resistance. The elastic support corresponds to the necessary increase in pressure P_{PPS} that will compensate the elastance. The total support is the sum of both. Figure 1-11 shows a scheme of resistive and elastic pressure support.

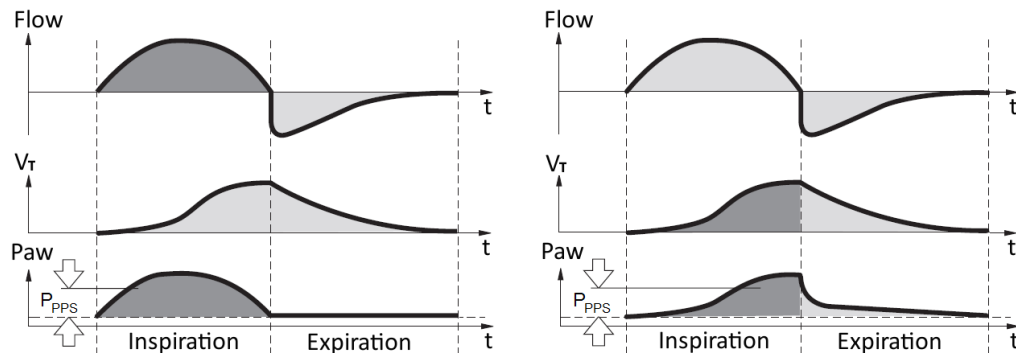


Figure 1-11: Flow and volume assistance in PPS. Figure adapted from [37].

V_T : tidal volume. P_{aw} : airway pressure. P_{PPS} : pressure support. t = time. The resistive pressure support (left) is proportional to the flow; the elastic pressure support (right) is proportional to the tidal volume.

Appendini et al. [38] found that PAV and CPAP can unload the inspiratory muscles of the ill patient to values close to those found in normal subjects. Nevertheless, the possibility to set the level of support according to the respiratory mechanics makes the proper determination of parameters critical: wrong determination of R and C may cause overcompensation making the system unstable and causing a situation called *runaway* in which the patient is over-assisted and would have to counteract the ventilator. The determination of respiratory mechanics is therefore particularly important for modern ventilation modes like PAV [12], [13], [39].

1.4 Definition of the Problem

1.4.1 Purpose

The review on state of the art makes clear that even recent methods have limitations and that there is still room for improvement and innovation. Although various modes of ventilatory assistance already exist and receive different names depending on their manufacturers, the principles are similar and none of them exhibits superiority regarding outcome parameters until now.

For this reason this work has the purpose to investigate and develop an alternative method that delivers a continuous non-invasive estimation of respiratory resistance, compliance, muscular pressure and respiratory effort represented by the pressure-time product at different levels of support ventilation, comparable to those estimations obtained by multiple linear regression in combination with the invasive measurement of transdiaphragmatic pressure. This method and its performance are to be implemented and validated with simulations and in a study with spontaneously breathing individuals with expectedly different respiratory mechanics.

1.4.2 Methodology

The introduction given in the previous sections included the motivation, the fundamental concepts and the state of the art. Knowing also the purpose of this project, the rest of this work is composed as follows.

Two methods are considered: the standard invasive method used as reference for validation and the novel non-invasive method called *Occlusion+Delta* (O+D). The novel method is initiated as a combination of existing procedures explained in the sections 2.1.1 to 2.1.4. The strategy designed to use them as partial procedures to build a new method is the topic of 2.1.5. Details and considerations for its implementation are concentrated in 2.1.6.

The following lines present a short summarized description of the method. The details are given in the next chapter.

The Occlusion+Delta (O+D) method: An introductory summary

Figure 1-12 shows flow (V'), volume (V), airway pressure (P_{aw}) and transdiaphragmatic pressure (P_{di}) of two breathing cycles. The last is used as a surrogate of the muscular pressure (P_{mus}) and is displayed here only as reference for the validation of the novel method. The times plotted are relative to each cycle.

As supported by the graphic the O+D method works as follows:

- During regular breathing, either spontaneous or with support ventilation flow and airway pressure are sensed and acquired.
- An expiratory occlusion of 200 ms is executed. This causes in the occluded cycle (see cycle 2) a visible short alteration to V' , V and P_{aw} (compare segments *b*) but not in P_{di} .
- Then, the values of all signals in the last 300 ms previous to the occlusion (see cycle 2 segment *a*) are selected. These are named V'_2 , V_2 , P_{aw_2} and P_{di_2} .
- The values of the volume previous to the occlusion are searched in each of the fifteen previous cycles (see cycle 1) to find the corresponding segments *a* (its duration may be different than in cycle 2).

- The values of all signals in the segment *a* of the undisturbed cycle are selected. These are named V'_1 , V_1 , Paw_1 and Pdi_1 .
- The slopes of the flow-volume loops of the occluded and the undisturbed cycles (V' vs. V) in the segments *a* are calculated and compared. Assumption: based on the equation of motion of the RC model, the smaller their difference, the more similar is the change of P_{mus} over the selected volume ranges.
- If the cycles are deemed similar the signals in the segments *b* are subtracted and the difference between Pdi_1 and Pdi_2 is neglected.
- The values are entered in the system of equations $(V'_2 - V'_1) \cdot R + (V_2 - V_1) \cdot E = Paw_2 - Paw_1$, which is solved for R and E by multiple linear regression. The compliance is calculated as the reciprocal of E , $C = 1/E$.
- All previous steps are done for one occlusion and fifteen cycles previous to it. The values of R and C from each pair are averaged into R_{curr} and C_{curr} .
- The averages are used in each cycle to reconstruct the muscular pressure using the formula: $P_{mus} = V' \cdot R + VE' - Paw$
- The area under the inspiratory part of P_{mus} is the pressure-time-product PTP_{O+D} , which can be compared for validation against the area under the invasively measured Pdi , respectively the area under the simulated pressure
- The occlusions can be periodically repeated to obtain a continuous assessment.

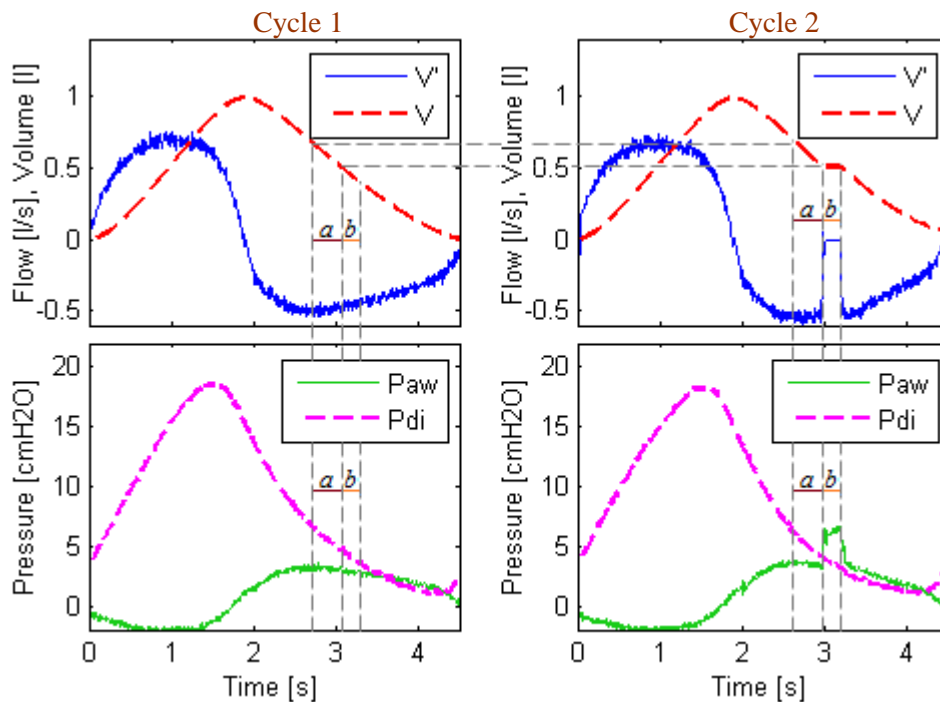


Figure 1-12: Scheme of signals for the O+D method.

Signals of an undisturbed (left) and an occluded (right) breathing cycle and selected segments for the non-invasive O+D method. The segment *b* on the right side indicates the expiratory occlusion of 200 ms. For more details see text.

Following this procedure the method can be suggested as a possible solution to the introduced problem. Still, the method, as it has been planned, has possible advantages and disadvantages as well:

The Occlusion+Delta (O+D) method: Pros and Cons

Pros:

- It does not require maximum relaxation because if the muscular pressure between the automatically selected pairs of cycles can be deemed similar, the variable P_{mus} can be removed from the algorithms, eliminating the need for invasive measurements.
- It does not require special cooperation from the patient, apart from normal breathing.
- It does not require extra hardware, since many modern ventilators are already able to produce fast short occlusions.
- Using multiple linear regression (MLR) it is possible to obtain both R and C.
- Through its reconstruction of the muscular pressure it periodically offers a definite assessment of the breathing effort.

Contras:

- It requires occlusion manoeuvres, whereby these are short and usually well tolerated.
- It is sensitive to leakages that may adulterate the measured signals and thus alter the values of R and C.
- Its suitability diminishes if the diaphragm does not produce the most of the pressure necessary for inspiration or if the respiratory system of the patient cannot be acceptably modelled by the single compartment RC model.

First validation of the method occurs using simulated data. This data is introduced in 2.2. It includes computer simulations and simulations with the bench simulator LS4000. Afterwards, validation with real data follows. The invasive method to measure transdiaphragmatic pressure (P_{di}) is described in 2.3. Both methods are used in a study with healthy volunteers, which was planned as section 2.4 shows. At each stage (simulation, modelling or validation) the results of the new method were validated against those of the established one. Section 2.5 explains the methods applied for the evaluation of data. A summary of the methods and data is presented as scheme in Figure 1-13.

Parallel to the development of the novel method, dedicated hardware and software were created to allow the implementation and validation of the proposed ideas. Figure 1-14 shows an overview of the tasks realised for this investigation.

The results are presented in chapter 3. Section 3.1 is limited to the application of the invasive reference method, whereas section 3.2 shows the results of the novel method. Both parts display their results separately for the simulated data and the data from the study with volunteers. In section 3.3 the results of both methods are compared to validated the proposed one. The last section summarizes in a simplified way the main results.

Chapter 4 contains the discussion. Section 4.1 includes observations about the work done to process and analyse real data. In section 4.2 the novel method is compared to the existing techniques introduced as the state of the art. Section 4.3 is devoted to the observations on the evaluated agreement between methods. Chapter 5 closes this work with the conclusions and outlook of this investigation.

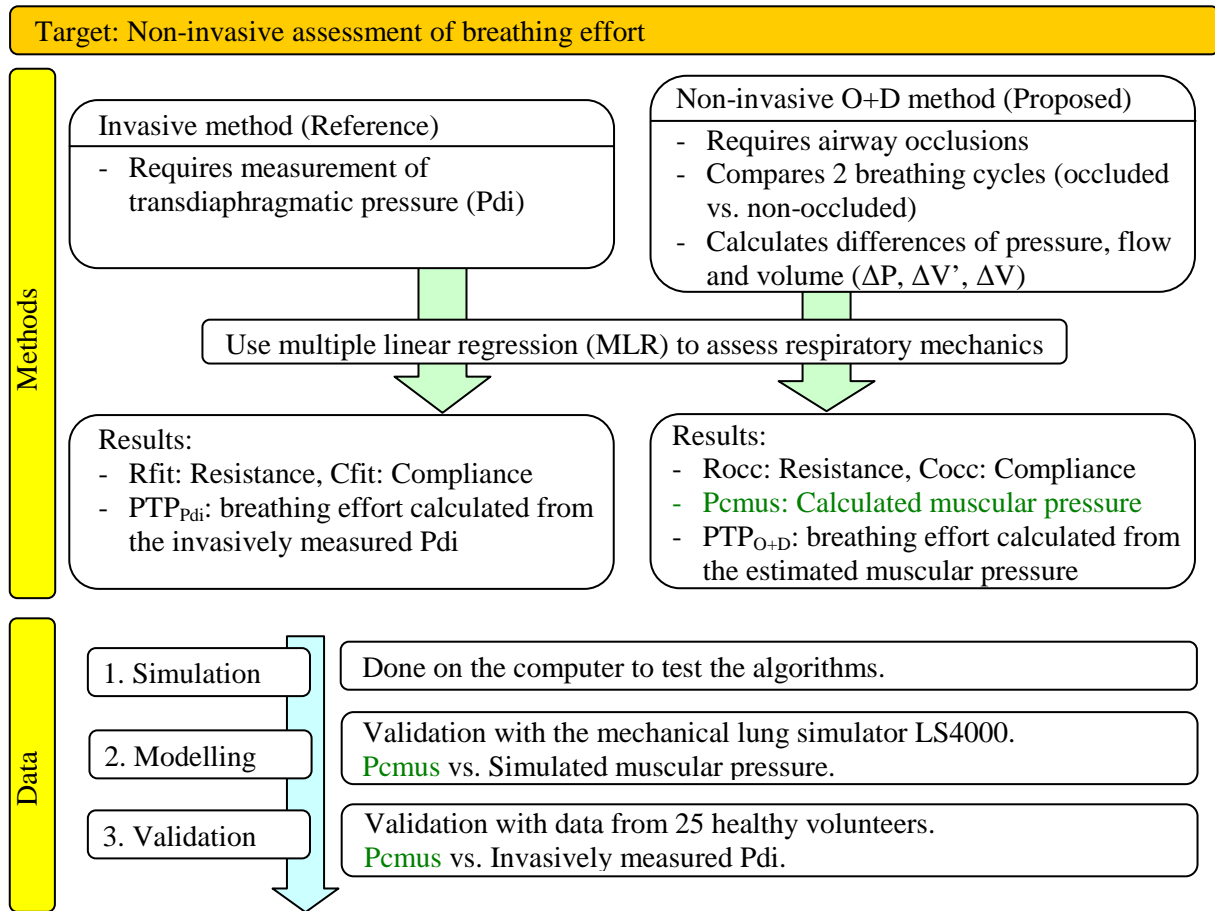


Figure 1-13: Overview of methods and data used in the present investigation on non-invasive assessment of respiratory effort in support ventilation.

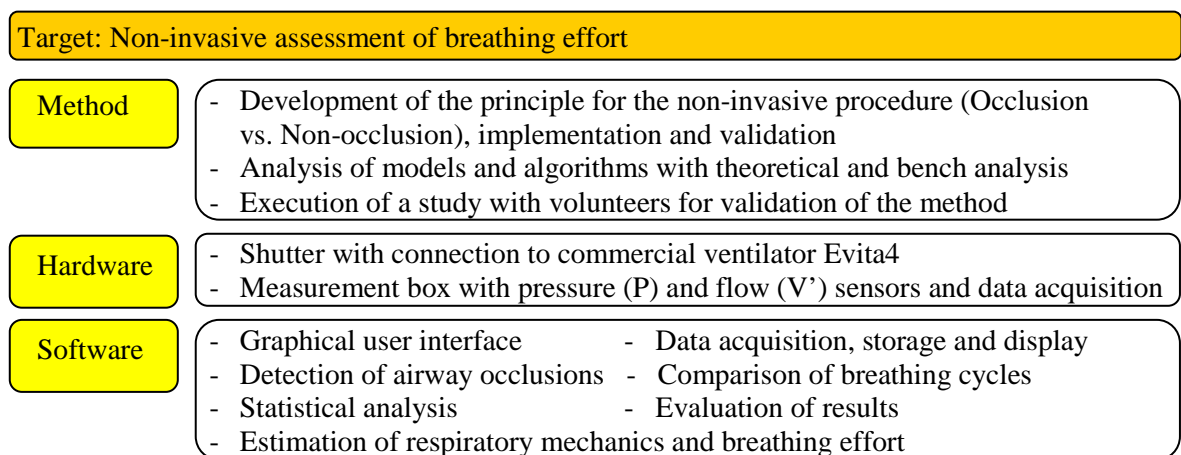


Figure 1-14: Overview of tasks performed for the present investigation

2 Materials and Methods

Advantageous ventilation modes like pressure support require an accurate setting of parameters based on the individual characteristics of the patient's respiratory system. This section deals with the materials and methods used in this work for the assessment of respiratory mechanics in spontaneously breathing subjects.

2.1 Basis methods

This section describes existing methods used as partial components for the novel method for non-invasive assessment of respiratory mechanics and how they were arranged together to build the novel one.

2.1.1 Expiratory occlusions

Short occlusions have been proven to be useful for the successful estimation of resistance but are not as strong for the determination of compliance (see 1.3.1.1). Despite of it, occlusions are common procedures barely perceived by the patients, which are fairly tolerable and are able to produce maximum changes in the respiratory signals and to deliver useful information. Furthermore, their potential implementation in a commercial respirator only requires minimum changes in hardware and the cooperation from the patient is not a requisite for success. For these reasons expiratory occlusions lasting approximately 200ms have been included in the methods selected for this work.

2.1.2 The Delta-Inst principle

Mathematical procedures like the Delta-Inst method [28] allow information to be gained out of the behaviour of pressures and flows at different times of the breathing cycle, that could only be obtained earlier by static techniques or with invasive procedures. The Delta-Inst method bases on the RC model of the respiratory system and the equation of motion (EOM) (Eq. 1.5, page 19) as introduced in 1.2.3.2. In the equation, the elastic pressure V/C can be expressed using the reciprocal of the compliance, the elastance E ($E=1/C$). This turns the formula into

$$P_{aw} + P_{mus} = V' R + V \cdot E + P_0 \quad (\text{Eq. 2.1})$$

with

P_{aw}	the airway pressure in mbar
P_{mus}	the muscular pressure in mbar
V'	the flow in l/s
R	the resistance of the respiratory system in mbar/l/s
V	the volume in litre
E	the elastance of the respiratory system in mbar/l
P_0	the positive end-expiratory pressure in mbar

The procedure starts with an increase or reduction in the level of pressure support for a given breathing cycle compared to the pressure given in the previous one. This is done without the patient being aware of each change in support.

Assuming linearity and constant values of R and E, the EOM for one specific breath can be written as

$$Paw_1 + Pmus_1 = V'_1 R + V_1 E + P_{0,1} \quad (\text{Eq. 2.2})$$

and, in an analogue way, the EOM for a second breath can be written as

$$Paw_2 + Pmus_2 = V'_2 R + V_2 E + P_{0,2} \quad (\text{Eq. 2.3})$$

whereby Pmus, V' and V change over time and P_0 represents the total intrapulmonary positive end-expiratory pressure [28].

Assuming that Pmus and P_0 do not significantly change between cycles (i.e. $Pmus_1 = Pmus_2$ and $P_{0,1} = P_{0,2}$) and that R and E remain constant, the differences Δ in airway pressure ($\Delta Paw = Paw_2 - Paw_1$), in volume ($\Delta V = V_2 - V_1$) and in flow ($\Delta V' = V'_2 - V'_1$) between the cycle with modified support and the previous one can be calculated by subtracting the equations and are related by the equation of differences

$$(Paw_2 - Paw_1) + (Pmus_2 - Pmus_1) = (V'_2 - V'_1) R + (V_2 - V_1) E + (P_{0,2} - P_{0,1}) \quad (\text{Eq. 2.4})$$

or equivalently

$$\Delta Paw = \Delta V' \cdot R + \Delta V \cdot E \quad (\text{Eq. 2.5})$$

Finally, multiple linear regression can be used to find the values of the parameters R and E [41]. In [28] the data for the equation of differences was derived from the signals measured in the interval between the starts of the inspiration and 0.25, 0.5 and 0.75 seconds later. The sampling rate was 160Hz.

Previous analysis of models and simulations [31] as well as the results of a study with COPD patients [28] support the feasibility of the Delta-Inst method inside the current project.

2.1.3 Multiple linear regression

Mathematical algorithms make it possible to fit the behaviour of a real system to a model characterized by a set of parameters and measurable variables. When the system has several input signals the modelling approach is called *multiple linear regression* (MLR). Regression models can be solved using *linear squares fitting* (LSF) which is a mathematical method to fit a model to real data described by an over-determined system² of linear equations. Its goal is to find the best approximation of model parameters that minimize the sum of the squared differences between the real data and its modelled values. It works as follows:

Given an over-determined system with input u and output y described by

$$y_i = \sum u_{ij} \cdot \theta_j \text{ with } i = 1, 2, \dots, m$$

which can be expressed in the matrix form of m linear equations and n unknown coefficients $\theta_1, \theta_2, \dots, \theta_n$ with $m > n$ as

$$\underline{y} = \underline{U} \cdot \underline{\theta}$$

² a system of equations with more equations than unknown variables

where

$$\underline{y} = \begin{pmatrix} y_1 \\ y_2 \\ \vdots \\ y_m \end{pmatrix}, \underline{U} = \begin{pmatrix} u_{11} & u_{12} & \cdots & u_{1n} \\ u_{21} & u_{22} & \cdots & u_{2n} \\ \vdots & \vdots & \ddots & \vdots \\ u_{m1} & u_{m2} & \cdots & u_{mn} \end{pmatrix}, \underline{\theta} = \begin{pmatrix} \theta_1 \\ \theta_2 \\ \vdots \\ \theta_n \end{pmatrix},$$

and the single errors between the output values from a modelled system of θ parameters and the real output values are given by

$$r_i = y_i - \sum u_{ij} \cdot \theta_j$$

the fitting algorithm finds the set of model parameters θ that best describe the behaviour of the real system, when the sum of the squared errors $S = \sum r_i^2$ reaches its minimum value.

In the case of the Delta-Inst method introduced in the previous section MLR is applied using the equation of differences $\Delta Paw = \Delta V' R + \Delta V E$ (Eq. 2.5, page 35). For this, the matrices are filled with the calculated differences of pressure, flow and volume between cycles (instead of using their absolute values) and the fitting algorithm finds the best estimates of R and E.

$$\begin{pmatrix} \Delta Paw_1 \\ \Delta Paw_2 \\ \vdots \\ \Delta Paw_n \end{pmatrix} = \begin{pmatrix} \Delta V'_1 & \Delta V_1 \\ \Delta V'_2 & \Delta V_2 \\ \vdots & \vdots \\ \Delta V'_n & \Delta V_n \end{pmatrix} \times \begin{pmatrix} R \\ E \end{pmatrix}$$

On the other hand, if a measurement or approximation to the muscular pressure as the transdiaphragmatic pressure, is available and if the flow, volume and airway pressure can be measured, the equation of motion $Paw + Pdi = V'R + V/C + P_0$ (Eq. 1.6, page 19) can be re-written in an equation of matrices using $P = Paw + Pdi$ and the parameters resistance R, elastance E ($E=1/C$) and offset pressure P_0 as

$$\begin{pmatrix} P_1 \\ P_2 \\ \vdots \\ P_n \end{pmatrix} = \begin{pmatrix} V'_1 & V_1 & 1 \\ V'_2 & V_2 & 1 \\ \vdots & \vdots & \vdots \\ V'_n & V_n & 1 \end{pmatrix} \times \begin{pmatrix} R \\ E \\ P_0 \end{pmatrix}$$

A least squares fitting algorithm can be then used to find the vector of respiratory parameters containing R, E and P_0 .

Note that in this work MLR will be treated as the application of MLR to find the set of parameters having knowledge of all inputs and outputs of the system, i.e. having knowledge of Pdi, and is therefore referred to as an invasive method.

The pressure signals measured in a real setup may contain offsets. In the real system the recorded airway pressure and the measured muscular pressure may contain a positive end-expiratory pressure and a relatively constant measurement offset. Both are determined inside the element P_0 of the parametric vector. Later when presenting the analysed data sources, it can be seen that while the offset of a simulated Pmus can easily be kept

constant, the offset of real signals may constantly vary during the measurement, even inside single breaths. The LSF finds the best constant value for P_0 , but it is also possible to approximate the real changing offset as a line between the minimum pressures of contiguous cycles.

In this work, the MLR method is used taking the signals of each respiratory cycle to obtain R, C and P_0 using a general least squares fit solved in LabWindows CVI. The data was sampled each 5ms and no smoothing was used before applying LSF.

2.1.4 Computation of muscular pressure

Knowing the respiratory parameters supports diagnostics and the assessment of respiratory work. R and C can be obtained whether from MLR including invasive measurement of Pdi or by using a non-invasive method like the Delta-Inst. In turn, the parameters, obtained in either way, can be used to calculate a *reconstruction* of the muscular pressure (Pcmus) as

$$P_{cmus} = V \cdot R + V / C + P_0 - P_{aw} \quad (\text{Eq. 2.6})$$

The reconstruction can be directly compared to the invasively measured Pdi, accepting the last as the best approximation to the real Pmus.

Thus, the reconstruction obtained with R and C from MLR with the invasive measurement of Pdi serves to determine how well the model represents the real system. The reconstruction obtained with R and C from a non-invasive method will serve to determine how well the new method is at assessing the real Pdi. Figure 2-1 shows an example of Pdi and a possible reconstruction of Pmus obtained with parameters estimated from MLR.

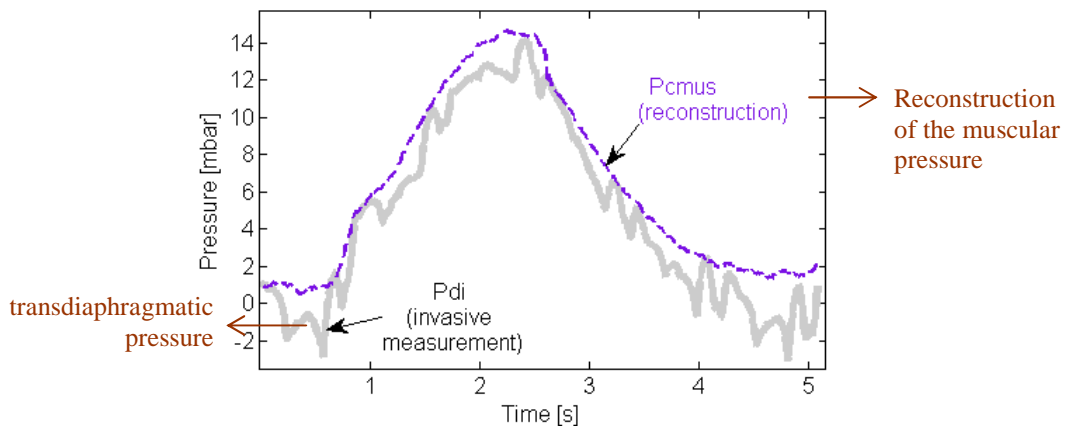


Figure 2-1: Example of measured Pdi and a possible reconstruction of the muscular pressure (Pcmus) in a breathing cycle.

2.1.5 Joining methods

This section describes the *structural concept* for the novel method. Its design joins the use of expiratory occlusions with the Delta-Inst method to make estimations of R and C that serve for the computation of muscular pressure and the calculation of breathing effort.

Concept

Note that not only the validation but also the development of the novel method itself was a goal of this work. The initial concept and methodology starts with the combination of the

previously introduced established methods – expiratory occlusions, the Delta-Inst principle, MLR and the computation of muscular pressure – towards the construction of a novel one. In consequence most details were at this early stage still open and had to be evaluated before a final decision was taken. This section introduces therefore only the rough concept and steps; the details about the method and its implementation are presented in the section 2.1.6.

The first step is the acquisition of respiratory signals. For this, flow (V') and airway pressure (Paw) are continuously measured, whereas the volume (V) is calculated for each cycle as the integral of the flow over time. Once the measurement of signals has started, the expiratory occlusions can be executed. The occlusions generate variations in the respiratory signals: during the 200ms after occlusion onset the flow goes to zero, the volume stops increasing and the airway pressure rises. When the valve of the ventilator reopens, the variables return to their normal course. Such short variations are useful to obtain pairs of breathing cycles that in principle will only differ after the start of the manoeuvre. If so, it is possible to find at least two cycles that, resembling the Delta-Inst method, have unchanged muscular pressures, at least until the onset of the occlusion. Their differences in the remaining variables can be calculated and MLR can be used afterwards to get R and C.

Important differences to the existing methods are that in the novel one the pairs of cycles do not necessarily have to be consecutive and that the intentional variations in the affected cycles start in the expiration and not already in the inspiration. Finally, the values of R and C are entered into Eq. 2.6 (page 37) to calculate the reconstructions of the muscular pressure. Its integral over the inspiratory time expresses the respiratory effort as the inspiratory pressure-time product (PTP_{insp}).

Steps

After starting the measurement a short occlusion of 200ms is performed during an expiration, which constitutes an alteration over the normal cycle. Sample signals from a normal cycle and an occluded cycle can be seen in Figure 2-2.

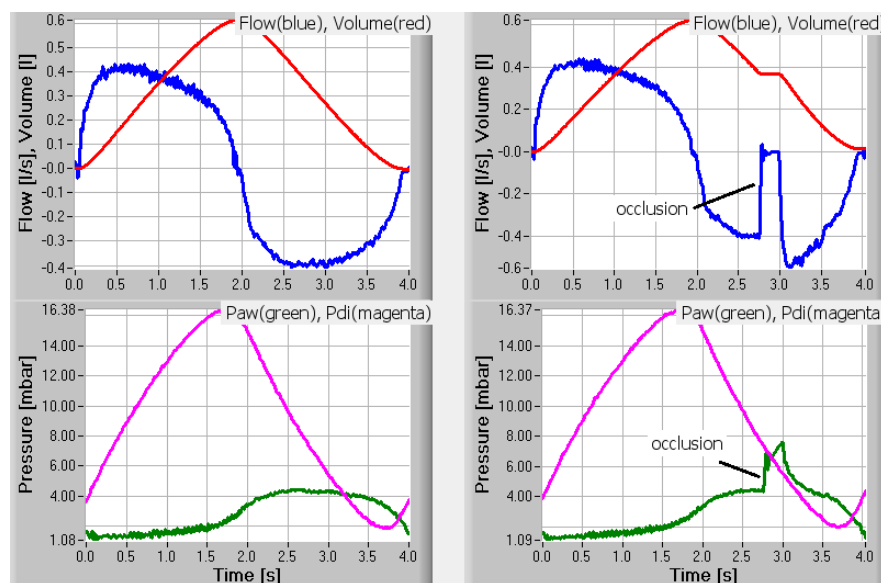


Figure 2-2: Signals of a normal and an occluded simulated cycles.

The transdiaphragmatic pressure (Pdi) serves as surrogate for the muscular pressure (P_{mus}) and is equal in the normal (left) and the occluded (right) cycles. The occlusion only causes changes to the flow, volume and airway pressure (Paw).

The occlusion is induced by shutting the expiratory valve of a commercial ventilator during the programmed time. To guarantee a safe manoeuvre the valve will reopen at the latest 500ms after occlusion onset in every case. The expiratory occlusions are executed with the expectation of producing an immediate change in airway pressure, flow and volume but not in muscular pressure or its surrogate, the transdiaphragmatic pressure.

In a similar way like in the Delta-Inst method (section 2.1.2) the variables of two cycles, one normal and one *altered* are selected to build the differences between their respective equations of motion. That the cycle is altered means in the Delta-Inst method, that the level of pressure support is modified. For the new method it means that a short expiratory occlusion has been done. Also here constant linear conditions are assumed.

Now the differences (Δ) between the equations of motion of the selected cycles are calculated and can be expressed as

$$\Delta P_{aw} + \Delta P_{mus} = \Delta V' R + \Delta V \cdot E \quad (\text{Eq. 2.7})$$

Note that this equation, in comparison to Eq. 2.5 (page 35) still contains the term ΔP_{mus} because no assumption has been yet. Only when the subject is breathing quietly and physiological reactions to the occlusion can be discarded, it can be assumed that the course of the muscular activity measured from two *similar cycles* is similar too. The mathematical procedure to determine whether two cycles are similar is explained in the next section (see 2.1.6). So, if P_{mus} during the occluded cycle is similar to that of the undisturbed one, their difference becomes negligible removing the term ΔP_{mus} from the equation and making the measurement of P_{mus} unnecessary. In the same manner, if a constant offset pressure P_0 is used in the equation and the cycles are similar, the difference in P_0 can be neglected too.

Next step is the application of linear squares fitting to obtain R and E from the equation of differences (Eq. 2.7). The result is a pair of values after each occlusion, whereby the compliance C is determined as reciprocal from the elastance E. Limits for R and C were established in order to reject outliers like negative resistances or extremely high compliances (see 2.5.1). For its validation, the resulting R and C can be compared to the values calculated from MLR with the invasively measured Pdi.

Besides the determination of R and C, the method is designed to make a reconstruction of the muscular pressure of each breathing cycle. The obtained values of R and C can be used to reconstruct P_{mus} as described in 2.1.4 by entering them into the corresponding equation of motion; but since R and C are expected to change slowly the parameters used for the reconstruction should be the averages of the results from an arbitrary number of previous occlusions. The reconstructed signal is the calculated muscular pressure (P_{cmus}) and its pressure-time-product is the non-invasive estimation of respiratory effort.

For the validation, the reconstructed muscular pressure (P_{mus}) and the invasively measured transdiaphragmatic pressure (Pdi) are compared through their areas under the curve, being the inspiratory part the one with major clinical significance. These values correspond to the inspiratory pressure-time-product (PTP_{insp}) and have been evaluated as section 2.5 shows.

2.1.6 The Occlusion+Delta method: implementation and considerations

The previous section presented the structural concept of the proposed method for non-invasive estimation of respiratory mechanics and respiratory effort. The method received the name *Occlusion+Delta* (O+D) and can be summarized in a few basic steps: first, expiratory occlusions are executed, and second, the differences of two similar cycles are calculated and entered into a fitting algorithm as described in 2.1.5 to obtain the model parameters R and C, which are then used to reconstruct the muscular pressure.

The most important link between these partial procedures is the definition of similarity between cycles. The reason: as far as the breathing pattern is homogeneous over several cycles, muscular relaxation is not crucial for the O+D method. This is an important advantage of it. How similarity between cycles was defined and further details of the O+D method are the topic of the following paragraphs. Later, Figure 2-4 in subsection 2.1.6.4 summarizes in a flow chart all steps required for the proposed method.

2.1.6.1 Similarity of cycles

Because the muscular pressure (P_{mus}) is unknown to the non-invasive method, the basic assumption of the O+D must be supported by determining the similarity of the cycles through their variables airway pressure (P_{aw}), flow (V') and volume (V) in the occluded and not occluded cycles. For the comparison of any pair of cycles containing one occluded and one non-occluded breath the slopes of both expiratory flow-volume curves (see Figure 2-3) are calculated in the 300ms previous to the occlusion onset for the occluded cycle and in the corresponding range of volumes for the non occluded cycle. According to recorded real data, 300ms is the duration of the segment previous to the occlusion, which permits to get the largest amount of samples while staying in the linear part of the flow-volume curve.

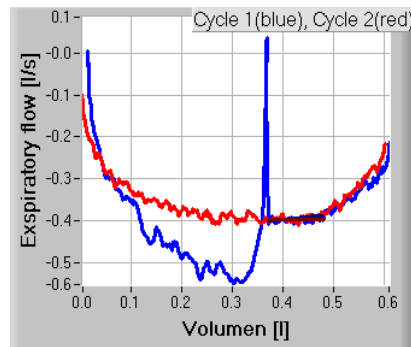


Figure 2-3: Similarity test using the flow-volume relationships in the expiration of two breaths, one normal (red) and one occluded (blue)

The equation of motion of a single cycle can be derived on both sides over the volume and reorganized as

$$\frac{dP_{mus}}{dV} + \frac{dP_{aw}}{dV} = \frac{dV'}{dV} R + \frac{dV}{dV} E \quad (\text{Eq. 2.8})$$

whereby the ventilator set to pressure support produces a stable airway pressure which hardly changes due to volume variations ($dP_{aw}/dV=0$) permitting to eliminate the second term of the equation. The difference in the variation of the muscular pressure over the volume between two cycles, 1 and 2, is then related to the variation of the flow with the volume as

$$\left(\frac{dP_{mus_1}}{dV_1} - \frac{dP_{mus_2}}{dV_2} \right) = \left(\frac{dV'_1}{dV_1} - \frac{dV'_2}{dV_2} \right) \cdot R + \left(\frac{dV_1}{dV_1} - \frac{dV_2}{dV_2} \right) \cdot E \quad (\text{Eq. 2.9})$$

The chosen segment of volume is equal for both cycles and both sides of the equation have units of elastance (mbar/l). Assuming that the variations of muscular pressure over the volume segment are identical, the error in the elastance E which arises from different slopes is defined by

$$\left(\frac{dP_{mus_1}}{dV_1} - \frac{dP_{mus_2}}{dV_2} \right) = \left(\frac{dV'_1}{dV_1} - \frac{dV'_2}{dV_2} \right) \cdot R \quad (\text{Eq. 2.10})$$

For this work the maximum error in the elastance must be by definition lower than 2 mbar/l. To check this, the slopes of the flow-volume curves (see Figure 2-3) in the selected range of volume are measured and their difference is calculated and multiplied by a resistance of 5 mbar/l/s, which is an assumed standard value used here only for tests. The difference of the slopes multiplied by the test constant returns the *similarity factor* E_err.

An absolute value of the similarity factor E_err smaller than 2 indicates a theoretical expected error in the elastance lower than 2 mbar/l and suggests that the compared cycles can be deemed similar. Afterwards, resistance and elastance can be calculated as introduced in 2.1.5 by solving the system of linear equations $\Delta P_{aw} = \Delta V' R + \Delta V E$ (Eq. 2.5, page 35) where $\Delta V'$ is the difference between the flow during the occlusion and the corresponding flow in the not occluded cycle. The same applies for ΔV and ΔP_{aw} .

2.1.6.2 Selected pairs of cycles

The equation of differences described in section 2.1.5 requires the variables from two similar cycles (one occluded and one undisturbed) to calculate its differences and then R and C. The occluded cycles are identified by searching inside the recorded expiratory flow signal the expected shape: a sudden change of the expiratory flow towards zero, a segment of about 200ms (minimum 100ms and maximum 350ms) of constant flow and a following rapid change of flow to a value close to that before the occlusion.

In the final implementation of the O+D method the occluded cycle is compared to each of the previous ten to fifteen undisturbed breaths previous to the occlusion. This increases the probability to find at least one cycle that is similar (see 2.1.6.1) to the occluded one and thus, to get at least one pair of values for R and C from the last occlusion: from each pair of similar cycles a value of R and C is obtained and these are averaged. The results from the pairs done with each occlusion are Rocc and Cocc.

After the determination of R and C, the method is designed to make a reconstruction of the muscular pressure (Pmus) in the inspiratory phase of each breathing cycle. The obtained values of R and C after each occlusion could be used to reconstruct Pmus (see 2.1.4), but since R and C are expected to change slowly, the parameters used for the reconstruction (Rcurr and Ccurr) are the averages of the results from the last ten previous occlusions.

2.1.6.3 Definition of outliers

After building the equation of differences in the O+D method LSF is used to get the parameters R and C. The results of this procedure are more reliable the more samples are available, but because the occlusion is very short (around 200ms) and the left and right

boundaries of the recorded signals include transients between normal and occluded breathing the number of samples for the fit is limited to less than 40. Additional factors like viscoelasticity and remaining external signals like gastric movements or pressures related to the heart beat can affect the form of ΔP_{aw} causing the fitting algorithm to produce unreal values of R and C. For those reasons constraints were established ($1 < R < 30$ mbar/l/s; $10 < C < 200$ ml/mbar) to reject extreme values and to calculate the averages (R_{curr} , C_{curr}) to be used for the reconstruction of muscular pressure only with results that lay inside the physiological range.

2.1.6.4 Graphical description

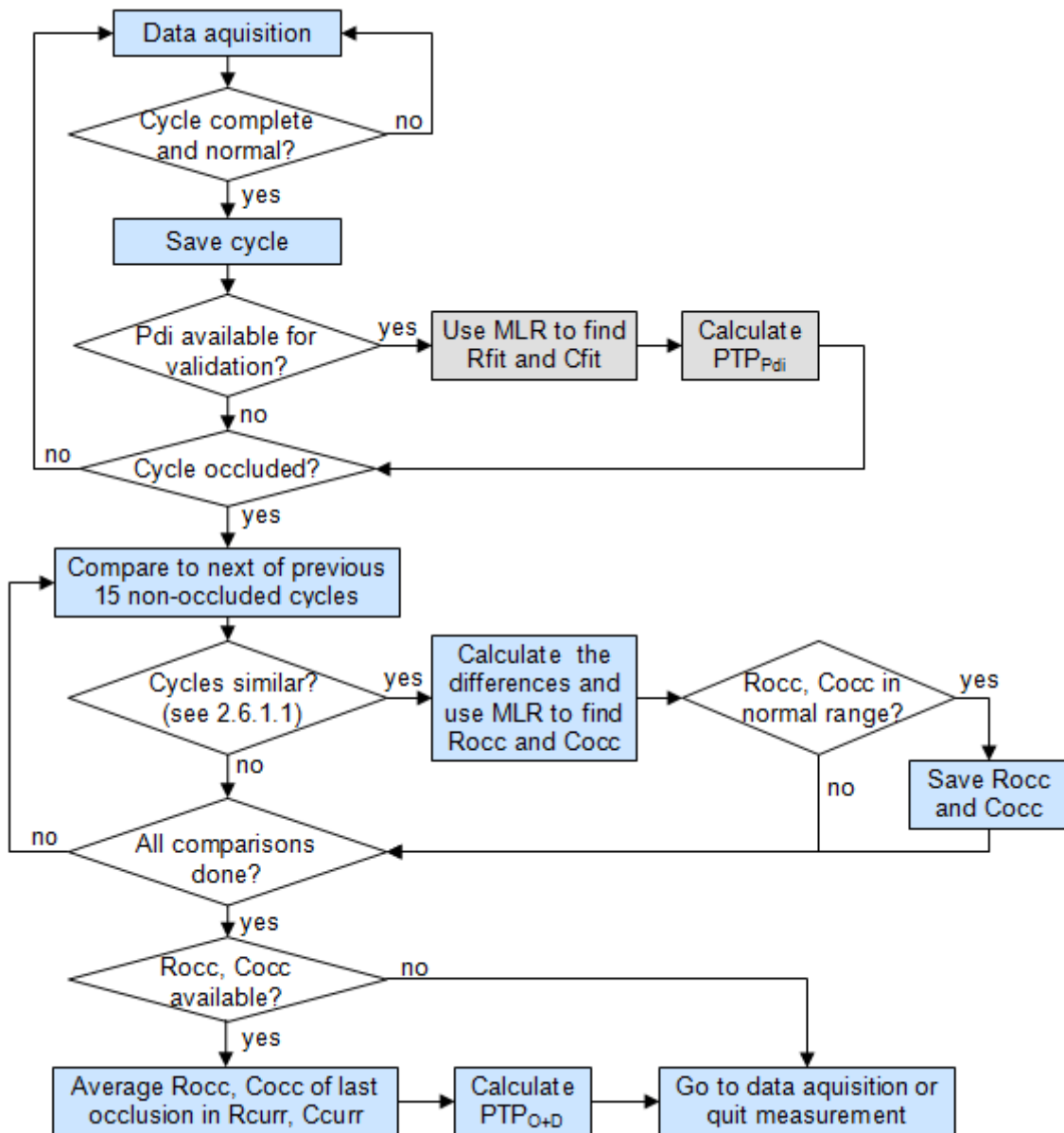


Figure 2-4: Summary of steps for the novel method

Pdi: transdiaphragmatic pressure. MLR: multiple linear regression. R: Resistance. C: Compliance. Rfit, Cfit: R and C from the invasive method. Rocc, Cocc: R and C from the novel method. Rcurr, Ccurr: averages for the current occluded cycle.

PTP_{insp}: inspiratory pressure-time product. PTP_{Pdi}: PTP_{insp} from the invasive method. PTP_{O+D}: PTP_{insp} from the pressure reconstructed with the novel method.

2.2 Simulated data

For the verification of the proposed novel method three sources of data were used: computer simulations, simulations with the mechanical simulator LS4000 and data from healthy volunteers. All data correspond to quiet spontaneous breathing with or without ventilatory support. This section gives an overview on the sources of simulated data.

2.2.1 Computer simulations

With the aid of the simulated data, the behaviour of the modelled system can be examined in an ideal environment. This allows testing the algorithms required for the novel method under known fixed conditions. For the first analysis, computer simulations were generated using the software Simulink.

Two series of simulations were done as basis for two diploma thesis realised as part of this work: a series of simulations of quiet spontaneous breathing and a series of simulations of spontaneous breathing with ventilatory support resembling the ASB mode. In both cases the input variable was the flow and the output variable was the driving pressure (Pdrive), which results from the sum of the airway pressure and the muscular pressure ($P_{drive} = P_{aw} + P_{mus}$).

The values of R and C ($R = 3.3, 4.5, 6.6$ or 7.5 mbar/l/s; $C = 25, 50, 75$ or 90 ml/mbar) were entered via the discrete transfer function $num(z)/den(z)$. The systems were simulated in ideal conditions but also including disturbances caused by an offset pressure and/or white noise. Figure 2-5 shows the Simulink model for a case where the system is affected by both.

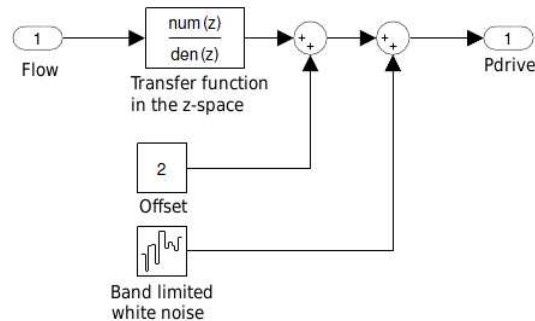


Figure 2-5: Simulink model of a system affected by offset and noise.

The input is the flow; the output is the driving pressure (Pdrive). In this simplified model only the output is affected by offset and noise.

The input flows to simulate spontaneous breathing with and without ASB had amplitudes in the range of -1 to 1 l/s and an approximated duration of 5 seconds per cycle (these values were selected because they resembled the explorative data). The offset was set to 2 mbar and the noise was band limited white noise [42]. Both disturbances are added to the system directly before the output. The data generated can be evaluated according to the methods introduced in 2.1 to test the suitability of the algorithms.

2.2.2 Simulations with the lung simulator LS4000

After testing the algorithms real signals were used to investigate their behaviour in real conditions. In this part, the signals were not simulated in the computer, but produced by a mechanical model, measured by real sensors and acquired in a real measurement system. This is an important step before acquiring data from a human respiratory system because possible measurement errors and safety risks can be identified and eliminated. Moreover, the real influence of noise and offsets can be examined.

Active lung simulators play a role for the investigation on methods to determine lung mechanics in non-sedated patients because they can reproduce the pressure generated by the respiratory muscles during spontaneous breathing (passive simulators can not). This permits to test safely software and hardware in a real environment previous to clinical research. For this work the active simulator LS4000 (Dräger, Lübeck, Germany) was updated to be controlled by software and used to generate simulated data.

2.2.2.1 The active lung simulator

The mechanical part of the LS4000 shown in Figure 2-6 is a voltage controlled piston which moves back and forth producing a pressure which resembles the muscular inspiratory force and is applied over the attached mechanical elements representing the respiratory resistance and compliance.

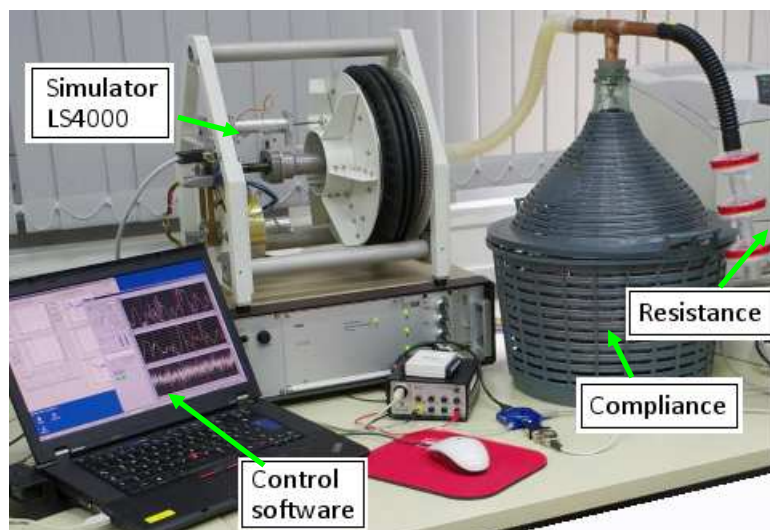


Figure 2-6: Simulation setup with the active lung simulator. It is controlled by software to produce pressure and flow over the mechanical elements representing resistance and compliance.

The resistances were made of a series of bacterial filters (Barr Vent, B+P Beatmungsprodukte GmbH, Neunkirchen-Seelscheid, Germany) to obtain values between 2.5 and 5 mbar/l/s. Two glass bottles were used to simulate compliances of 25 and 50 ml/mbar. Connecting their openings in parallel builds a compliance of approximately 75 ml/mbar. These values give a wide range of the parameters that can be measured in adult patients.

The voltage levels required to make the LS4000 produce a determined pressure over R and C are calculated by dedicated software according to the inputs from the user interface and transmitted to the simulator through a data acquisition card USB-6009 (National

Instruments Germany GmbH, München, Germany) via USB. The simulator is connected to a computer and a ventilator as the scheme in Figure 2-7 shows.

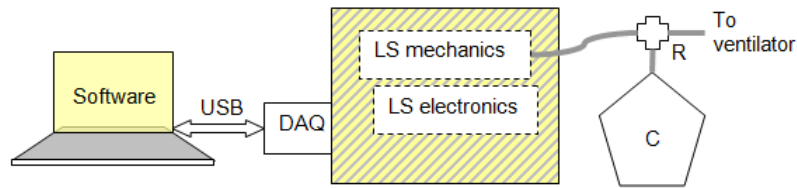


Figure 2-7: Scheme of the simulation setup.

The simulator (LS) is connected to a ventilator and via USB to a computer with dedicated software.

2.2.2.2 Resistance and compliance

The pressure changes measured when putting a series of constant flows through the resistive parts, or a series of additional volumes into the compliant elements respectively, delivered the characteristic curves to determine their resistances and compliances. Depending on the amount of disposable bacterial filters attached in series, the values available for simulation were ~ 2.5 mbar/l/s (2 filters) and ~ 5.0 mbar/l/s (4 filters). These values were determined with a flow generator (F.A.T. GmbH & Co. KG, Lüdenscheid, Germany) for flows between 5 and 80 l/min. The pressure-volume relationships revealed the compliances of the bottles to be 25.1 and 50.5 ml/mbar.

For this work the active lung simulator LS4000 was used to generate simulations with the characteristics summarized in Table 2-1.

Case	R [mbar/l/s]	C [ml/mbar]
25--2	2.5	25
50--2	2.5	50
75--2	2.5	75
25--4	5.0	25
50--4	5.0	50
75--4	5.0	75

Table 2-1: Model parameters for simulation with the lung simulator.
R: Resistance. C: Compliance (rounded)

2.2.2.3 Software control

In each case or combination of R and C the simulator was controlled to produce defined forms of P_{mus} with three different maximum amplitudes. For this, a software program was written using LabWindows CVI to enable control of the simulator and to produce the different patterns simulating muscular pressure. Examination of real signals concluded in making the pressure wave as the sum of an exponential and a sinusoidal component. Figure 2-8 shows the user interface of the control program.

The calibration constants for the simulator are preset; the offsets are automatically measured before starting signal generation. All other parameters like amplitude and frequency of the pressure to be generated can be entered. The sends and acquires signals through a data acquisition card USB-6009. The measured signals are displayed and saved in netCDF format.

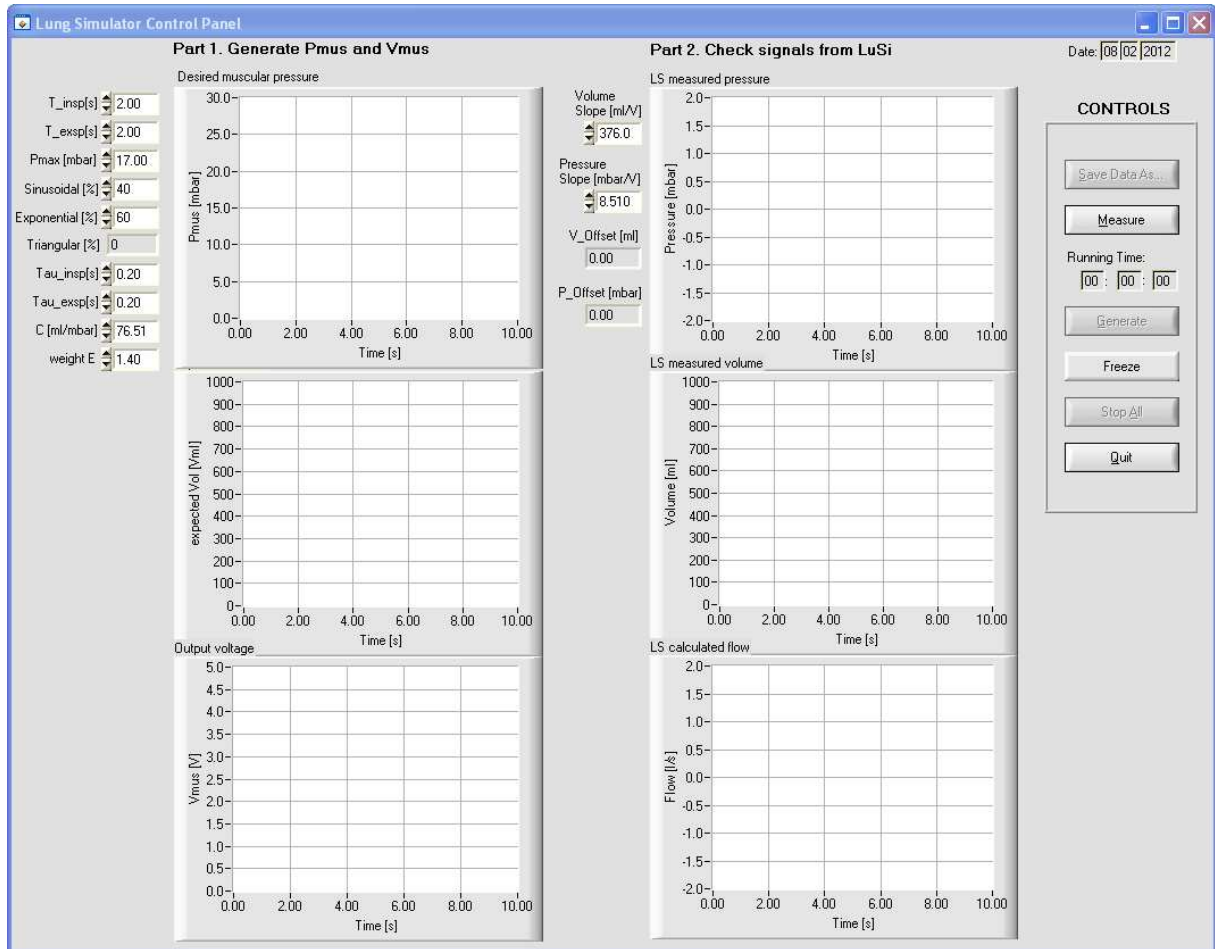


Figure 2-8: User interface of the software to control the simulator. The input fields on the left side permit to select times, form and amplitudes of the pressure wave to be generated with the simulator.

The simulations using the LS4000 were done only for spontaneous breathing. Simulations of ASB make only sense if the simulator can respond to ASB as a human would do. This was not the case, so that the simulations with the LS4000 were limited to different levels of spontaneous breathing without support.

2.3 Invasive measurement of transdiaphragmatic pressure

Whereas the simulations with the LS4000 permitted the direct pressure measurement from the model, the acquisition of data from volunteers requires the invasive measurement of transdiaphragmatic pressure, which is essential part of the reference method.

The *transdiaphragmatic pressure* (P_{di}) is calculated as the difference between the pressures in the pleura and the abdomen, whose values are estimated from oesophageal (P_{es}) and gastric pressure (P_{ga}). These measurements have been used in numerous studies to analyse lung and chest wall compliance, work of breathing, respiratory muscle function and the presence of diaphragm paralysis [7]. Because the pressures are measured immediately above and below the diaphragm, the transdiaphragmatic pressure gives a direct estimation of the muscular force required for the inspiration. A review on the historical background, techniques for placement of the sensing devices and potential clinical applications of oesophageal and gastric pressure measurements can be found in [7].

Some studies like [43], [44], [45] only use the measurement of oesophageal pressure and neglect the fluctuations of the gastric pressure. For the measurement of either oesophageal pressure alone or oesophageal and gastric pressures, balloon-tipped catheters are frequently used. Detailed explanations about this technique and alternative methods like using liquid-filled catheters or micro-transducers are available in [46]. Because of its widespread use and common safe employment, the balloon catheter technique was chosen in this work for the measurement of Pdi as described below.

2.3.1 The balloon catheter technique

For the measurement of oesophageal pressure a thin catheter with a balloon located at its end is introduced via nose or mouth until the balloon is placed in the lower third of the oesophagus [47], [48]. The catheters (see Figure 2-9) are hollow, thin (2-3mm outer diameter) and have at the upper end connections for the measurement of the pressure signal. The measurement with one single balloon catheter has been successfully used for example in [43], [44], [45].

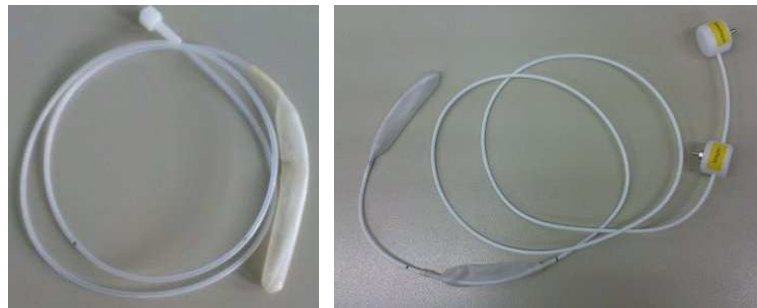


Figure 2-9: Single and double balloon catheters. Single balloon catheters (left) are used to measure oesophageal pressure. With double balloon catheters (right) the gastric pressure can be measured at the same time.

If the measurement of gastric pressure is desired as well, two single balloon catheters can be used. Figure 2-10 [49] shows how two single balloon catheters are placed in the oesophagus and the stomach to measure Pes and Pga. Pairs of single balloon catheters have been used for instance in [50], [51], [52], [53], [54].

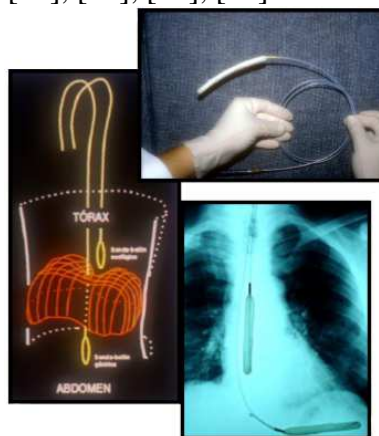


Figure 2-10: Pressure measurement with two single balloon catheters [49]

An improvement of this technique is given by the use of *double balloon catheters* (see Figure 2-9): the distance between oesophageal and gastric balloons is kept constant during the whole measurement and insertion of the catheter is required only once. This reduces

the burden on the patient. Double balloon catheters have been used previously for instance in [55]. Figure 2-11 shows schematically how the double balloon catheter is placed.

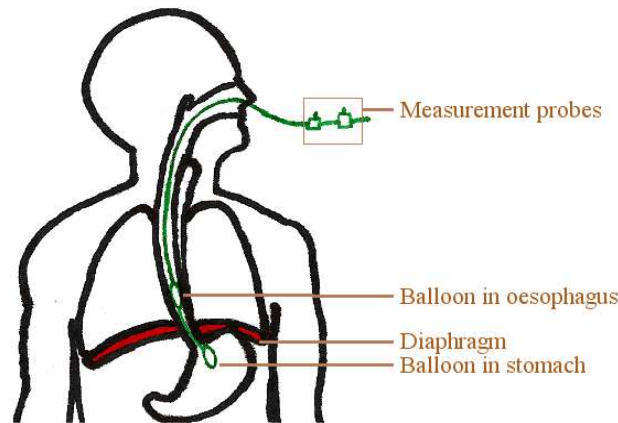


Figure 2-11: Pressure measurement with a double-balloon catheter

For the present investigation custom-made double balloon catheters (nSpire Health GmbH, Oberthulba, Germany) were used to measure both oesophageal and gastric pressures. The catheters are 100cm long and have two latex balloons, each 7cm long, separated by a distance of 10cm. Prior to insertion, a local anaesthetic (Xylocain® 2%) was sprayed into the subject's nose and throat. During the insertion cold water was given to the subject to support the placement of the catheter by swallowing. After shifting the balloons to the approximated depth to be able to reach the stomach, the upper ends of the catheter were connected to the measurement system ZAN 400 (ZAN Messgeräte GmbH, Oberthulba, Germany) and the measurement was started.

After the positioning of the catheter was completed, the balloons were inflated with 2 to 3ml of air. Since inadequate filling of the balloons may lead to wrong measurements of pressure, those volumes were determined according to the mechanical characteristics of the catheters bought; for this, the balloons were pressurized and depressurized with known pressures and the range of volumes where the measurement is correct was documented. The correct placement of the balloons was determined by a negative swing of P_{es} and a positive deflection of P_{ga} during inspiration. The proximal end of the catheter line was fixed to the cheeks to avoid displacement. For convention, the inspiratory P_{di} was considered positive. All pressures were measured in mbar.

The invasive measurement of P_{di} was part of the study with volunteers (see section 2.4), which was approved by the Committee of Ethics of the University of Lübeck (Lübeck, Germany) (Reference 11-074, date: 17th of June 2011).

2.3.2 Filtering artefacts and offset correction

A few cycles of recorded P_{di} are shown in Figure 2-12. Superimposed signals of higher frequency (around 1Hz, typical for the heart rate) can be recognized. Such components, known as *cardiogenic oscillations* [5], appear as a consequence of the physiologic proximity of the heart to the oesophagus and might cause errors in the estimation of model parameters or strongly decrease the goodness of fit between the reconstructed P_{di} and the original signal. Therefore, a filter must be used to suppress waves with frequencies around the frequency of the heart beat.

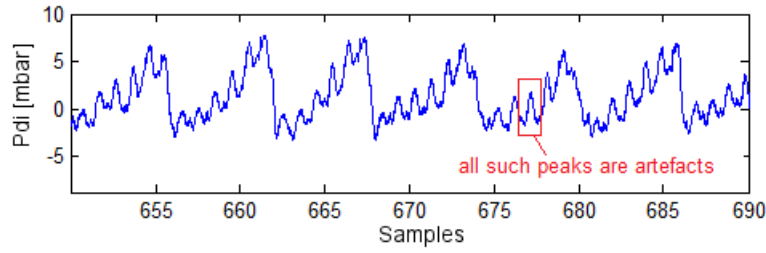


Figure 2-12: Cardiac artefacts in the measured transdiaphragmatic pressure(Pdi)

The cut-off frequencies for the filter are determined from the analysis of frequencies of the measured Pdi. An excerpt of the spectrum of a sample Pdi is shown as example in Figure 2-13. Zooming in on the values displayed permits a better visualization of the components that must be eliminated.

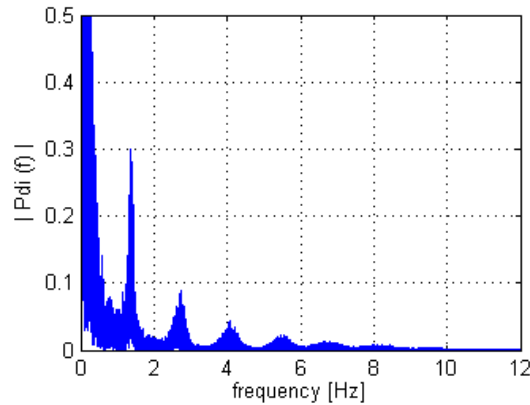


Figure 2-13: Single-sided amplitude spectrum of the measured Pdi. Signals of frequency between 1 and 2 Hz, typical for the heart rate, appear superimposed to the frequency components of the transdiaphragmatic pressure (Pdi).

To filter the undesired frequencies without losing quality in the original signal, a Butterworth high-pass filter and a Butterworth low-pass filter, both of fifth order, were combined to build a band-rejection filter to safely eliminate the components with frequencies between 0.8 and 8 Hz. The filter was implemented with the functions *butter* and *filtfilt* of MATLAB. Using the order n and cut-off frequency ω_n , the function *butter* obtains the coefficients b and a of the transfer function

$$F(z) = \frac{b_1 + b_2 z^{-1} + \dots + b_{n+1} z^{-n}}{1 + a_2 z^{-1} + \dots + a_{n+1} z^{-n}} \quad (\text{Eq. 2.11})$$

Once the transfer functions are defined, the signal is filtered using the function *filtfilt* with the parameters for low and high pass. The resulting signals are added to obtain Pdi after band-rejection. An important characteristic of the function *filtfilt* is that the signal is filtered in the forward and reverse directions, producing zero-phase distortion and actually using a filter order that is double the order of the filter specified by b and a .

Similarly, the involuntary action of neighbouring smooth muscles (peristalsis) influences the measured pressures causing a slow variation of the offset in Pdi. Assuming full relaxation of the muscles at the end of the expiration, the offset can be defined as the average of the initial values in each breathing cycle, but was rather determined, considering its variability, as the baseline connecting the minima of filtered Pdi in consecutive cycles.

An important requirement, before establishing the varying offset of Pdi and using the signal to calculate PTP_{insp} and the model parameters, is the opportune recognition and exclusion of cycles with abnormal Pdi, i.e. with Pdi signals that do not belong to quiet or assisted spontaneous breathing, but rather to coughs, sighs, speaking, etc. This is done by testing the Pdi of each cycle already during the measurement, against a series of conditions described mathematically. Details are given in 2.5.1.

2.4 Study with volunteers

After the validation with simulations, a study with test persons followed. The goal of the study was the analysis of the proposed novel method for assessment of respiratory mechanics in a group of healthy subjects with expectedly different respiratory mechanics. For this, the study included a group of long-time smokers and a group of non-smokers. This section describes the study.

In order to test the method the study included 25 healthy adults with normal respiratory systems. For all examinations the commercial ventilator Evita4 (Dräger, Lübeck, Germany) was used. In order to obtain enough usable values, direct testing with humans (instead of animals, which could not be examined without sedation) was necessary. This study was designed to test the reliability of the assessment of the activity of the respiratory muscles and of the respiratory resistance and compliance, gained through the proposed novel method. The activity of the respiratory muscles varies however between subjects and in the time, depending on the ventilatory requirements. It must be examined therefore, if such variations are opportunely recognized.

The study was approved by the Committee of Ethics of the University of Lübeck (Lübeck, Germany) and informed written consent was obtained from the volunteers prior to their inclusion in the study. The study was covered by an insurance for clinical studies done by universities (company: Allianz AS, insurance number 9100160845).

2.4.1 Study design

For the acquisition of respiratory signals, the test subjects breathed spontaneously with and without support from the ventilator in ASB mode. In addition, the dead-space³ was increased for a short time to augment the respiratory demand. The test subjects were informed in each phase about the procedure and were asked to evaluate subjectively their current breathing effort. A poster was displayed during all examinations, such that all participants had a clear overview on the procedure step by step. The poster and the letter from the committee of ethics can be found in [Annex A1](#) and [Annex A2](#). All test subjects were interviewed and examined before the measurement to discard any source of increased risk. Particularly the heart and lung function as well as the state of mouth and oro-pharynx were examined.

Following criteria was used for the selection of the test subjects:

Group 1: Non-smokers between 18 and 40 years old

Group 2: Smokers between 30 and 70 years old, having smoked regularly for at least 10 years

³ volume of air that is not used for gas exchange

The criteria for exclusion from the study included: allergy to local anaesthesia, disease or malformation of the airways, lung, thorax or abdomen, regular intake of medication, pregnancy, sleep apnoea syndrome, allergy to latex and problems with swallowing. Only subjects with physical status class 1 of the American Society of Anaesthesiologists, i.e. normal healthy, participated in the study. Data from 10 smokers and 15 non-smokers, all men, was used for the validation. Both groups were required to avoid drinking and eating during four to six hours before starting the measurement.

2.4.2 Validation setup

The assessment of lung mechanics requires measurement of flow and pressure. Figure 2-14 displays the validation setup used in this study, which is composed of several devices used to get the relevant signals. In this graphic a person is connected via facemask to the system, but a mechanical simulator can be connected instead.

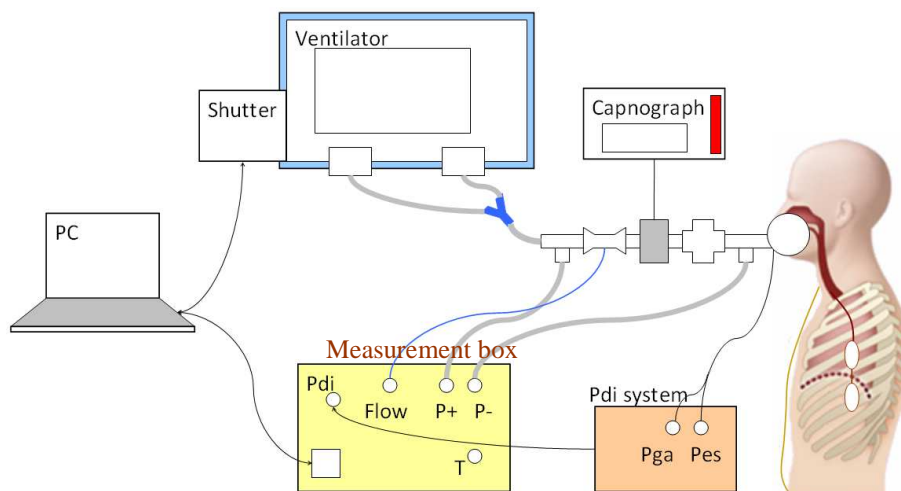


Figure 2-14: Validation setup

Pdi: transdiaphragmatic pressure. Pga: gastric pressure. Pes: oesophageal pressure. P+, P-: differential pressure. T: Temperature.

This section describes the components of the validation setup and their functions.

- a) PC: Dedicated software (see [Annex B](#)) controls the shutter to close the expiratory valve of the ventilator triggering the occlusions required for the method when desired. It also receives the signals read by the data acquisition card (DAQ) (USB-6009, National Instruments Germany GmbH, München, Germany) of the measurement box.
- b) Ventilator: A commercial intensive care ventilator (Evita4, Dräger, Lübeck, Germany) was used to monitor the respiratory signals of the subjects and partially to give support under CPAP or ASB mode. The setup was however designed independently of the ventilator, giving the possibility to use any other device. Disposable CPAP masks (B+P Beatmungsprodukte GmbH, Neunkirchen-Seelscheid, Germany) connected the volunteers to the Evita4. The figure below shows the ventilator with the shutter (small black box) attached to it.



Figure 2-15: Evita4 and shutter, front side and back side

- c) Capnograph: During the study with volunteers the levels of carbon dioxide (CO_2) and arterial oxygen saturation (SpO_2) were supervised using a mainstream capnograph (CO_2SMO^+ , Novamatrix medical systems Inc., Wallingford, CT USA) calibrated according to the steps described by the manufacturer. The device and its sensors are shown below.



Figure 2-16: Capnograph and sensors of CO_2 and SpO_2

- d) Flow sensor: A hot-wire anemometer (Spirolog, Dräger, Lübeck, Germany) was used to measure flow. The recognition of flow direction was done in the measurement box (see item i)) by measuring differential pressure over the row of sensors.
- e) Sensors: Several sensors were placed close to the mouth and nose of the test subject (or the distal tube of the simulator). The next figure shows the row of sensors and connectors: 1) connection port to the ventilator with luer-lock opening for differential pressure measurement, 2) flow sensor with cable, 3) CO_2 sensor with cable, 4) disposable bacterial filter (B+P Beatmungsprodukte GmbH, Neunkirchen-Seelscheid, Germany) and 5) connection port to mask with luer-lock opening for airway pressure measurement.

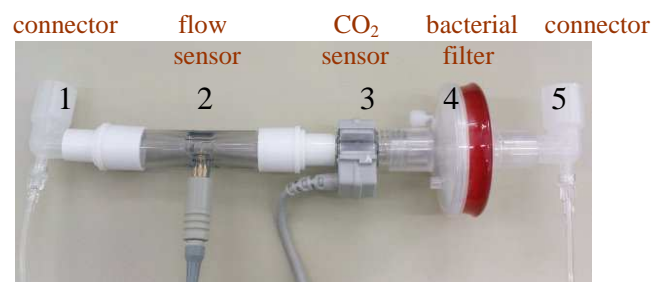


Figure 2-17: Sensing system to be connected between the mask and the ventilator.

- f) Balloon catheter: The oesophageal and gastric pressures were measured as described in 2.3.1 using double-balloon catheters (nSpire Health GmbH, Oberhulba, Germany).



Figure 2-18: Double-balloon catheter for invasive measurement of oesophageal and gastric pressures. (This measurement is only for reference).

- g) Pdi measurement system: The pressures acquired with the balloon-catheter were measured by pressure sensors in the ZAN400 TDP (nSpire Health GmbH, Oberhulba, Germany).



Figure 2-19: Device for measurement of oesophageal and gastric pressure

- h) The shutter

The shutter constitutes a fundamental part of this work because it produces the occlusions needed for the designed method. It was implemented using the electrical control lines of an Evita4 ventilator. According to a digital signal sent from the computer, the shutter closes the expiratory valve of the Evita4 during approximately 200ms. Over the dedicated software one can decide how often the occlusions occur; as default each 5 breathing cycles. Figure 2-20 shows the shutter (black box on the right side) with its red-black cable connected to the backside of the Evita4. Further details on the shutter can be found in [Annex C](#).

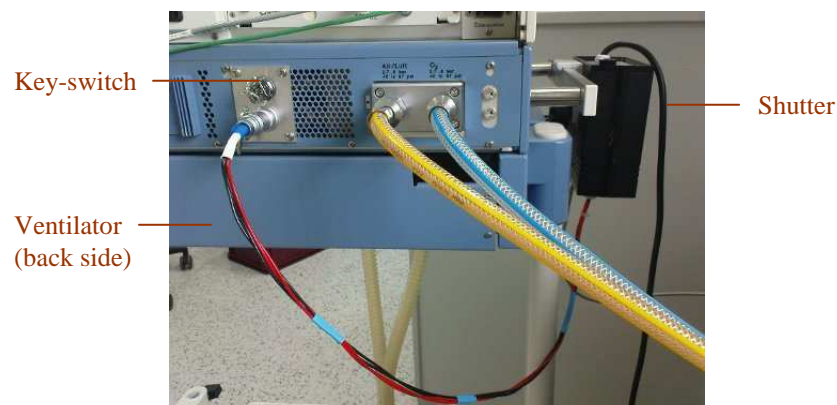


Figure 2-20: Interface shutter-ventilator

i) The measurement box

In order to have a system that is independent of the ventilator used, a device capable of receiving and transmitting the measured signals was constructed for the validation setup.

The measurement box (see Figure 2-21) is composed by four parts: 1) the flow signal is sent to a processor for flow measurement (LP-Flow, Dräger, Lübeck, Germany), 2) the differential, airway and barometric pressures are measured by miniaturized pressure transducers (HCE series, Sensortechnics GmbH, Puchheim, Germany), 3) a precision sensor (LM35, National Semiconductors) measures the ambient temperature, and 4) all measured signals are read by a DAQ USB-6009 with a sampling rate of 200Hz and transmitted to the computer for data analysis. A second power supply SNP-Z061 energizes the boards of the box.



Figure 2-21: Measurement box

With inputs for the acquisition of transdiaphragmatic pressure (Pdi), flow, airway pressure (Paw), differential pressure (P+, P-) and temperature (Temp).

2.4.3 Methodology

a) Preparation

The volunteer sits on a chair with approximately 45 degrees of inclination. Pulse-oxymetry, electrocardiographic signals and non-invasive blood pressure are measured with a clinical monitor (S5, Datex-Ohmeda GmbH, Freiburg im Breisgau, Germany) and a winged infusion set is placed as precaution. Topic anaesthesia is applied to the nose and the epilarynx. The balloon-tipped catheter is then prepared for insertion through the nose. After passing the nares, the catheter is shifted through the oesophagus down to the stomach. By continuous swallowing while drinking cold water the volunteer facilitates the insertion of the catheter. Once the catheter has reached the approximated deep, the measurement of pressure is started. Correct positioning is confirmed by negative deflections in the measured oesophageal pressure and positive deflections in the gastric pressure during the inspiration. If positioning is not correct, the catheter must be carefully pulled or pushed. After proper positioning of the balloons, the proximal end of the catheter is fixed with skin-friendly tape to the cheeks and the test subject is connected to the validation setup through a nose-mouth mask.

The communication is done by signs, because the subject cannot speak when using the mask. Moving the left foot means that there is some problem; moving the right foot indicates that everything goes well. The mask can be removed anytime if necessary. After a short period of habituation to the mask and to the situation, the measurement is started. In the single examination phases the subject is asked to evaluate his inspiratory effort in a

scale between 0 and 10, where 0 means no effort and 10 means maximum stress. The subject answers with his fingers. This is done as part of the monitoring.



Figure 2-22: Setup in the study with volunteers

b) Examination phases

The examination was divided in seven phases planned as described below:

- Phase 1: habituation. In this phase the volunteer can habituate to breath with the mask and the ventilator set to CPAP or ASB mode and a small positive pressure (PEEP between 0 and 5mbar). In order to overcome the additional resistance from the devices, the support can be adjusted in such way that the persons can breath as usual. A maximum pressure of 15mbar can be given. This value depends on the test person. Phase 1 takes about 3 minutes.
- Phase 2: spontaneous breathing. In this phase normal breathing cycles are recorded. This phase takes around 10 minutes.
- Phase 3: phase change and habituation. The work of breathing is increased by removing assistance (ASB is set to 0mbar) and adding a row of up to six bacterial filters increasing the dead space between the sensors and the ventilator. Phase 3 takes about 3 minutes.
- Phase 4: spontaneous breathing with increased work of breathing. In this phase, breathing cycles requiring more effort than in phase 1 are recorded. This phase lasts around 10 minutes. If the effort becomes too high for the volunteer, it can be shortened.
- Phase 5: phase change and habituation. The work of breathing is reduced by removing all additional filters and giving high positive pressure support (ASB is set to 10 to 15mbar). This value depends on the subject. Phase 5 takes about 3 minutes.
- Phase 6: spontaneous breathing with reduced work of breathing through ventilatory support by ASB. In this phase breathing cycles requiring minimum effort are recorded. This phase takes around 10 minutes. If the assistance is too high for the volunteer, the support level can be lowered or the phase can be shortened.
- Phase 7: normalization. In the last phase the subject breaths in the same conditions as in phase 1 during about 3 minutes.

Pressures, flow and partial pressure of CO₂ are supervised, acquired and recorded during each phase. Every 3 to 7 breaths an occlusion is started by the software and the novel method is applied to determine the respiratory parameters. After phase 7 the mask is

removed. The examination including preparation and the seven phases takes about 90 minutes. The following table gives an overview on the timing for the different phases.

Min. after start →	3	6	9	12	15	18	21	24	27	30	33	36	39
Phase 1	■												
Phase 2		■	■	■	■								
Phase 3					■	■	■	■					
Phase 4						■	■	■	■	■			
Phase 5									■	■	■	■	
Phase 6										■	■	■	■
Phase 7													■

Table 2-2: Timing for the examination phases

During the examination following variables are directly measured:

- Flow
- Airway pressure
- Oesophageal pressure and gastric pressure

Following variables are derived from the previous ones:

- Transdiaphragmatic pressure
- Tidal volume, inspiratory and expiratory times, cycle time and frequency
- Pressure time product from transdiaphragmatic pressure

And following variables are measured for supervision:

- Heart rate
- Non invasive blood pressure
- Arterial oxygen saturation (SpO₂)
- Expiratory partial pressure of carbon dioxide (CO₂)

For the measurement of the first group of variables the sensors of the validation setup (see 2.4.2) were used. The calculation of the second group of variables was done by the dedicated software (see [Annex B](#)) during the measurement. The last group of variables was measured with the clinical monitor and the capnometer. The subjective opinion of the volunteer about the assistance was documented too.

c) End of the examination

After finishing the data acquisition, the balloon catheter is carefully removed. The volunteer is asked to describe any problem or discomfort that could arise from the examination. After checking that breathing and swallowing continue to be normal, the examination is finished.

2.4.4 Safety

Any of the following criteria leads to the termination of the examination:

- Decision of the volunteer or the supervising physician
- Dyspnoe or thoracic pain
- Cardiac dysrhythmia
- Heart frequency under 50/min or over 110/min
- Systolic pressure under 80 mbar or over 160 mbar
- Other unwanted events

For any incident safety arrangements were defined.

2.5 Evaluation of results

As seen before, the correct implementation of the algorithms for the identification of the model parameters was evaluated with computer simulations done in the software Simulink, data collected from a lung simulator and data from healthy volunteers and patients. In all cases, at least three signals were required: flow, airway- and transdiaphragmatic pressure (as control).

2.5.1 Abnormal signals and outlying estimates

Once respiratory signals were acquired and saved, the usability and quality of the recordings had to be evaluated. High levels of noise, for example, diminish the quality of the signals and produce problems in their application. Especially difficult is the measurement of Pdi, due to the challenge of finding the correct position of the balloon-catheter, but also due to the superposition of cardiac pressure waves or muscular activity that does not belong to quiet breathing, for example during coughs, sighs or peristaltic movements. Therefore, it was necessary to establish rules to define what normal Pdi (in the sense of pertinent to quiet breathing cycles) should look like.

Signs of abnormal Pdi are extreme differences ($>15\text{mbar}$) between its minima in inspiration and expiration, pressures being higher in the expiration than in the inspiration or a pressure decrease already at the start of the inspiration. These conditions may not apply during ASB.

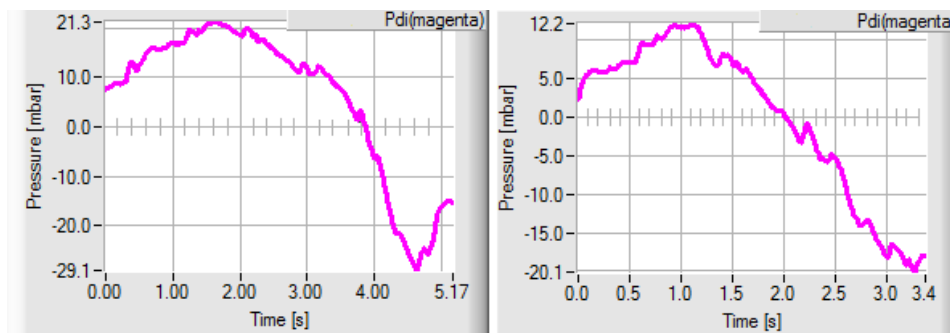


Figure 2-23: Two examples of abnormal Pdi
Extreme differences between the minima in inspiration and expiration are signs of a Pdi signal abnormal for quiet breathing.

Unwanted signals can also appear in flow (V') or airway pressure (P_{aw}), for example when the volunteer swallows or coughs. Examples of these are shown in Figure 2-24. Through the separation of flow in inspiration and expiration, most interruptions to the normal cycle can be recognized.

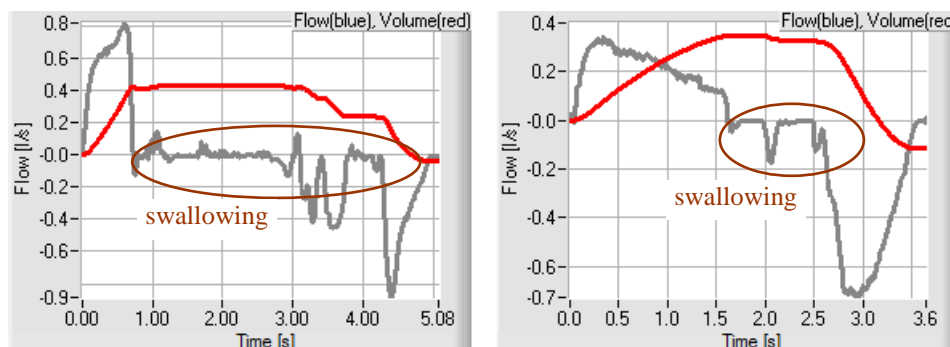


Figure 2-24: Examples of disturbances in flow due to swallowing

Any abnormal signals should be discarded before the determination of the model parameters. However, remaining erroneous signals may still enter into the least squares fitting to find R and C. For such cases a range of normal (in the sense of physiologic) values was established as 1 to 30 mbar/l/s for R and 10 to 200 ml/mbar for C. Only cycles with values inside these ranges were used to reconstruct the muscular pressure.

Once the variables of each simulation or each test subject were measured and recorded, the quality of the measurements and records was compared according to: the number of cycles with abnormal Pdi, the number of cycles with R and C inside the physiological range or respectively the amount of outliers in R and C, and the number of occluded cycles effectively recognized as such.

2.5.2 Statistics

Agreement between methods was evaluated by comparing their pressure-time product (PTP_{insp}) values with linear regression, correlation and Bland-Altman analysis. The 3 levels of effort, i.e. the phases, were compared by one-way ANOVA and post-tests of their PTP_{insp} values per case or subject (given that there are more than 30 values per phase), or their mean values for overall evaluation. The statistical methods used in this work are described in the following paragraphs.

- Mean, standard deviation and relative error

Each non-occluded cycle described by normal signals of quiet breathing can be used to obtain the model parameters by MLR. Each occluded cycle can be used to obtain the model parameters by the novel method. After using the fitting algorithms to find the parameters R and C, several values of them may be available at any time of a measurement and are summarized by their *mean and standard deviation*. In the simulations the calculation of absolute and *relative errors* is possible because the values of the real (measured directly in the simulation setup) parameters are known.

- Linear regression analysis and Correlation

Linear regression analysis is used to investigate the relationship between two variables X and Y. Assuming a linear relationship, linear regression finds the best line $y = mx + b$ with slope m and intercept b , that predicts Y from X by minimizing the sum of the squares of the vertical distances of the points from the regression line [56]. In this work linear regression was used to analyze the relationships between the PTP_{insp} values calculated from the measured Pdi (PTP_{Pdi}), from the reconstruction of Pdi using the parameters obtained from MLR (PTP_{MLR}) and from the reconstruction using the parameters obtained by the novel method (PTP_{O+D}).

The Pearson product-moment *correlation coefficient* r quantifies the direction and magnitude of the joint variation of the two variables X and Y. Its value ranges from -1 to 1: r is 0 if there is no correlation, 1 if the correlation is perfect and -1 if the correlation is perfect and inverse. An r between -1 and 0 indicates converse directions of the variation; r between 0 and 1 indicates the same direction of the variation. Correlation is appropriate to analyse data if X and Y are measured independently, if the X values are not controlled but measured and if the covariation is linear (for example if X only increases Y only increases too).

The squared value of r is the *coefficient of determination* R^2 , which represents the fraction of the variance in the two variables X and Y that is shared [56]. The value of R^2 varies between 0, which means no relation between the data, and 1, which reflects a perfect match. R^2 can be also used as a measurement of goodness of fit, which expresses the fraction of variation in the data accounted for by the model according to

$$R^2 = 1 - \frac{S}{\sum_{i=1} (P_i - \bar{P})^2} \quad (\text{Eq. 2.12})$$

where S is the sum of the squared residuals and \bar{P} is the mean value of the measured pressure signal [5]. In this investigation R^2 was principally used to express the shared variance of the PTPinsp values from two different methods.

○ Bland-Altman analysis

Bland-Altman analysis is a modern effective method to measure agreement between methods. It consists on two steps: a) plotting the differences between two variables (one from each method) against its means and b) estimating confidence intervals for the limits of agreement. The results are summarised into the mean difference \bar{d} and the standard deviation of the differences sd . The limits of agreement are defined as $\bar{d} - 2sd$ and $\bar{d} + 2sd$. The 95% confidence intervals go from $\bar{x} - tSE$ to $\bar{x} + tSE$ where \bar{x} takes the value of \bar{d} or the desired limit, t is the critical t-value of a distribution with $n-1$ degrees of freedom and n the number of samples, and SE is the standard error of the selected limit. This analysis is particularly useful when correlation analysis is misleading [57], [58].

In cases where the differences vary systematically over the range of measurement, for example if the scatter of the differences increases as the mean increases, the previous limits of agreement may be inappropriate, because they would be too large for small means and too narrow for large means. If the differences are proportional to the mean, logarithmic transformation can be used [57], [59], [60]. Additional considerations include the use of multiple observations per individual [61] where a correction of the sd may be appropriate. Bland-Altman analysis was used in this work to measure the agreement between the invasive and non-invasive methods to assess PTPinsp.

○ T-test and ANOVA

The t-test proofs the null hypothesis H_0 that the mean values μ_x and μ_y of two populations are equal, against the alternative hypothesis that one mean is smaller than the other. The null hypothesis of a *two-tailed t-test* can be rejected if the absolute value of the *t-statistic* is lower than or equal to the *critical-t*. The calculation of the t-statistic depends on the sample sizes, the sample means and the variances of the populations. The critical-t is obtained according to the significance level p and the number of degrees of freedom.

There are t-tests for independent samples and t-tests for dependent samples. In this work the values of the respiratory parameters from smokers and non-smokers are clearly independent. Similarly, the mean PTPinsp values of different phases are independent from each other. In its simplest form the ANOVA test proofs whether or not the means of several groups are all equal and constitutes a generalization of the t-test if comparison of more than two groups is required. One-way ANOVA and the Bonferroni post-test with $n > 30$ and $p = 0.05$ were used to compare the PTPinsp values of the 3 recorded phases.

3 Results

For the verification of the *Occlusion+Delta* (O+D) method its results were compared to those obtained through the invasive measurement of transdiaphragmatic pressure (Pdi) and multiple linear regression (MLR). The evaluated data⁴ was gained from 6 simulations with the lung simulator LS4000 and from 25 measurements with healthy volunteers. The results are organised in this chapter as the table below shows. Additionally, a summary of the main results can be found in 3.4.

	Results from the reference method	Results from the O+D method	Comparison and validation
Introduction	3.1	3.2	3.3
Simulations with the LS4000	3.1.1	3.2.1	3.3.1
Study with volunteers	3.1.2	3.2.2	3.3.2

Table 3-1: Overview of the chapter Results.
The numerals indicate the section number.

According to the goals set for this work, this chapter presents the results for the single studied cases and from overall analysis, to determine:

- To which extent the results (R, C and PTP_{insp}) obtained by the non-invasive and by the invasive methods agree
- Whether there are significant differences between the examined phases

Most of the plots shown in this chapter serve as example of the results; these and all other plots can be found in the attached CD. An overview of the contents is given in [Annex D](#). The following abbreviations are used in the tables:

Abbreviations and titles used in the tables:	
nr. Occls	Amount of occlusions
Rfit, Cfit	R and C obtained from multiple linear regression with Pdi
Rocc, Cocc	R and C obtained with the non-invasive O+D method
Rcurr, Ccurr	Gliding (current) average of the last 10 Rocc and Cocc; these values are used to calculate the estimation of muscular pressure
nPdi	Amount of cycles with normal Pdi, undisturbed flow and airway pressure and values of R and C inside the physiological range ($1 < R < 30$ mbar/l/s; $10 < C < 200$ ml/mbar)
m, b	Coefficients of the regression line of PTP _{Pdi} and PTP _{O+D}
R ²	Coefficient of determination
BA	Bland-Altman analysis - mean: mean difference - sd: standard deviation of the differences
outl.	Amount of outliers in the differences of PTP _{insp}
PTP _{insp}	inspiratory Pressure Time Product
PTP _{Pdi}	PTP _{insp} calculated from the invasively measured Pdi
PTP _{O+D}	PTP _{insp} calculated with the non-invasive O+D method

Table 3-2: Abbreviations used in the tables of results

⁴ The computer simulations just confirmed the successful performance of the model and the algorithms. The detailed results can be found in the diploma theses of E. Rother [42] and M. Strutz [62].

○ Basic data for the simulations

The lung simulator LS4000 was used to simulate 6 combinations of R and C and to produce signals of flow and pressure that represent spontaneous breathing with a cycling frequency of 4 seconds and 3 levels of simulated muscular pressure. The ventilator was set to CPAP mode with PEEP= 2mbar; the occlusions were executed each third cycle. Table 3-3 shows the list of simulated cases and their parameters.

Case	25--2	25--4	50--2	50--4	75--2	75--4
Resistance [mbar/l/s]	2.5	5	2.5	5	2.5	5
Compliance [ml/mbar]	25	25	50	50	75	75

Table 3-3: Cases simulated for the validation of O+D

○ Demographic data of the volunteers

A total of 30 volunteers participated in the study. The first 2 measurements (subject 1 and 2) served as general test and there were 3 cases (subject 17, 18 and 30) where adequate measurement of Pdi was not feasible. Thus, the data for study involved 25 healthy men, including 10 smokers and 15 non-smokers, breathing spontaneously in 3 phases: quiet normal breathing (phase 1), breathing with augmented dead-space (phase 2) and breathing with assistance (phase 3). Note that the setup changes deliberately in phase 2 by the presence of a row of six bacterial filters between the ventilator and the sensors and in phase 3 through the action of the Evita4 set to ASB mode.

Table 3-4 shows the demographic data of the participants of the study. The parameter *pack-year* is commonly specified for the smokers and is calculated as the product of packs of cigarettes smoked per day and the amount of years as a smoker. A comparison of R and C between smokers and non-smokers can be found in [Annex E](#).

Non-smokers n=15			Smokers n=10			
Nr.	Pseudonym	Age	Nr.	Pseudonym	Age	Pack-year
4	n25dg	25	3	r45lr	45	4.5
5	n28gd	28	9	r46cl	46	25
6	n24wb	24	10	r68js	68	4.5
7	n21tj	21	13	r32rd	32	33
8	n24sw	24	20	r46jf	46	12.5
11	n24as	24	22	r41tr	41	22
12	n21jt	21	24	r32sb	32	18
14	n26es	26	26	r59do	59	21
15	n19kb	19	27	r48rb	48	39
16	n27jn	27	28	r49vg	49	16
19	n19dr	19		mean	46.6	19.6
21	n19fr	19		sd	10.4	10.6
23	n33aa	22				
25	n23ks	23				
29	n34ag	34				
	mean	23.7				
	sd	3.9				

Table 3-4: Demographic data of the participants of the study

3.1 Results from the invasive reference method

This section presents the results from the reference method, which requires knowledge of Pdi in combination with MLR. In the initial part Pdi was simulated, whereas in the study with volunteers invasive measurement of transdiaphragmatic pressure was required, so that the results also refer to the invasively acquired signals.

3.1.1 Simulations with the lung simulator

3.1.1.1 Results per simulation case

Each simulated breathing cycle was entered to an MLR to obtain Rfit and Cfit. Their means and standard deviations are shown in Table 3-5. The column nPdi indicates the amount of cycles used to get the parameters.

Case	Rfit [mbar/l/s]		Cfit [ml/mbar]		nPdi
	mean	sd	mean	sd	
25—2	1.92	0.55	23.9	0.5	98
25—4	4.82	0.45	24.6	0.32	97
50—2	1.92	0.27	49.5	0.82	98
50—4	5.04	0.26	48.6	0.67	97
75—2	2.05	0.12	73.7	0.58	97
75—4	4.71	0.17	71.1	0.91	97

Table 3-5: R and C from the simulated cases by the control method.

Rfit: Resistance. Cfit: Compliance. sd: standard deviation. nPdi: number of cycles.

3.1.1.2 Analysis of phases per case

During the simulation of each case 3 maximum values of simulated muscular pressure were set to represent 3 levels of effort during spontaneous breathing. The efficacy of such design was confirmed by comparison of the PTP_{insp} values simulated during the different phases. According to the analysis of variance, the mean PTP_{insp} values from the simulated Pdi (PTP_{Pdi}) were significantly different ($p < 0.05$) between all phases in all simulated cases. As expected for the simulator, there were no considerable differences in Rfit or Cfit between phases. Their means and standard deviations calculated for each phase separately are listed in [Annex F](#), Table F-1.

3.1.2 Results of the study with volunteers

The acquisition and analysis of real signals required special considerations. Particularly the invasive measurement of Pdi required thorough preparation for the correct utilisation of the validation setup and the interpretation of data. The results follow.

3.1.2.1 Preparation and pre-processing of data

- Characterisation of the balloon catheters

To confirm the adequate measurement of pressure, the balloons of the acquired catheters were placed under water. A constant PEEP was applied and the pressure on the balloons was recorded. The balloons were filled each with 1 to 4ml of air. Table 3-6 shows the pressures in mbar measured by each balloon according to their filling volume. Clearly the balloons need 2 to 3ml of air to give a correct measurement of pressure.

PEEP	1ml		2ml		3ml		4ml	
	Pes	Pga	Pes	Pga	Pes	Pga	Pes	Pga
0	-4.5	-1.8	-0.5	-0.5	0.5	0	14.3	12.5
5	0	3	3.8	3.9	4.8	4.5	16	14.6
10	3.5	7.5	8.9	8.9	9.8	9.5	18.3	16.8
15	8.3	12.5	13.5	13.8	14.5	14.3	20.5	19.3
20	12.5	17	18.5	18.7	19.3	19	23.2	22
25	16.7	21.8	23.3	23.5	24	23.8	26.3	25.2
30	20.5	26	28	28.2	28.7	28.3	30.5	29

Legend:
 Error >3mbar
 Error 2-3mbar

Table 3-6: Characterisation of the balloon catheters

o Invasive measurement of Pdi

Correct placement of the balloons in the lower third of the oesophagus and in the stomach was confirmed by negative swings of oesophageal pressure (Pes) and positive swings of gastric pressure (Pga) during the inspiration. This method worked successfully as the following figure shows.

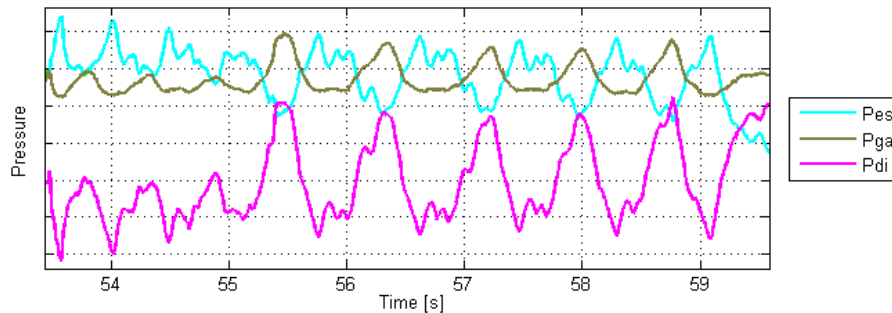


Figure 3-1: Pressure signals for placement of the balloon-catheters (example excerpt of measurement with subject 6).

o Effort levels

Setting three levels of effort was possible and is visible in the amplitudes of the measured pressures as well as in the values of PTP_{insp} for 21 out of 25 subjects. In 4 cases (10, 12, 16, 21) the separation of phases was not that clear. Figure 3-2 shows an example of the measured Pes, Pga and Pdi from three cycles measured in each of the three phases. Note that this cycles correspond to the same subject but the baselines of the signals differ between cycles.

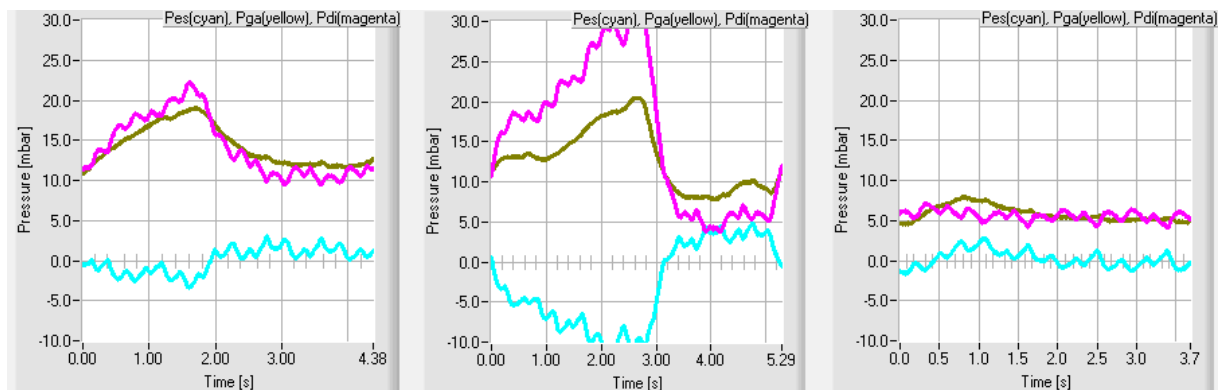


Figure 3-2: Examples of Pes, Pga and Pdi in the different levels of effort

○ Filtering cardiogenic oscillations

Heart artefacts were filtered as described in 2.3.2. The frequencies in the stop-band (0.8 to 8 Hz) were adequate for all subjects. This is confirmed by the frequency analysis of their Pdi signals. The natural differences between subjects are also reflected by the frequency analysis of their Pdi. The next figure shows some excerpts of the analysis of the frequencies to be filtered. The axis have been limited for better visualisation.

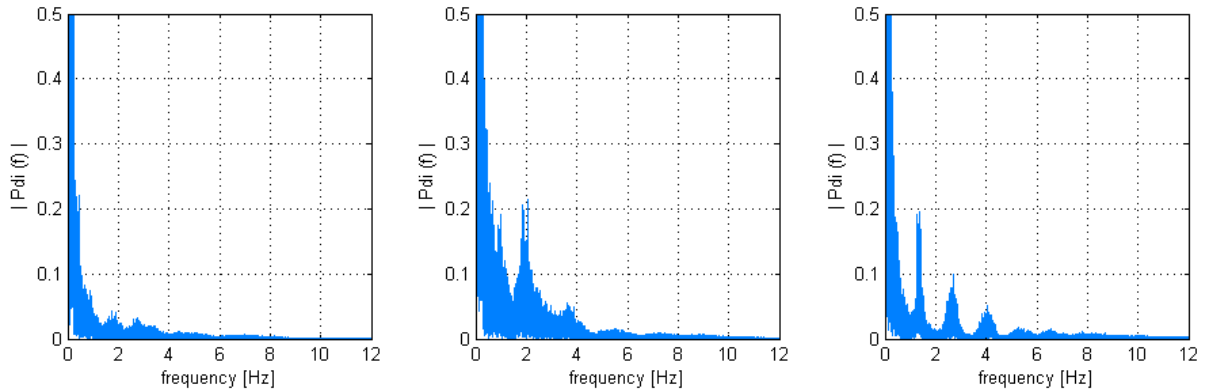


Figure 3-3: Analysis of frequencies of Pdi of three different subjects

Even if the signals with frequencies in the stop band coincide with the heart rate, it cannot be excluded that other sources interact here. In the present work this can be disregarded because the respiratory system is being modelled by a simple RC compartment. An example of the successful filtration of the desired frequencies is shown in the next figure.

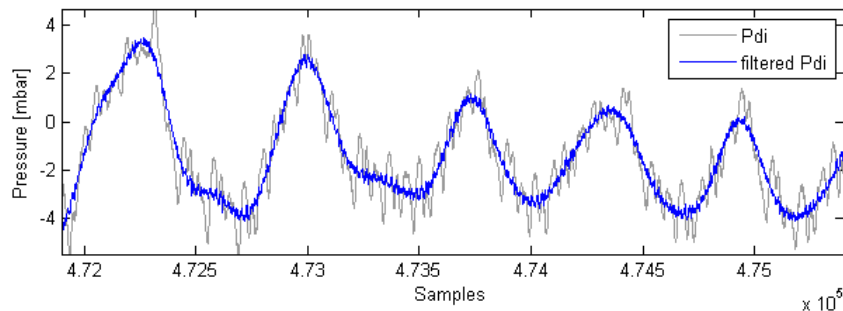


Figure 3-4: Example of original and filtered Pdi

○ Recognition of abnormal Pdi

The figure below shows the percentage of cycles with abnormal Pdi (see 2.5.1) over the total amount of cycles recognized per subject. These values give a hint on the quality of the invasive measurement.

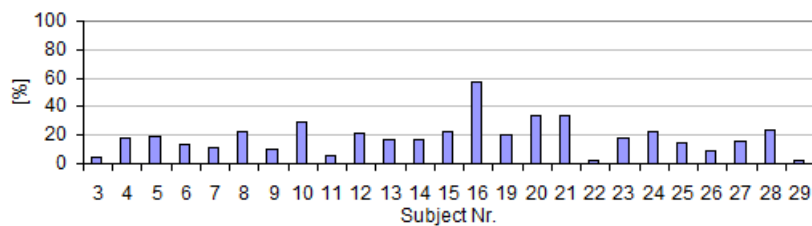


Figure 3-5: Percentage of cycles with abnormal Pdi per subject

- Determination of baseline

The determination of the offset line of Pdi was achieved as the next figures show. The upper plots shows the measured Pdi and offset line (bsl); the lower plots shows the effective offset-corrected Pdi. These are examples using the data from 3 subjects. All other plots are available in the attached CD.

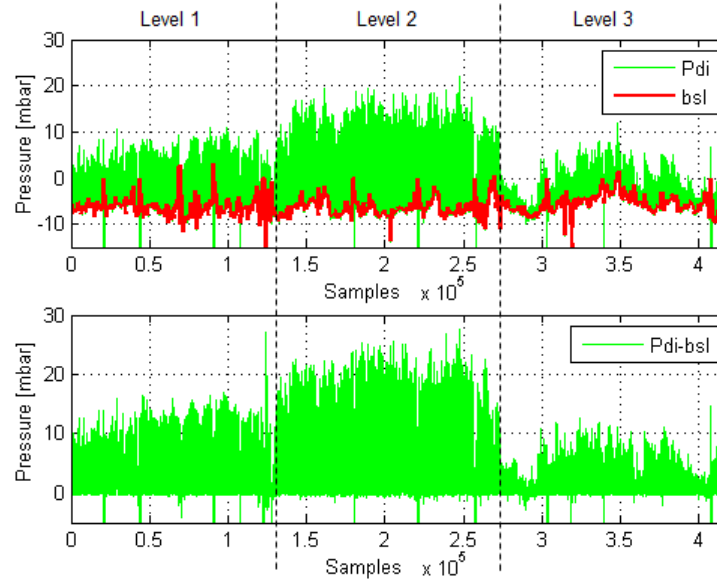


Figure 3-6: Example of offset correction in Pdi.

Pdi: transdiaphragmatic pressure; bsl: determined baseline.

In the previous figure the offset, or baseline, of Pdi varies little and remains most of the time (except for some peaks) between 0 and -10mbar. In other cases the variation of the baseline was greater, as the next figure shows. Also in these cases the determination of baseline and its correction was possible.

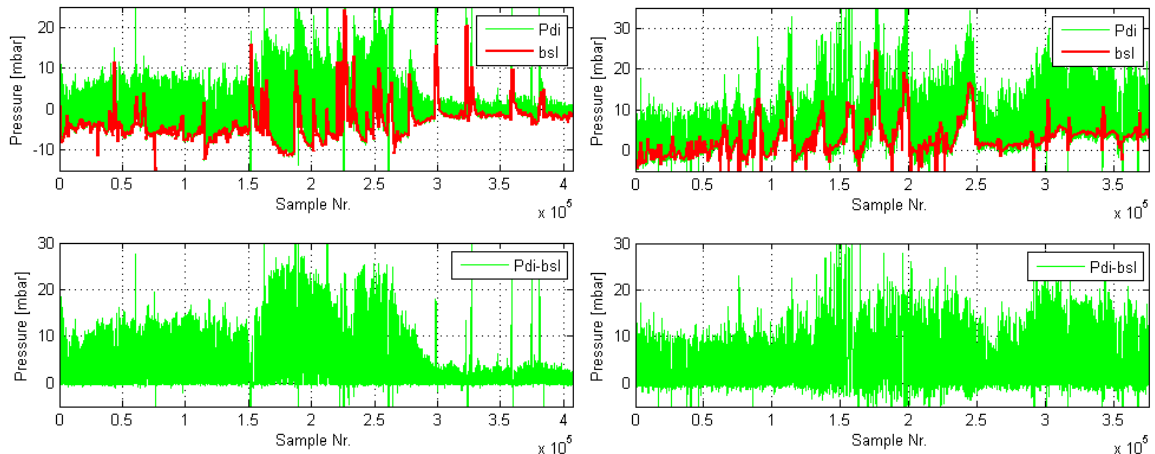


Figure 3-7: Offset correction in Pdi from subject 23 and 27.

Pdi: transdiaphragmatic pressure; bsl: determined baseline.

- Recognition of leaks

Besides the invasive measurement of Pdi, the MLR requires the flow and the airway pressure as inputs. Even with the invasively placed balloon-catheters, the interface between volunteer and ventilator in the validation setup was a nose-mouth mask, as for non-invasive ventilation, for the application of either method, the invasive and the non-invasive.

A disadvantage of the non-invasive ventilation is the presence of leaks. Due to the fact that all faces are different and that the subjects move, there is no ideal mask that avoids leaks completely. Particularly in the data recorded from subject 16 during ASB, a big leak was found. Figure 3-8 shows the flow and volume recorded from a sample cycle. The inspired volume ($\sim 1.5\text{ l}$) is much higher than the expired volume ($\sim 0.7\text{ l}$). The real inspired volume is actually much smaller than the volume calculated from the recorded flow (max. $\sim 0.8\text{ l/s}$) because part of this flow ($\sim 0.3\text{ l/s}$) delivered by the Evita4 leaks.

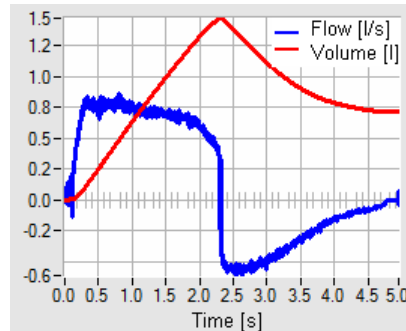


Figure 3-8: Cycle with high end expiratory volume

Figure 3-9 shows that the leak was present over a long time during the measurement with subject 16. The plot shows the maximum volumes (V_{\max}) from each cycle and the end expiratory volumes (V_{ee}) which, without leak, should be near zero. Such cycles cannot be correctly modelled if the leak is neglected. Therefore, as a solution to this problem, all cycles with V_{ee} over 0.5 liter were excluded from the analysis of all subjects.

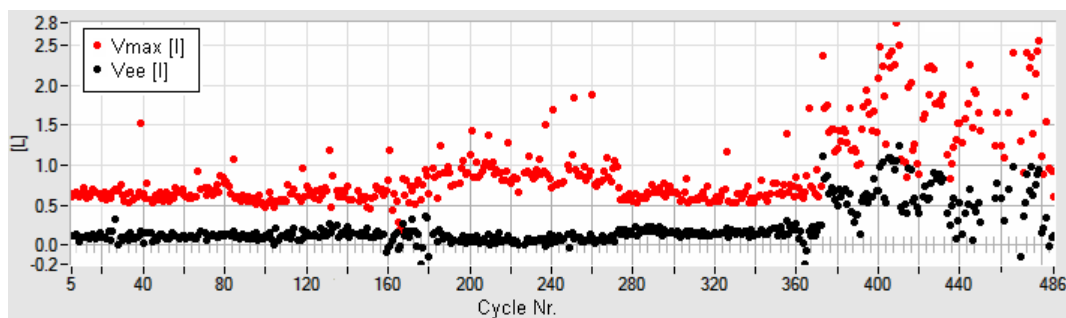


Figure 3-9: End-expiratory volumes in cycles without and with leak
 V_{\max} : maximum volume. V_{ee} : end expiratory volume.

o Recognition of swallowing

Also here there were large differences between subjects because some swallowed much often than others. More than 90% of the cycles expected to be have disturbances in V' and P_{aw} were recognized successfully by the program and were therefore not used to reconstruct the muscular pressure. However, the subsequent changes in the overall results were very small: in all cases the amount of cycles rejected was less than 3% and the reduction in the dispersion of the differences of PTP_{insp} (between PTP_{Pdi} and $PTP_{\text{O+D}}$) was smaller than 5%.

3.1.2.2 Results per subject

Each recorded breathing cycle was entered to MLR to obtain Rfit and Cfit. Table 3-7 summarizes the results for the complete measurement with each volunteer. The subject numbers in grey correspond to the smokers. The numbers in red are outliers. The column nPdi indicates the amount of cycles used to get the parameters.

Subj.	Rfit [mbar/l/s]		Cfit [ml/mbar]		nPdi
	mean	sd	mean	sd	
3	5.12	1.87	101.1	22.1	417
4	3.15	1.33	74.4	18.9	493
5	4.57	2.34	119.0	26.7	321
6	6.43	2.08	104.9	27.4	286
7	7.95	3.8	85.2	23.7	541
8	4.85	1.77	126.6	34.0	330
9	4.42	1.94	66.0	11.2	495
10	7.28	3.94	67.7	21.0	280
11	5.3	2.15	62.1	10.3	456
12	6.12	2.11	85.3	11.7	176
13	7.69	2.66	88.4	14.6	343
14	3.66	1.78	94.9	16.9	332
15	6.28	3.05	61.9	19.8	446
16	5.89	2.06	112.7	41.0	169
19	6.89	2.53	97.7	25.5	318
20	6.77	2.04	110.0	33.5	192
21	4.2	2.92	106.6	25.7	131
22	4.11	1.19	117.1	26.0	570
23	6.64	2.19	90.5	20.6	271
24	7.99	2.41	101.0	33.5	356
25	7.43	3.31	98.6	18.8	249
26	7.02	2.13	101.2	22.6	288
27	7.38	3.31	68.5	13.3	397
28	7.87	3.1	118.7	34.5	273
29	6.74	1.61	70.8	24.4	421
Min	3.15	1.19	61.9	10.3	131
Max	7.99	3.94	126.6	41.0	570

Table 3-7: R and C from the volunteers by the invasive method.

Rfit: Resistance. Cfit: Compliance. sd: standard deviation. nPdi: number of cycles.

3.1.2.3 Analysis of phases per subject

During the examination the volunteers breathed spontaneously at 3 different levels of effort. The efficacy of the augmentation of effort by increasing dead space and of the reduction of effort by giving ventilatory support was confirmed by comparison of the PTP_{insp} calculated during the different phases. The analysis of variance revealed that the mean PTP_{insp} values from the invasive method (PTP_{Pdi}) were significantly different between all phases in 22 of 25 subjects.

In contrast to the simulations, the parameters Rfit and Cfit of the volunteers presented considerable variations between phases. Their means and standard deviations calculated for each phase separately are listed in [Annex F](#), Table F-2.

3.2 Results from the non-invasive O+D method

The Occlusion+Delta (O+D) method was applied as introduced in 2.1.5 and 2.1.6. The occlusions were executed each 3 cycles in the simulations and each 3 to 7 cycles in the study with volunteers. The time of onset of the occlusions varied between 300 and 1000ms after the begin of the expiration depending on the trend duration of the expiratory time. This section reports the results of the designed method.

3.2.1 Simulations with the lung simulator

3.2.1.1 Results per simulation case

Each occlusion was used to obtain Rocc and Cocc. Their means and standard deviations are in Table 3-8. The column nPdi indicates the amount of cycles used to get the parameters.

Case	Rocc [mbar/l/s]		Cocc [ml/mbar]		nPdi
	mean	sd	mean	sd	
25--2	1.94	0.5	27.5	1.99	98
25--4	4.54	0.27	26.8	1.37	97
50--2	2.24	0.21	52.3	4.6	98
50--4	4.82	0.29	50.2	2.76	97
75--2	2.49	0.13	81.0	6.03	97
75--4	4.69	0.22	69.7	9.75	97

Table 3-8: R and C from the simulated cases by the O+D method.

Rocc: Resistance. Cocc: Compliance. sd: standard deviation. nPdi: number of cycles.

3.2.1.2 Analysis of phases per case

During the simulation of each case, 3 levels of muscular pressure were simulated. The mean PTP_{insp} values from the Occlusion+Delta method (PTP_{O+D}) were also significantly different ($p < 0.05$) between all phases in all simulated cases. As expected, there were no considerable differences in Rocc or Cocc between the phases. All means and standard deviations calculated for each phase separately are given in [Annex F](#), Table F-1.

3.2.2 Results of the study with volunteers

After the verification of the O+D method with simulations followed the analysis of data from the study with volunteers. The setup for acquisition of real data included signal measurement with minimized susceptibility to artefacts, improved control of mechanical disturbances and a sampling rate of 5ms. During the measurements each trigger signal sent from the program to the shutter caused an occlusion. When reading the measured signals, the recognition of occlusions was correct in over 96% of the cases. Figure 3-10 shows sample signals of occluded cycles in all 3 phases.

Most of the volunteers (22 of 25) noticed the occlusions, sometimes just due to the clicking noise of the electric relay of the shutter. All volunteers said that the occlusions did not disturb them. Three volunteers had problems accepting the ventilatory support during ASB. This appears in the signals as false triggers. Note that the occlusions are not executed on a regular basis to avoid that the volunteer is prepared for the next occlusion, which could influence his physiological reactions.

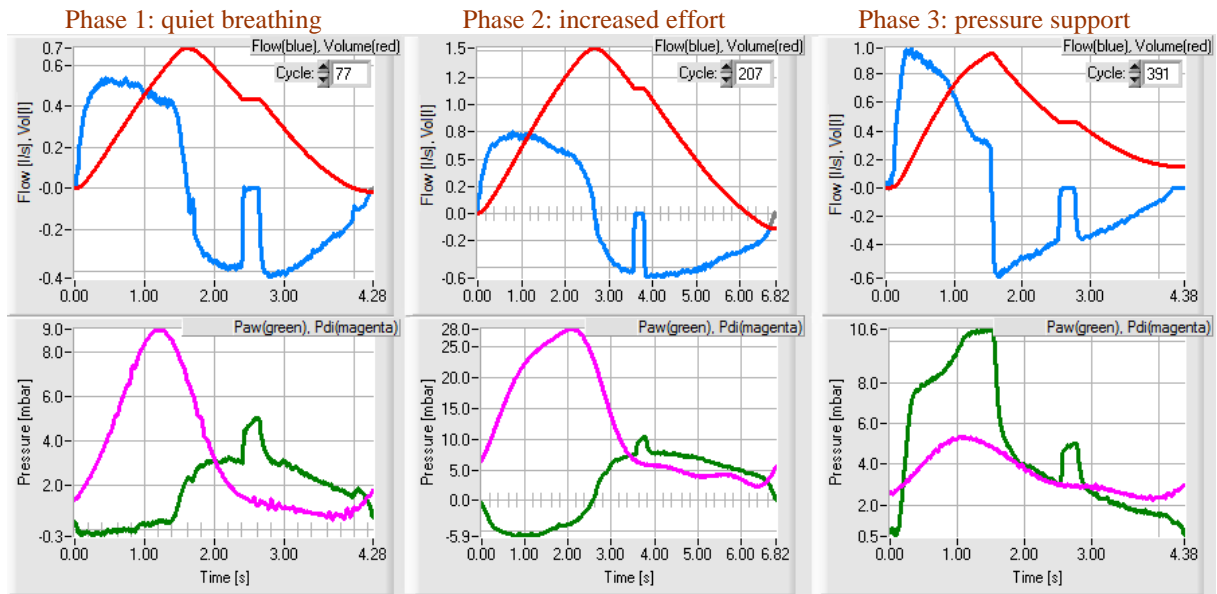


Figure 3-10: Examples of signals in occluded cycles at 3 levels of respiratory effort.
 Paw: airway pressure. Pdi: transdiaphragmatic pressure.

3.2.2.1 Results per subject

Each occlusion was used to get Rocc and Cocc. Table 3-9 shows the results for the complete measurement with each volunteer. The subject numbers in grey correspond to the smokers.

Subj.	Rocc [mbar/l/s]		Cocc [ml/mbar]		nPdi
	mean	sd	mean	sd	
3	3.71	0.68	98.2	20.9	417
4	3.21	0.64	86.2	19.1	493
5	3.44	0.73	92.3	28.8	321
6	6.11	1.66	82.5	28.5	286
7	7.09	2.94	71.4	26.5	541
8	3.65	1.01	85.1	24.9	330
9	4.01	1.50	91.7	28.3	495
10	5.02	1.52	95.2	28.5	280
11	4.57	1.53	58.9	20.8	456
12	4.36	0.98	90.5	33.3	176
13	7.03	1.43	73.2	25.9	343
14	2.38	0.58	85.4	24.8	332
15	4.26	1.47	81.1	26.2	446
16	5.10	2.94	76.8	27.0	169
19	6.97	2.25	87.6	30.9	318
20	6.75	1.86	67.9	20.7	192
21	2.35	0.54	100.1	28.2	131
22	3.76	1.0	113.2	32.9	570
23	3.6	1.19	104.4	28.9	271
24	5.27	1.58	91.6	26.1	356
25	4.74	2.43	71.7	22.4	249
26	4.02	1.09	70.6	18.8	288
27	6.06	1.43	86.8	27.3	397
28	4.41	1.89	91.5	25.8	273
29	5.06	1.13	68.7	15.6	421

Table 3-9: R and C from the volunteers by the O+D method.

Rocc: Resistance. Cocc: Compliance. sd: standard deviation. nPdi: number of cycles.

3.2.2.2 Analysis of phases per subject

The volunteers breathed at three levels of respiratory effort (normal, augmented and reduced) during spontaneous breathing. The efficacy of setting the levels was confirmed by the comparison of the PTP_{insp} values obtained during the different phases. According to the analysis of variance, the mean PTP_{insp} values from the non-invasive method (PTP_{O+D}) were significantly different between all phases in all subjects⁵. The parameters Rocc and Cocc also presented considerable variations between phases. Their means and standard deviations calculated for each phase separately are listed in [Annex F](#), Table F-2.

3.3 Validation of the non-invasive O+D method

This section presents the comparison of the results from the non-invasive method against the results of the standard invasive procedure.

3.3.1 Simulations with the lung simulator

3.3.1.1 Validation results per simulation case

The estimates of R and C from the O+D method, Rocc and Cocc, gained after each occlusion were used to reconstruct the pressure from the upcoming cycles. Figure 3-11 shows two examples of reconstructions from case 50--2 compared against the simulated pressure: one was successful and one has poor fit.

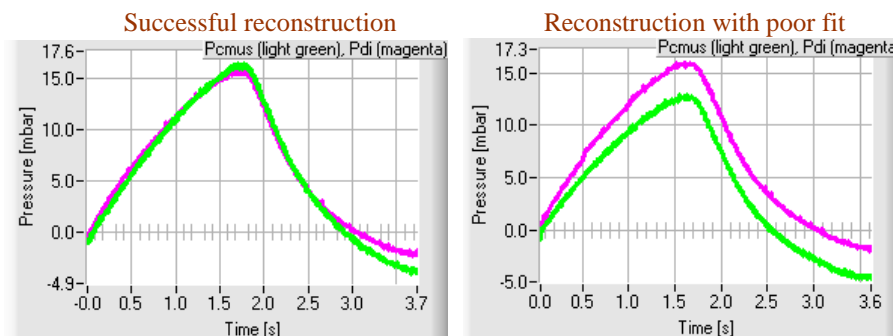


Figure 3-11: Examples of simulated Pdi and its reconstructions.
Pdi: the simulated pressure, Pcmus: the calculated muscular pressure.

The following table shows, as example, the results of the validation obtained for case 75--4. The resulting parameters Rocc and Cocc from the O+D method can be directly compared to the parameters Rfit and Cfit from the reference method. The table also displays the results of regression and Bland-Altman analysis.

Rocc		Cocc		Rfit		Cfit		BA						
[mbar/l/s]		[ml/mbar]		[mbar/l/s]		[ml/mbar]		nPdi	m	b	R ²	[mbar*s]	outl.	
mean	sd	mean	sd	mean	sd	mean	sd					mean	sd	
4.69	0.22	69.7	9.75	4.71	0.17	71.12	0.91	97	1.01	0.14	0.95	0.34	0.44	2

The results of all single cases were plotted in graphics organised like Figure 3-12. This graphic shows, as example, the results obtained for case 50--2 (LS502).

⁵ Note that this affirmation is weak for phase 3 of subject 10 and phase 1 of subject 21 which had only 19 and 5 cycles respectively ($n < 30$); in all other cases $n > 30$.

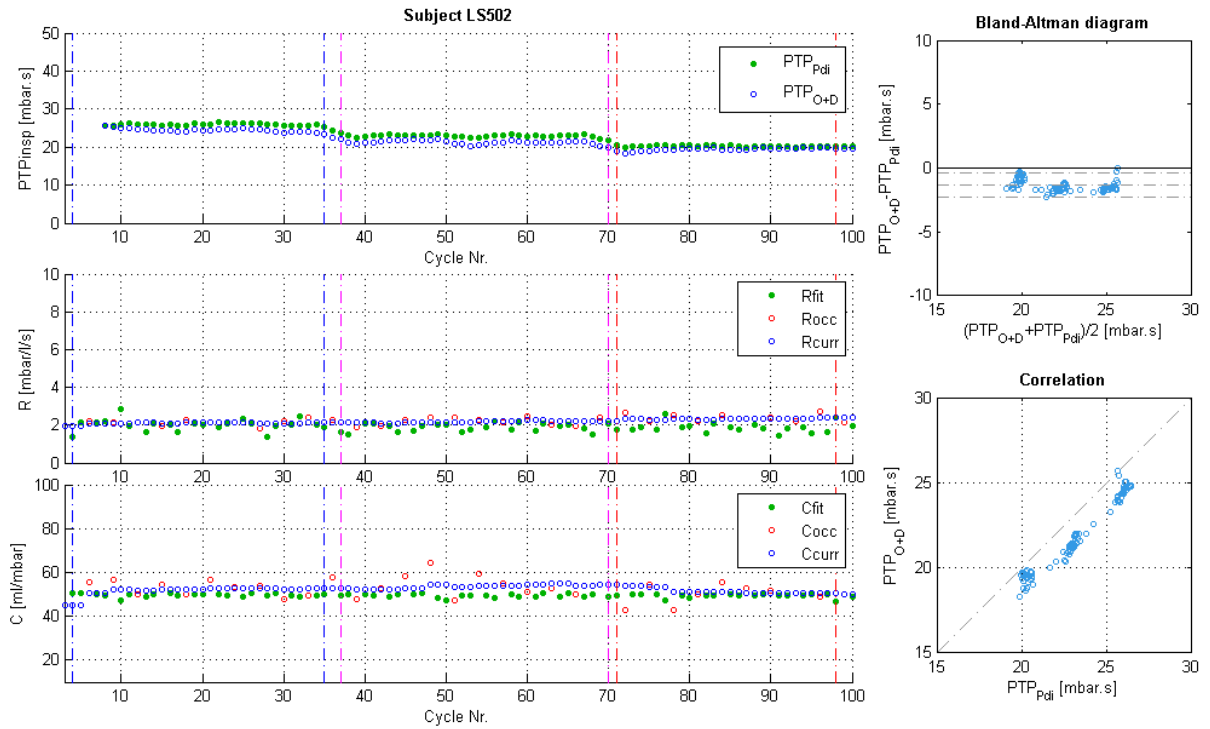


Figure 3-12: Summary of results for a single simulation case. The left panels show PTPinsp, R and C by the reference method (PTP_{Pdi}, Rfit, Cfit) and from the new procedure (PTP_{O+D}, Rocc, Cocc, Rcurr, Ccurr). The dashed lines mark the begin and end of the examined phases. The right panels compare the PTPinsp values from both methods with one point per cycle.

The single tables and plots of all simulations are available in the attached CD. Table 3-10 summarizes the results of the validation for all 6 simulated cases.

Case	Rocc		Cocc		Rfit		Cfit		nPdi	m	b	R ²	BA	
	[mbar/l/s]	[ml/mbar]	[mbar/l/s]	[ml/mbar]	[mbar/l/s]	[ml/mbar]	[mbar/l/s]	[ml/mbar]					mean	sd
25--2	1.94	0.5	27.5	1.99	1.92	0.55	23.9	0.5	98	0.96	-2.98	0.96	-4.56	0.66
25--4	4.54	0.27	26.8	1.37	4.82	0.45	24.6	0.32	97	0.87	1.84	0.98	-3.50	0.60
50--2	2.24	0.21	52.3	4.6	1.92	0.27	49.5	0.82	98	0.90	1.02	0.96	-1.35	0.49
50--4	4.82	0.29	50.2	2.76	5.04	0.26	48.6	0.67	97	0.97	0.18	0.99	-0.53	0.24
75--2	2.49	0.13	81.0	6.03	2.05	0.12	73.7	0.58	97	0.94	0.44	1.00	-0.80	0.18
75--4	4.69	0.22	69.7	9.75	4.71	0.17	71.1	0.91	97	1.01	0.14	0.95	0.34	0.44

Table 3-10: Validation results from simulated cases

The small absolute differences between the mean values of R and C are plotted in Figure 3-13. The real values of R and C directly measured in the setup (see 2.2.2.2) did not change during the simulation.

For all cases, analyzed separately, linear regression reveals high agreement in the PTPinsp from the simulated and the reconstructed muscular pressure ($0.87 < m < 1.01$, $-2.98 < b < 1.84$, $R^2 > 0.95$). This demonstrates that the changes in PTP_{O+D} correctly follow the changes in PTP_{Pdi}. Also Bland-Altman analysis shows positive results (mean differences between -4.56 and 0.34 mbar*s; standard deviations of the differences between 0.18 and 0.66 mbar*s). Although there are significant differences in agreement between cases, all differences are acceptable when compared to the absolute values of PTPinsp.

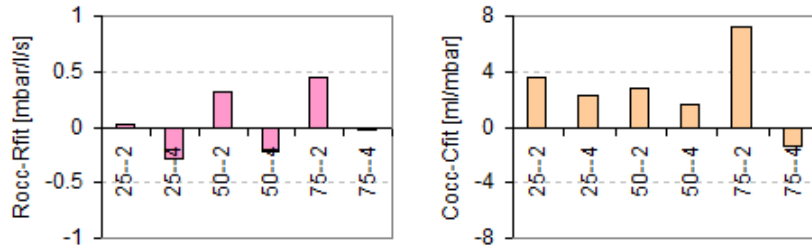


Figure 3-13: Differences in R and C between methods in the simulated cases. R: Resistance. C: Compliance. Rfit, Cfit: R and C obtained with the simulated muscular pressure. Rocc, Cocc: R and C obtained with the Occlusion+Delta method

3.3.1.2 Analysis of phases per case

Although the experimental setup of the model did not change between phases, a separated analysis for each phase was done in preparation for the analysis of real data. The results of each phase are organized in tables as the example below (results for case 75--4).

Phase	cycles	nr. Occls	Rfit		Cfit		Rocc		Cocc		nPdi	BA		outl.
			[mbar/l/s] mean	[mbar/l/s] sd	[ml/mbar] mean	[ml/mbar] sd	[mbar/l/s] mean	[mbar/l/s] sd	[ml/mbar] mean	[ml/mbar] sd		[mbar*s] mean	[mbar*s] sd	
1	27	9	4.84	0.15	71.3	0.94	4.64	0.22	63.9	7.31	27	0.15	0.56	0
2	34	12	4.71	0.13	71.2	0.91	4.67	0.14	70.9	5.01	34	0.64	0.25	0
3	28	10	4.57	0.12	70.8	0.8	4.70	0.26	71.0	12.9	28	0.17	0.26	0

Additionally, the agreement in PTPinsp inside the phases was measured by Bland-Altman analysis. Its results are plotted in graphics that look like Figure 3-14. This graphic shows, as example, the results obtained for case 50--2 (LS502). All single tables and plots are available in the attached CD.

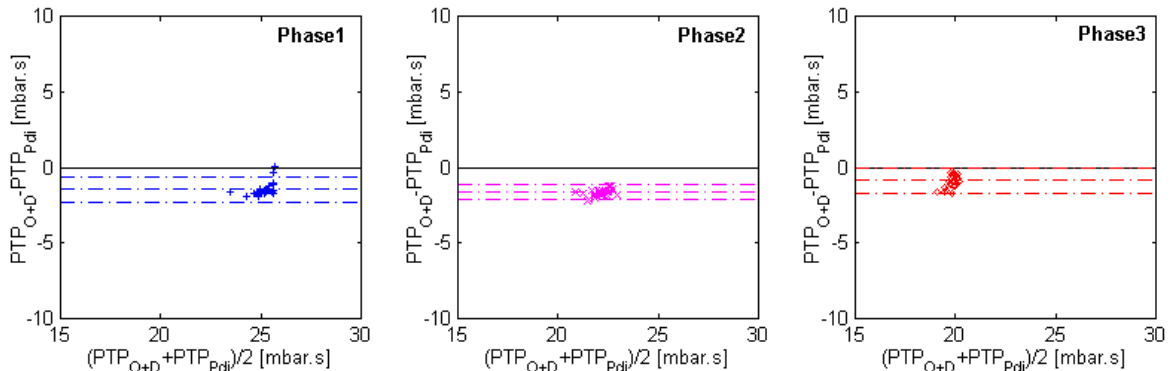


Figure 3-14: Analysis of phases by Bland-Altman of PTPinsp per simulation.

PTPinsp: inspiratory pressure-time product. PTP_{Pdi}: PTPinsp from the simulated pressure. PTP_{O+D}: PTPinsp from the pressure reconstructed with the O+D method.

As expected for the simulations, there were no representative differences in R, C or in the mean differences of PTPinsp between the phases. [Annex F](#), Table F-1 shows all validation results for all three phases of all 6 simulated cases.

3.3.1.3 Overall analysis of simulation cases

Linear regression and Bland-Altman analysis of the R and C values reveal high agreement between methods for the simulations:

- $R_{occ} = 0.85 \cdot R_{fit} + 0.55$, $R^2 = 0.99$; Differences in R = 0.04 ± 0.57 mbar/l/s
- $C_{occ} = 1.00 \cdot C_{fit} + 2.48$, $R^2 = 0.98$; Differences in C = 2.67 ± 5.62 ml/mbar

The single differences in mean R and C from both methods vary strongly between the cases and are compared here as relative values:

	25--2	25--4	50--2	50--4	75--2	75--4
100(R _{occ} -R _{fit})/R _{fit} [%]	1.0	-5.8	16.7	-4.4	21.5	-0.4
100(C _{occ} -C _{fit})/C _{fit} [%]	15.0	9.2	5.6	3.3	9.8	-2.0

At least 92 pairs of PTP_{insp} were available for each simulated case. For a balanced analysis of all cases together, the same amount of pairs ($n'=92$) was used per case ($n=552$). Linear regression and Bland-Altman analysis also reveal high agreement between the PTP_{insp} calculated from both methods in the simulations:

- $PTP_{O+D} = 0.83 \cdot PTP_{Pdi} + 2.85$
- 95% confidence bounds 0.825 to 0.844 for m and 2.582 to 3.124 for b , $R^2 = 0.98$
- Differences = -1.73 ± 3.58 mbar*s

Figure 3-15 presents the corresponding plots. The colours indicate the cases. The Bland-Altman diagram shows that the differences in 25--2 and 25--4 are bigger than in the others, although still acceptable, but also their mean PTP_{insp} values are greater. This is related to the small selected compliance: these simulations were done with a very low compliance, which would represent a very stiff lung. Correspondingly, the regression analysis shows an offset in 25--2 and 25--4.

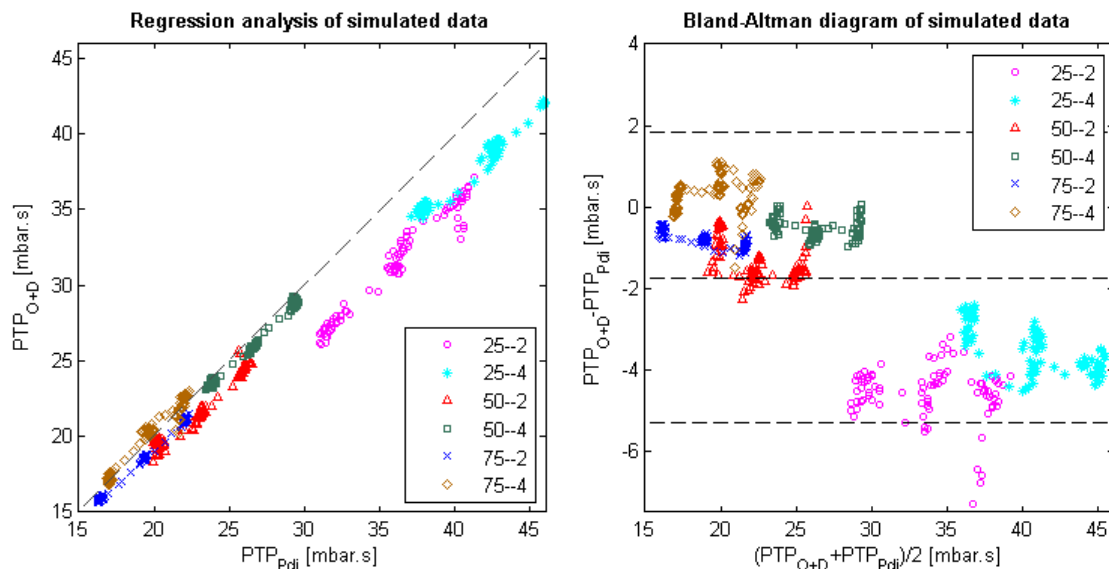


Figure 3-15: Results of O+D with simulations

PTP_{insp}: inspiratory pressure-time product. PTP_{Pdi}: PTP_{insp} from the simulated pressure. PTP_{O+D}: PTP_{insp} from the pressure reconstructed with the O+D method.

In conclusion, the simulations served to successfully verify the principle and function of the O+D method. The next step is the analysis of the method with data from volunteers.

3.3.2 Results of the study with volunteers

3.3.2.1 Validation results per subject

Like for the simulations, all results for single subjects are plotted in graphics organized as Figure 3-16. The plots show as example the results obtained for subject 3 and subject 10.

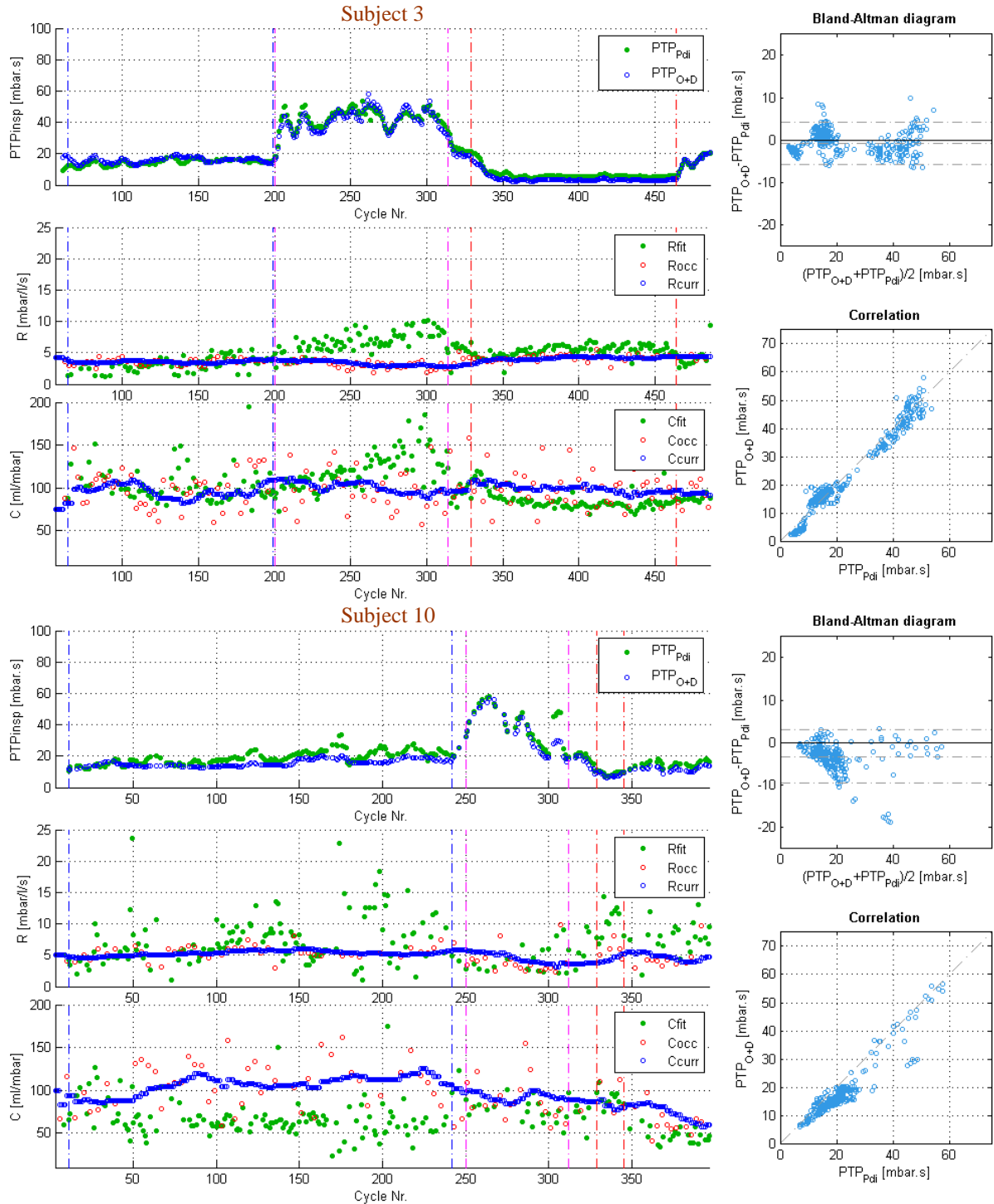


Figure 3-16: Summary of results for single subjects
The left panels show PTPinsp, R and C by the reference method (PTP_{Pdi} , R_{fit} , C_{fit}) and from the new procedure (PTP_{O+D} , R_{occ} , C_{occ} , R_{curr} , C_{curr}). The dashed lines mark the begin and end of the examined phases. The right panels compare the PTPinsp values from both methods with one point per cycle.

In most cases a look on the plots of PTP_{insp} suffices to recognize the phases (delimited in the plots by dashed lines), but for the subjects 10, 12, 16 and 21 that differentiation was not that clear. All plots available in the attached CD.

Main validation results per subject

Table 3-11 summarizes the validation results for the complete measurement with each volunteer. The numbers in grey correspond to the smokers. The numbers in red are outliers.

Subj.	Rocc		Cocc		Rfit		Cfit		nPdi	m	b	R ²	BA	
	[mbar/l/s]		[ml/mbar]		[mbar/l/s]		[ml/mbar]						[mbar*s]	
	mean	sd	mean	sd	mean	sd	mean	sd					mean	sd
3	3.71	0.68	98.2	20.9	5.12	1.87	101.1	22.1	417	1.00	-0.80	0.97	-0.83	2.52
4	3.21	0.64	86.2	19.1	3.15	1.33	74.4	18.9	493	1.25	-3.23	0.97	-0.08	3.14
5	3.44	0.73	92.3	28.8	4.57	2.34	119.0	26.7	321	1.07	0.55	0.86	1.71	4.15
6	6.11	1.66	82.5	28.5	6.43	2.08	104.9	27.4	286	1.2	0.02	0.96	4.4	4.05
7	7.09	2.94	71.4	26.5	7.95	3.8	85.2	23.7	541	1.23	-1.30	0.94	1.86	2.85
8	3.65	1.01	85.1	24.9	4.85	1.77	126.6	34.0	330	1.16	-1.25	0.93	2.32	4.32
9	4.01	1.5	91.7	28.3	4.42	1.94	66.0	11.2	495	1.20	-3.44	0.95	-0.35	3.03
10	5.02	1.52	95.2	28.5	7.28	3.94	67.7	21.0	280	0.88	-0.94	0.88	-3.4	3.24
11	4.57	1.53	58.9	20.8	5.3	2.15	62.1	10.3	456	1.11	-0.16	0.92	1.89	5.1
12	4.36	0.98	90.5	33.3	6.12	2.11	85.3	11.7	176	1.01	0.33	0.95	0.64	5.95
13	7.03	1.43	73.2	25.9	7.69	2.66	88.4	14.6	343	1.06	2.46	0.91	3.8	4.02
14	2.38	0.58	85.4	24.8	3.66	1.78	94.9	16.9	332	1.03	1.50	0.82	2.09	5.61
15	4.26	1.47	81.1	26.2	6.28	3.05	61.9	19.8	446	1.08	-1.79	0.86	-0.61	3.46
16	5.1	2.94	76.8	27.0	5.89	2.06	112.7	41.0	169	1.01	6.42	0.68	6.53	3.9
19	6.97	2.25	87.6	30.9	6.89	2.53	97.7	25.5	318	1.44	-6.28	0.88	3.96	8.43
20	6.75	1.86	67.9	20.7	6.77	2.04	110.0	33.5	192	0.98	4.39	0.97	4.01	2.97
21	2.35	0.54	100.1	28.2	4.2	2.92	106.6	25.7	131	1.97	-23.3	0.65	6.47	22.04
22	3.76	1.0	113.2	32.9	4.11	1.19	117.1	26.0	570	0.95	1.45	0.98	1.02	0.77
23	3.6	1.19	104.4	28.9	6.64	2.19	90.5	20.6	271	1.25	-7.24	0.87	-2.85	3.91
24	5.27	1.58	91.6	26.1	7.99	2.41	101.0	33.5	356	0.87	1.27	0.9	-0.88	3.93
25	4.74	2.43	71.7	22.4	7.43	3.31	98.6	18.8	249	0.92	9.34	0.84	6.69	8.52
26	4.02	1.09	70.6	18.8	7.02	2.13	101.2	22.6	288	1.38	-2.96	0.96	7.57	8.4
27	6.06	1.43	86.8	27.3	7.38	3.31	68.5	13.3	397	0.83	-0.75	0.89	-4.22	4.93
28	4.41	1.89	91.5	25.8	7.87	3.1	118.7	34.5	273	1.11	0.84	0.8	2.79	5.09
29	5.06	1.13	68.7	15.6	6.74	1.61	70.8	24.4	421	1.36	-9.7	0.95	-0.98	6.23
Min	2.35	0.54	58.9	15.6	3.15	1.19	61.9	10.3	131	0.83	-23.3	0.65	-4.22	0.77
Max	7.09	2.94	113.2	33.3	7.99	3.94	126.6	41.0	570	1.97	9.34	0.98	7.57	22.04

Table 3-11: Results of measurements with volunteers

R and C present large variation independently of the method used: the mean standard deviations using the results of all subjects are 1.44 mbar/l/s for Rocc, 2.38 mbar/l/s for Rfit, 25.6 ml/mbar for Cocc and 23.1 ml/mbar for Cfit.

In 23 of 25 cases the mean Rocc was smaller than the mean Rfit. The differences in C vary largely. These mean values were calculated for the whole measurement. The differences in mean R and C between methods are plotted in Figure 3-17.

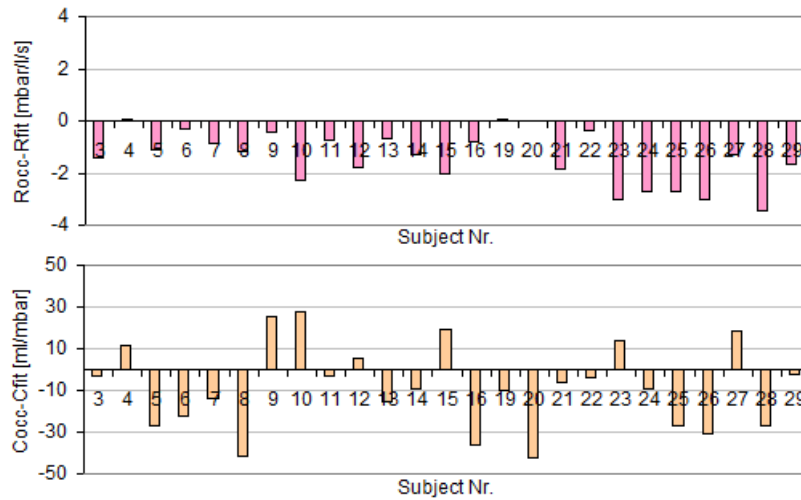


Figure 3-17: Differences in mean resistance and compliance between methods
 R: Resistance. C: Compliance. Rfit, Cfit: R and C obtained with the measured muscular pressure. Rocc, Cocc: R and C obtained with the Occlusion+Delta method

For all cases, analyzed separately, linear regression shows positive agreement:

- $0.65 < R^2 < 0.98$
- $0.83 < m < 1.44$ (outlier in subject 21 $m=1.97$)
- $-9.7 < b < 9.34$ (outlier in subject 21 $b=-23.3$)

whereas Bland-Altman analysis shows acceptable agreement:

- mean differences between -4.22 and 7.57 mbar*s
- standard deviation of the differences between 0.77 and 8.52 mbar*s
- (outlier in subject 21 $sd= 22.04$)

with large differences between subjects.

Figure 3-18 summarizes in a box plot all the differences in PTP_{insp} per subject. Clearly the measurement of subject 21 had a much larger dispersion than all others, although no signs of it appeared during the measurement. On the contrary, the best results (mean closest to zero and smallest deviation) correspond to subject 22.

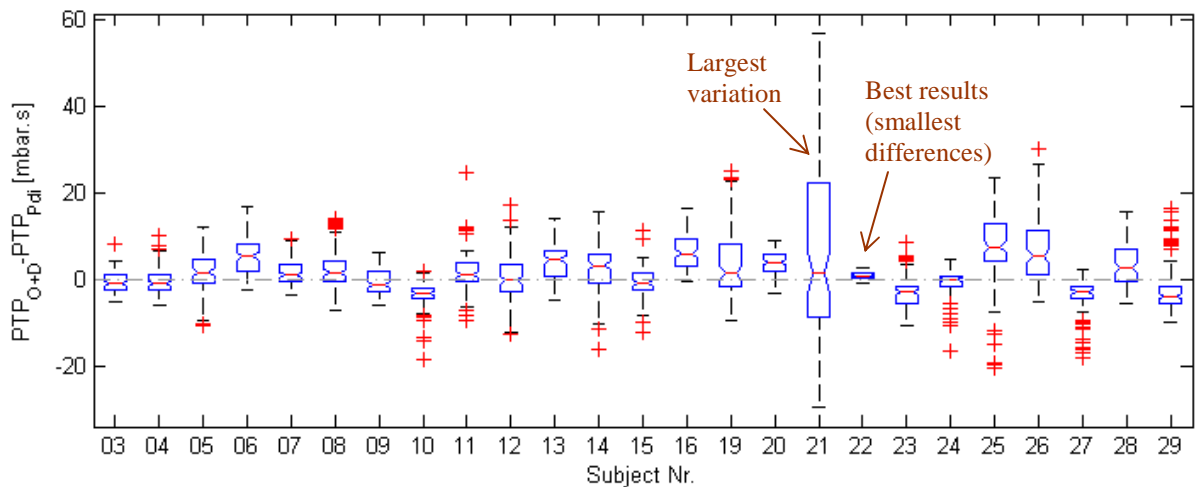


Figure 3-18: Differences in PTP_{insp} for all 25 volunteers
 PTP_{insp}: inspiratory pressure-time product. PTP_{Pdi}: PTP_{insp} from the simulated pressure. PTP_{O+D}: PTP_{insp} from the pressure reconstructed with the O+D method.

3.3.2.2 Analysis of phases per subject

Due to the previously revealed differences between phases for the volunteers, a separated analysis was done for each. The results of each phase are organized in tables as the example in Table 3-12 shows (subject 29). This table presents a case, where there is a big change of Cfit in phase 2 that has remarkable consequences in the differences of PTP_{insp}.

Phase	cycles	nr. Occls	Rfit		Cfit		Rocc		Cocc		nPdi	BA		outl.
			[mbar/l/s]		[ml/mbar]		[mbar/l/s]		[ml/mbar]			[mbar*s]		
			mean	sd	mean	sd	mean	sd	mean	sd		mean	sd	
1	126	28	7.07	1.2	60.8	7.48	5.23	0.78	73.72	13.9	126	-4.22	1.63	0
2	117	23	6.08	1.61	101.7	26.66	3.96	1.39	71.13	12.1	112	7.58	5.56	0
3	168	38	6.99	1.73	57.7	7.88	5.58	0.67	63.56	16.7	167	-4.43	1.83	1

Table 3-12: Sample results of measurements per phase (subject 29). The higher compliance Cfit in phase 2 is reflected by a higher mean difference in respiratory effort.

Also the values of subject 7 and subject 9 are good examples of a notable difference between phases in relation to the results of the Bland-Altman analysis. Figure 3-19 shows the Bland-Altman diagrams of these subjects with separated markers for each phase.

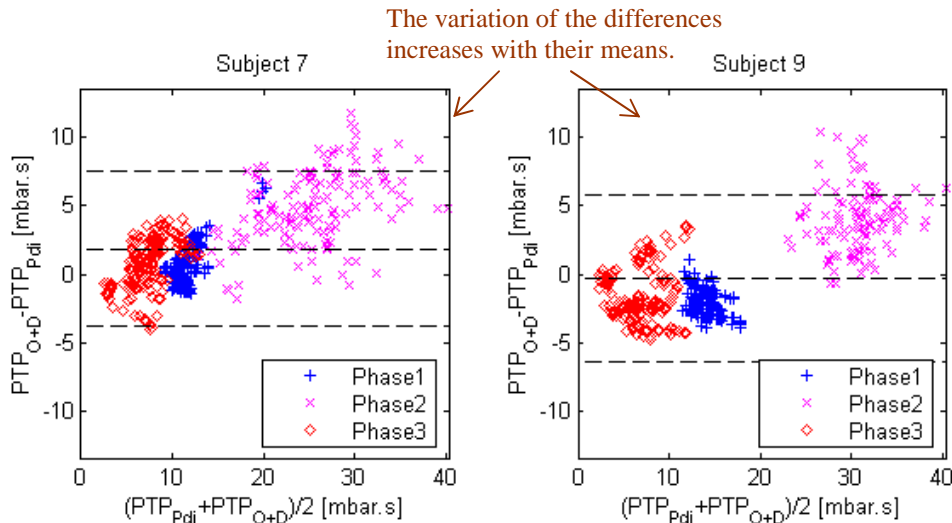


Figure 3-19: Analysis of phases by Bland-Altman diagram of two subjects. PTP_{insp}: inspiratory pressure-time product. PTP_{Pdi}: PTP_{insp} from the simulated pressure. PTP_{O+D}: PTP_{insp} from the pressure reconstructed with the O+D method. Phase 1: quiet breathing; Phase 2: increased effort; Phase 3: pressure support.

That the mean values of PTP_{insp} increase in phase 2 and decrease in phase 3 was part of the experimental design, but not that the variances of the differences change.

The results of the phase analysis for each subject were plotted in graphics like Figure 3-20. This plots show, as example, the agreement obtained for the three phases of the measurement with subject 28. As explanation to the repetitive increase of the mean difference in PTP_{insp} during phase 2 a possible delay of the measured Pdi with respect to the flow was considered, but did not result consistent between subjects.

The single tables and plots of all 25 subjects are available in the attached CD. The validation results for all three phases of all volunteers are shown in [Annex F](#), Table F-2.

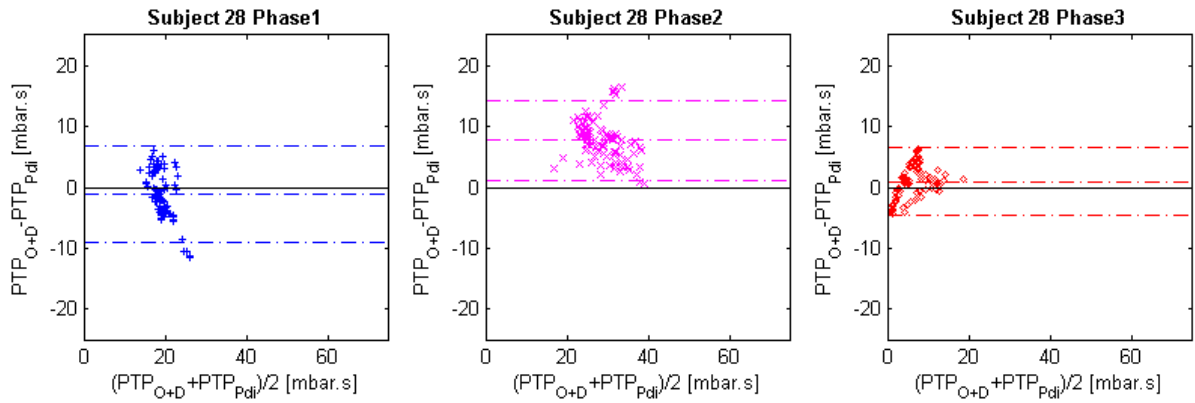


Figure 3-20: Analysis of phases by Bland-Altman diagram of PTP_{insp} per subject. PTP_{insp}: inspiratory pressure-time product. PTP_{Pdi}: PTP_{insp} from the simulated pressure. PTP_{O+D}: PTP_{insp} from the pressure reconstructed with the O+D method. Phase 1: quiet breathing; Phase 2: increased effort; Phase 3: pressure support.

3.3.2.3 Overall analysis of data from volunteers

As the values of R and C also changed between phases (see results in [Annex F](#), Table F-2) linear regression and Bland-Altman analysis were done using their means for each phase and each volunteer ($n = 75$). Figure 3-21 shows the plots.

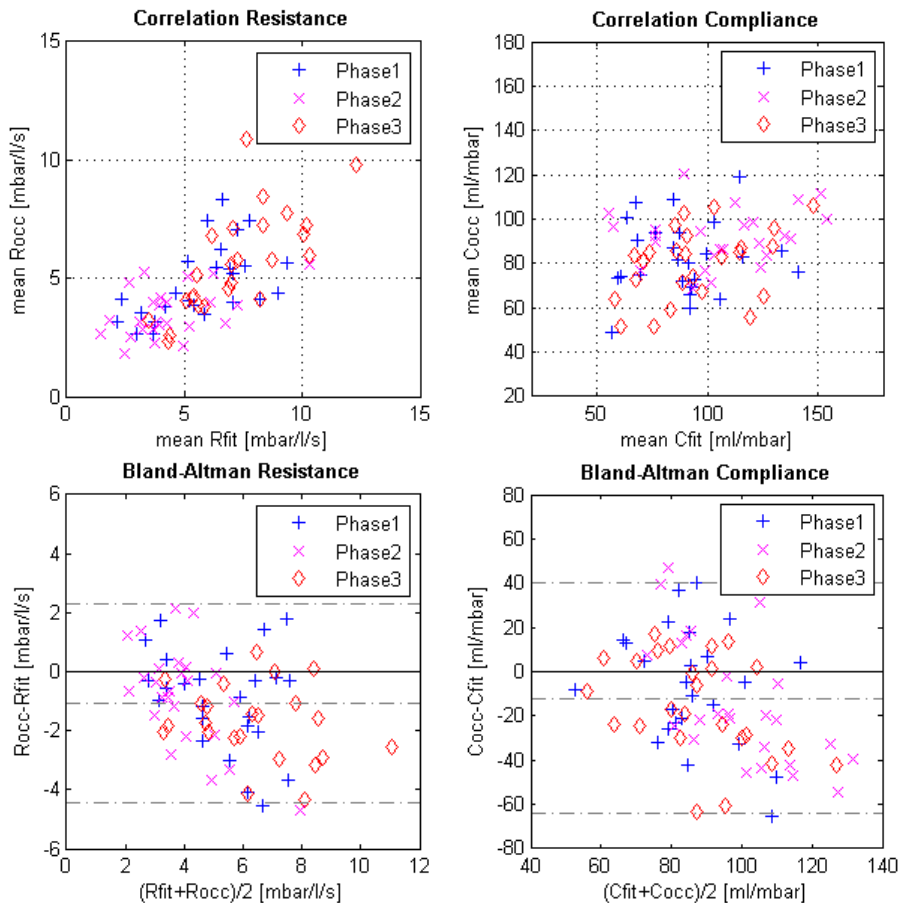


Figure 3-21: Analysis of mean R and C of all subjects per phase. R: Resistance. C: Compliance. Rfit, Cfit: R and C obtained with the simulated muscular pressure. Rocc, Cocc: R and C obtained with the Occlusion+Delta method. Phase 1: quiet breathing; Phase 2: increased effort; Phase 3: pressure support.

Main validation results for all subjects

The previous linear regression analysis shows low correlation, especially for C:

- $R_{occ} = 0.69 \cdot R_{fit} + 0.47$, $R^2 = 0.54$
- $C_{occ} = 0.17 \cdot C_{fit} + 68.67$, $R^2 = 0.07$.
- The differences are -1.39 ± 2.07 mbar/l/s for R and -8.33 ± 40.66 ml/mbar for C.

According to these results the O+D method can help to identify R but the determination of C is not precise enough.

The number of pairs of PTPinsp for each subject varied greatly (between 131 and 570). For a balanced analysis of all measurements together the same amount of pairs ($n'=100$) for each case was selected ($n = 2500$). The pairs were randomly selected.

Both linear regression and Bland-Altman analysis demonstrate positive agreement between the PTPinsp calculated from both methods:

- $PTP_{O+D} = 1.13 \cdot PTP_{P_{di}} - 0.85$, $R^2 = 0.84$
- mean differences (mean \pm 2SD) = 1.78 ± 7.18 mbar*s.

Figure 3-22 presents the corresponding plots showing only 10 points per volunteer for clarity.

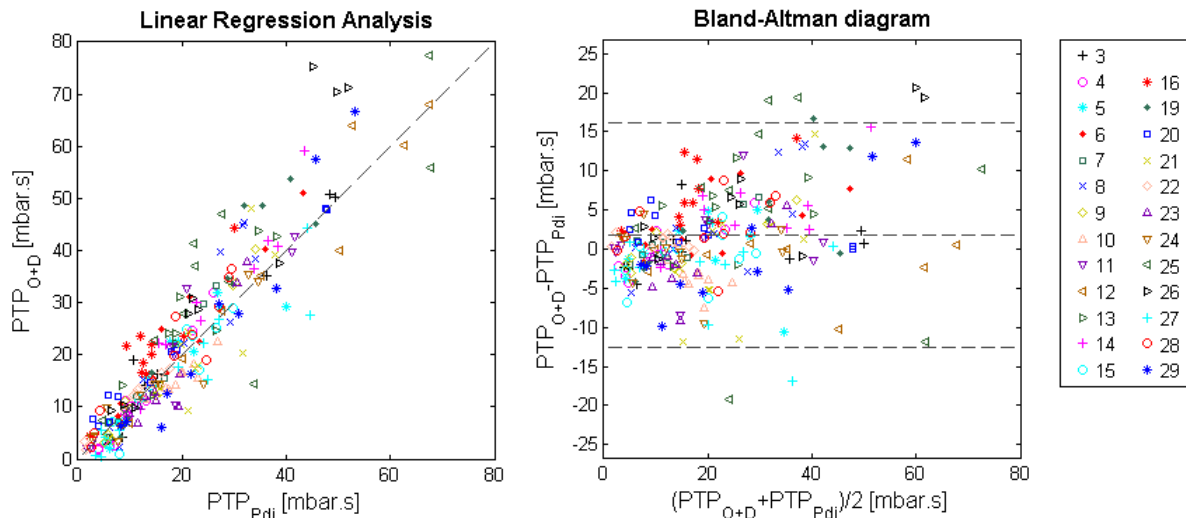


Figure 3-22: Regression and Bland-Altman analysis of PTPinsp from all volunteers
 PTPinsp: inspiratory pressure-time product. $PTP_{P_{di}}$: PTPinsp from the simulated pressure. PTP_{O+D} : PTPinsp from the pressure reconstructed with the O+D method.

3.3.2.4 Overall comparison of phases

As seen before, the differences in PTPinsp also varied between phases. The left panel of Figure 3-23 shows a box plot of the differences per phase. The outlier in phase 2 corresponds to subject 21. The mean differences of PTPinsp in mbar*s are 1.67 for phase 1, 5.44 for phase 2 and -0.43 for phase 3.

In the right panel of Figure 3-23 the values of subject 21 were omitted. The mean differences of PTP_{insp} in mbar*s are 1.62 for phase 1, 3.93 for phase 2 and -0.24 for phase 3.

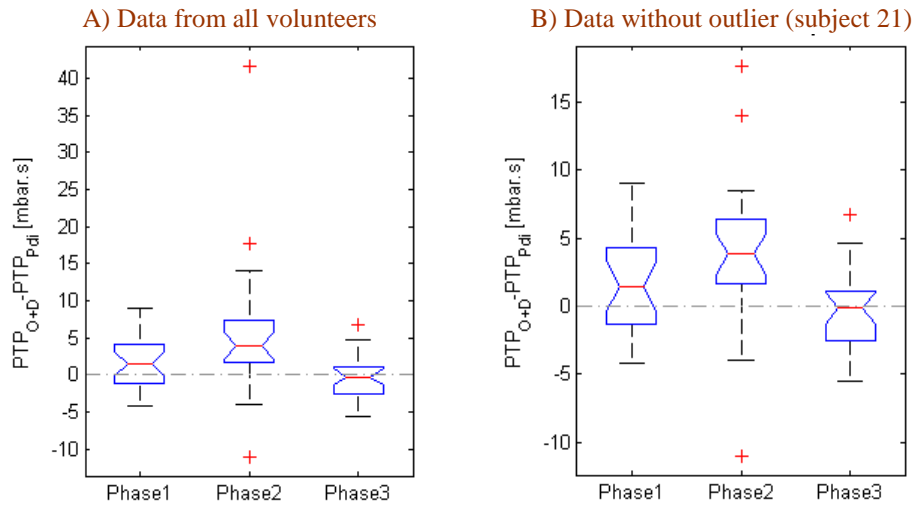


Figure 3-23: Overall mean differences in PTP_{insp} between phases.

PTP_{insp}: inspiratory pressure-time product. PTP_{Pdi}: PTP_{insp} from the simulated pressure.

PTP_{O+D}: PTP_{insp} from the pressure reconstructed with the O+D method.

Phase 1: quiet breathing; Phase 2: increased effort; Phase 3: pressure support.

3.4 Summary of main results

This section gives a simplified overview on the main results. Tables and figures can be found in the next two pages.

As seen in 3.3.1.3 the simulations served to successfully verify the principle and function of the O+D method. Next step was the validation with data from the study with volunteers.

Table 3-13 (same as Table 3-11) summarizes the results of the validation with each volunteer. It includes the mean values of R and C from each method. The results of linear regression (m, b), correlation (R^2) and Bland-Altman (mean and standard deviation of the differences) refer to the comparison of the effort by both methods.

As Figure 3-24 (same as Figure 3-17) shows, the mean R_{occ} was in 23 of 25 cases smaller than the mean R_{fit}, whereas the differences in mean C largely varied.

Figure 3-25 (same as Figure 3-18) presents all the differences in PTP_{insp} per subject.

Since R and C changed between phases, linear regression and Bland-Altman analysis were done using their mean values for each phase and each volunteer ($n = 75$). Regression analysis showed low correlation, especially for C ($R_{occ} = 0.69R_{fit} + 0.47$, $R^2 = 0.54$; $C_{occ} = 0.17C_{fit} + 68.67$, $R^2 = 0.07$). The differences were -1.39 ± 2.07 mbar/l/s for R and -8.33 ± 40.66 ml/mbar for C. As noted before, these results suggest that the O+D method can help to identify R but the determination of C is not precise enough.

Subj.	Rocc		Cocc		Rfit		Cfit		nPdi	m	B	R ²	BA	
	[mbar/l/s]	[mbar/l/s]	[ml/mbar]	[ml/mbar]	[mbar/l/s]	[mbar/l/s]	[ml/mbar]	[ml/mbar]					[mbar*s]	[mbar*s]
	mean	sd	mean	sd	mean	sd	mean	sd					mean	sd
3	3.71	0.68	98.2	20.9	5.12	1.87	101.1	22.1	417	1.00	-0.80	0.97	-0.83	2.52
4	3.21	0.64	86.2	19.1	3.15	1.33	74.4	18.9	493	1.25	-3.23	0.97	-0.08	3.14
5	3.44	0.73	92.3	28.8	4.57	2.34	119.0	26.7	321	1.07	0.55	0.86	1.71	4.15
6	6.11	1.66	82.5	28.5	6.43	2.08	104.9	27.4	286	1.2	0.02	0.96	4.4	4.05
7	7.09	2.94	71.4	26.5	7.95	3.8	85.2	23.7	541	1.23	-1.30	0.94	1.86	2.85
8	3.65	1.01	85.1	24.9	4.85	1.77	126.6	34.0	330	1.16	-1.25	0.93	2.32	4.32
9	4.01	1.5	91.7	28.3	4.42	1.94	66.0	11.2	495	1.20	-3.44	0.95	-0.35	3.03
10	5.02	1.52	95.2	28.5	7.28	3.94	67.7	21.0	280	0.88	-0.94	0.88	-3.4	3.24
11	4.57	1.53	58.9	20.8	5.3	2.15	62.1	10.3	456	1.11	-0.16	0.92	1.89	5.1
12	4.36	0.98	90.5	33.3	6.12	2.11	85.3	11.7	176	1.01	0.33	0.95	0.64	5.95
13	7.03	1.43	73.2	25.9	7.69	2.66	88.4	14.6	343	1.06	2.46	0.91	3.8	4.02
14	2.38	0.58	85.4	24.8	3.66	1.78	94.9	16.9	332	1.03	1.50	0.82	2.09	5.61
15	4.26	1.47	81.1	26.2	6.28	3.05	61.9	19.8	446	1.08	-1.79	0.86	-0.61	3.46
16	5.1	2.94	76.8	27.0	5.89	2.06	112.7	41.0	169	1.01	6.42	0.68	6.53	3.9
19	6.97	2.25	87.6	30.9	6.89	2.53	97.7	25.5	318	1.44	-6.28	0.88	3.96	8.43
20	6.75	1.86	67.9	20.7	6.77	2.04	110.0	33.5	192	0.98	4.39	0.97	4.01	2.97
21	2.35	0.54	100.1	28.2	4.2	2.92	106.6	25.7	131	1.97	-23.3	0.65	6.47	22.04
22	3.76	1.0	113.2	32.9	4.11	1.19	117.1	26.0	570	0.95	1.45	0.98	1.02	0.77
23	3.6	1.19	104.4	28.9	6.64	2.19	90.5	20.6	271	1.25	-7.24	0.87	-2.85	3.91
24	5.27	1.58	91.6	26.1	7.99	2.41	101.0	33.5	356	0.87	1.27	0.9	-0.88	3.93
25	4.74	2.43	71.7	22.4	7.43	3.31	98.6	18.8	249	0.92	9.34	0.84	6.69	8.52
26	4.02	1.09	70.6	18.8	7.02	2.13	101.2	22.6	288	1.38	-2.96	0.96	7.57	8.4
27	6.06	1.43	86.8	27.3	7.38	3.31	68.5	13.3	397	0.83	-0.75	0.89	-4.22	4.93
28	4.41	1.89	91.5	25.8	7.87	3.1	118.7	34.5	273	1.11	0.84	0.8	2.79	5.09
29	5.06	1.13	68.7	15.6	6.74	1.61	70.8	24.4	421	1.36	-9.7	0.95	-0.98	6.23
Min	2.35	0.54	58.9	15.6	3.15	1.19	61.9	10.3	131	0.83	-23.3	0.65	-4.22	0.77
Max	7.09	2.94	113.2	33.3	7.99	3.94	126.6	41.0	570	1.97	9.34	0.98	7.57	22.04

Table 3-13: Results of measurements with volunteers.

R: resistance. C: Compliance. Rfit, Cfit: R and C from invasive method. Rocc, Cocc: R and C from the novel method. nPdi: amount of cycles. m, b, R²: results of linear regression. BA: Bland-Altman analysis. The numbers in red are outliers.

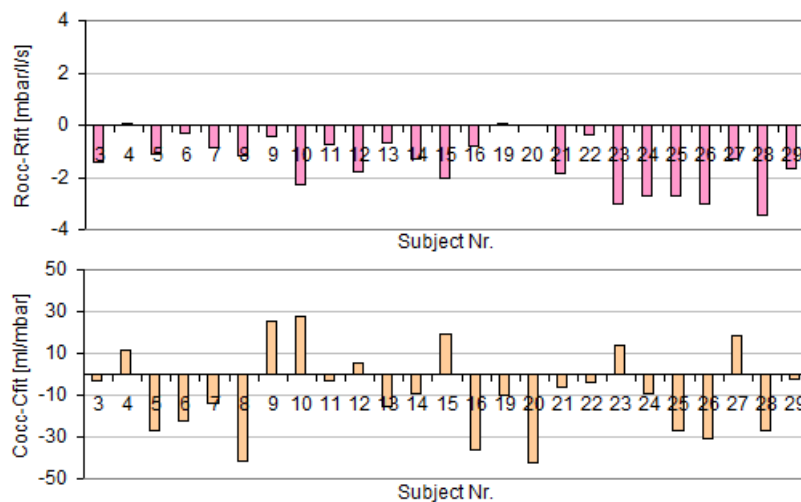


Figure 3-24: Differences in mean resistance and compliance between methods R: Resistance. C: Compliance. Rfit, Cfit: R and C obtained with the measured muscular pressure. Rocc, Cocc: R and C obtained with the Occlusion+Delta method

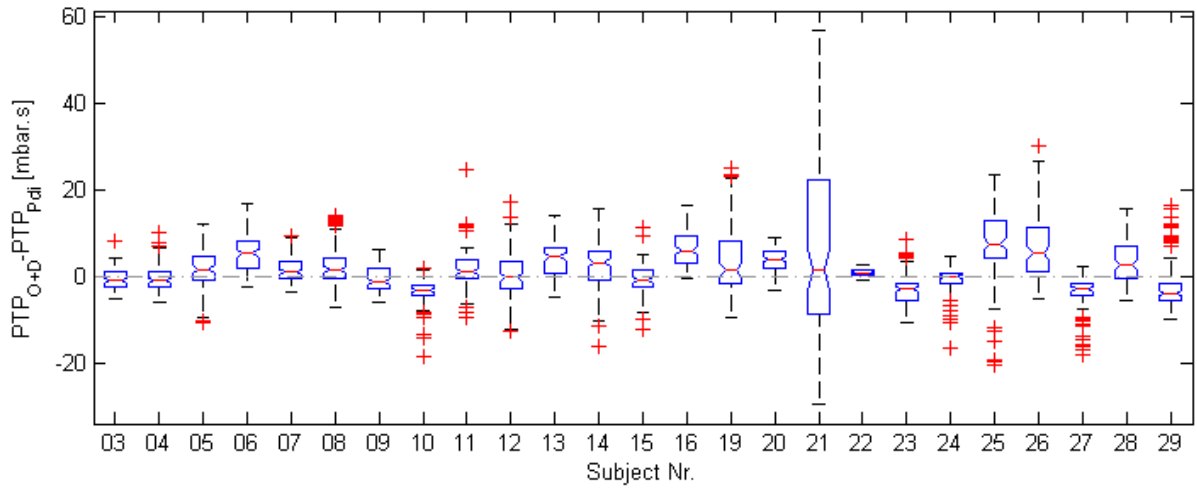


Figure 3-25: Differences in PTPinsp for all 25 volunteers
 PTPinsp: inspiratory pressure-time product. PTP_{Pdi}: PTPinsp from the simulated pressure. PTP_{O+D}: PTPinsp from the pressure reconstructed with the O+D method.

Finally, linear regression and Bland-Altman analysis were done using 100 randomly selected pairs of PTPinsp for each subject ($n = 2500$).

Both demonstrated acceptable agreement between the breathing effort measured as PTPinsp calculated from both methods:

- $PTP_{O+D} = 1.13PTP_{Pdi} - 0.85$, $R^2 = 0.84$
- mean differences (mean \pm 2SD) = 1.78 ± 7.18 mbar*s.

Figure 3-26 (same as Figure 3-22) presents the plots with 10 points per volunteer for clarity.

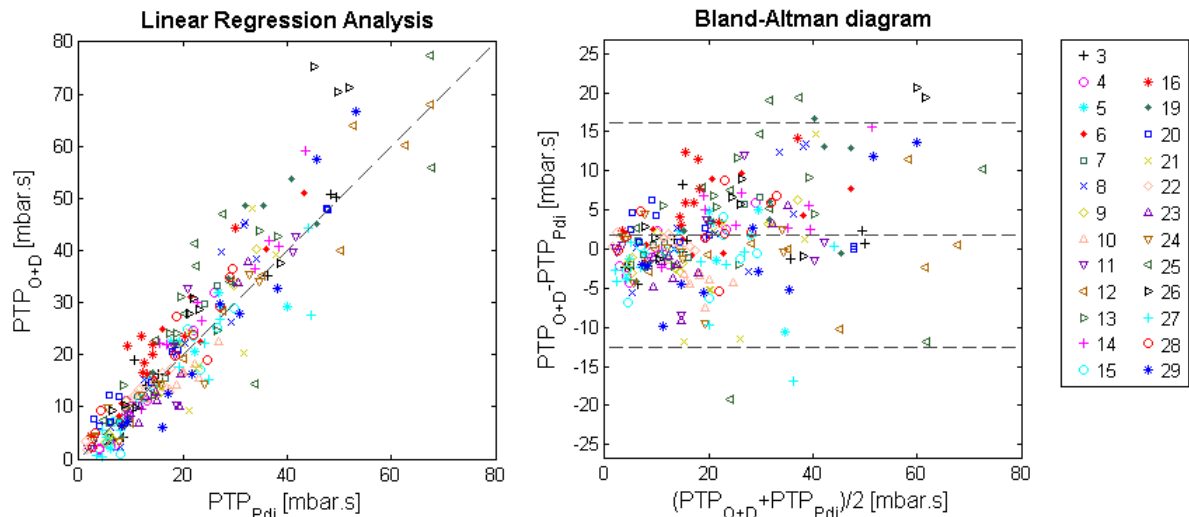


Figure 3-26: Regression and Bland-Altman analysis of PTPinsp from all subjects.
 PTPinsp: inspiratory pressure-time product. PTP_{Pdi}: PTPinsp from the simulated pressure. PTP_{O+D}: PTPinsp from the pressure reconstructed with the O+D method.

4 Discussion

This chapter is devoted to the discussion on some important aspects observed during the implementation and the validation of the results of the proposed Occlusion+Delta (O+D) method. It contains as well a comparison of it to the methods introduced as the state of the art.

4.1 Dealing with real data

4.1.1 Invasive measurement of Pdi

The use of a standard invasive method to measure transdiaphragmatic pressure (Pdi) was indispensable to have a reference for the verification of the non-invasive method O+D. For that reason, the results presented in the previous chapter involve data gained from the invasive measurement of Pdi using balloon-tipped catheters.

Previous studies have demonstrated that this technique gives a good approximation to the transdiaphragmatic pressure [7] but also that some issues must still be considered. In [63] the authors state that “It is commonly accepted that, in spite of some technical limitations and lack of accuracy, oesophageal pressure variations give a reliable estimate of pleural pressure variations” and then “Whereas oesophageal pressure has generally been used to accurately estimate the cyclical breathing variation of pleural pressure (...) the reliability of the absolute value of pleural pressure is somehow less defined”.

Since the invasive measurement of Pdi bases on the calculation of the difference between oesophageal and gastric pressure, their absolute values had to be carefully defined. The first step was the confirmation of the proper measurement of pressure by the balloons as done in 3.1.2.1. Besides this technical issue, numerous aspects must be taken into account: not only the artefacts caused by the heart beat and peristaltic or voluntary movements, but also the exact positioning of the balloons may influence the recorded signal. Implementing the steps previously introduced and discussed in this chapter, it was possible to measure and record Pdi getting the expected changes in its amplitude during the study with the volunteers.

4.1.1.1 Measurement of gastric pressure

Contrarily to previous studies like [43], [44], [45] this work also regards the measurement of gastric pressure for the estimation of muscular effort. During normal quiet breathing Pga is expected to have a relatively constant amplitude that is smaller than the amplitude of Pes. This was the case in 22 of the 25 subjects, as example A) in Figure 4-1 shows (subject 3), whereas the Pga of the subjects 11, 23 and 28 presented considerable variations of baseline and amplitude, as example B) shows (subject 11). In some cases Pga was relatively constant in amplitude, but was comparatively big in comparison to Pes, as the example C) shows (subject 7). In that sense, the overall analysis indicates that the measurement of Pga indeed carried important information in all cases for the calculation of Pdi. Finally, the plot in example D) of Figure 4-1 shows the signals recorded from subject 17 (not listed above): even after repeating complete placement of the catheter, no useful signals could be observed.

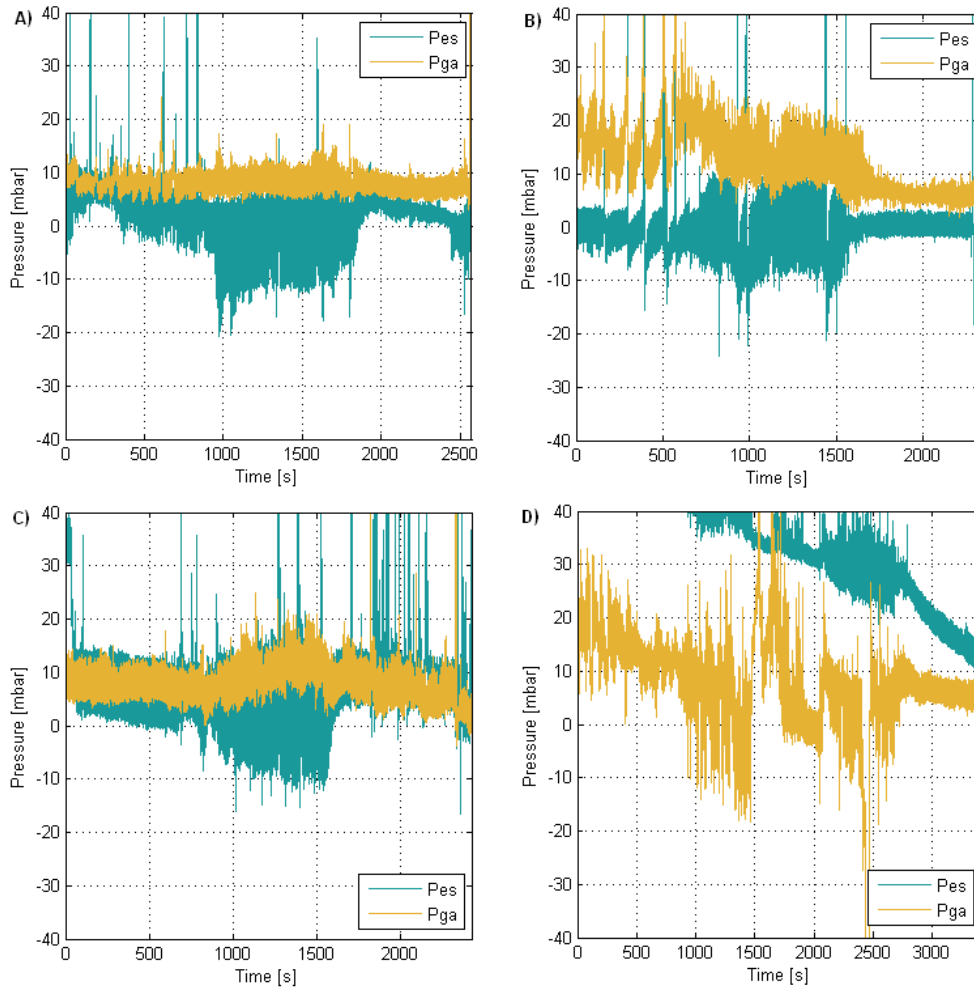


Figure 4-1: Observations on the invasively measured pressures
 Pes: oesophageal pressure. Pga: gastric pressure.

4.1.1.2 Disturbances, presumed reactions and cardiac artefacts

o Disturbances

The respiratory effort was quantified as the area under the inspiratory part of the measured Pdi (PTP_{Pdi}). A difficulty appears however if the measured signal presents disturbances. An example of this is illustrated in Figure 4-2 where Pdi contains a large deflection at the beginning of the cycle, which cannot be satisfactorily described by the linear single compartment model (see 1.2.3.1). In this case the unexpected form of Pdi returns a very low or even negative value for PTP_{Pdi} .

It is possible, indeed, that every now and then negative values for the area appear, but if this happens too often during quiet breathing one should suspect that the measurement of Pdi was problematic, particularly if flow, volume and airway pressure have standard forms like in the figure. In such a case the reconstruction of Pdi obtained with any positive values of R and C will logically also have a standard form, i.e. increasing in the inspiration and decreasing in the expiration. The area under the reconstructed pressure (PTP_{O+D}) would be larger. The difference between the areas from such cycles would be high. In the figure the magenta line represents Pdi; the reconstructed pressure (Pcmus) is shown in light green.

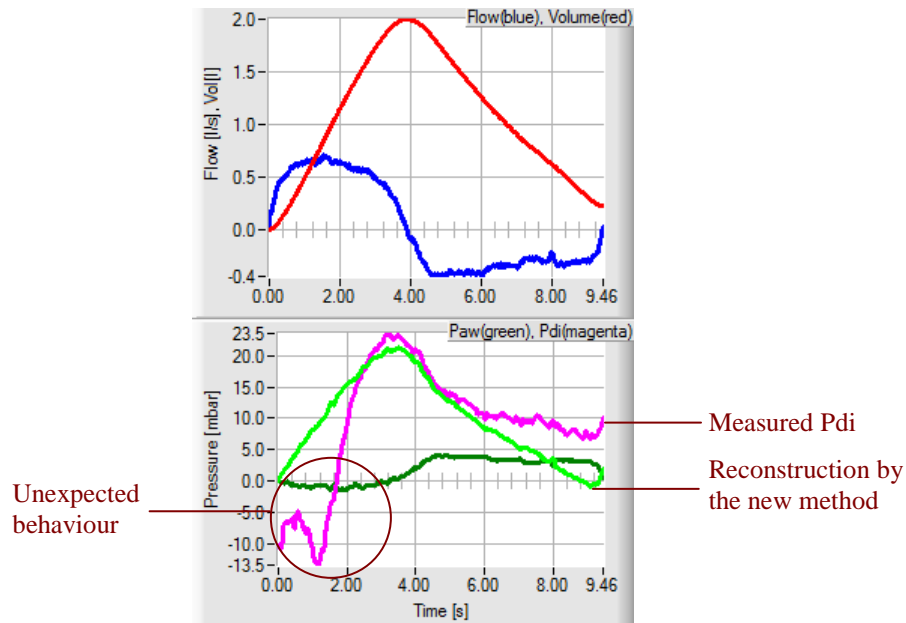


Figure 4-2: Divergence of areas due to a disturbance in Pdi.
Paw: airway pressure. Pdi: transdiaphragmatic pressure.

○ Presumed reactions to the occlusion

In some cycles a notable change in Pdi (suggesting a notable change in muscular pressure) can be seen after the occlusion onset. Figure 4-3 (left) shows an example of this. On the one hand, the MLR method applied on the whole cycle can not deliver physiological values of R and C. On the other hand, the assumption of Pdi being similar in this cycle and a previous one is weak and the O+D method will probably deliver outliers.

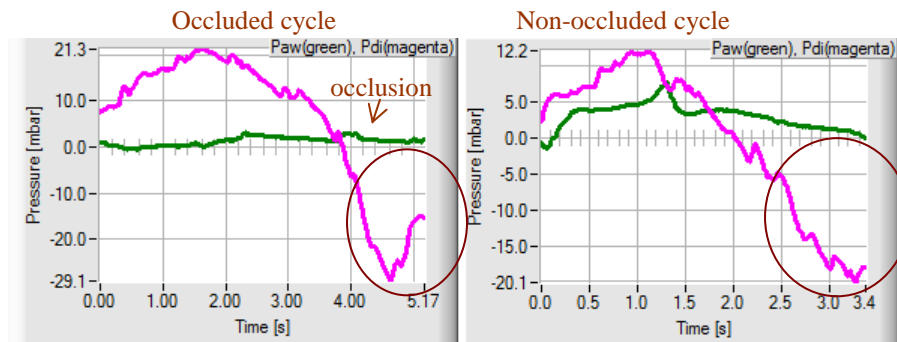


Figure 4-3: Presumed reactions of Pdi in an occluded and an undisturbed cycle
Paw: airway pressure. Pdi: transdiaphragmatic pressure. The large negative variation of Pdi may produce outliers in the model parameters.

The high negative variation of Pdi could be interpreted as a voluntary reaction to the occlusion, contradicting the theory about the normal reaction time of the diaphragm (<300 ms), or as artefacts due to internal displacement of the balloons. The second interpretation is rather acceptable because such changes of Pdi not only appear in occluded cycles but at any time of the measurement as Figure 4-3 (right) shows. Thus, such reactions cannot be directly related to the manoeuvre but rather to measurement artefacts.

- Filtering cardiac artefacts

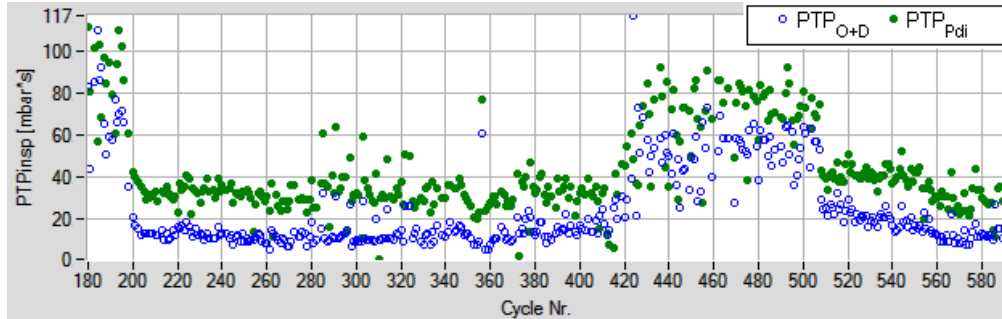
In this project the cardiac pressure waves observed in Pdi were filtered out after recording the data. The frequencies selected (0.8 to 8 Hz) covered the measured frequencies of the heart beat during quiet breathing. The process was not limited to a low-pass filter because noise that affects Pdi in the same manner as the other signals might contain important information for the fitting methods used in the MLR. Besides this, smoothed data would violate some of the assumptions of nonlinear (and linear) regression, because the residuals are no longer independent [64].

4.1.1.3 Constant and variable offset

The positioning of the balloon catheter requires a zero line which depends, among others, on the volume of air inflating the balloons. This may cause that a relatively constant offset appears in the measured Pdi. It is relatively constant because displacement of the catheter can also change the initial value. This is countered by fixing the position of the catheter during the measurement with skin-friendly tape to the cheeks. If Pdi is shifted by a relatively constant offset, the areas calculated under Pdi (PTP_{Pdi}) and the reconstruction Pcmus (PTP_{O+D}) differ even if the waveforms are virtually identical.

A constant offset can be corrected by identifying the baseline of Pdi, which can be obtained from the parameter P_0 delivered by the MLR method, and subtracting it from the measured signal. Figure 4-4 A) shows an example of the PTP_{insp} values from a recording with constant offset in Pdi. Figure 4-4 B) shows the results of the same file after subtracting the offset.

A) Before correction



B) After offset correction

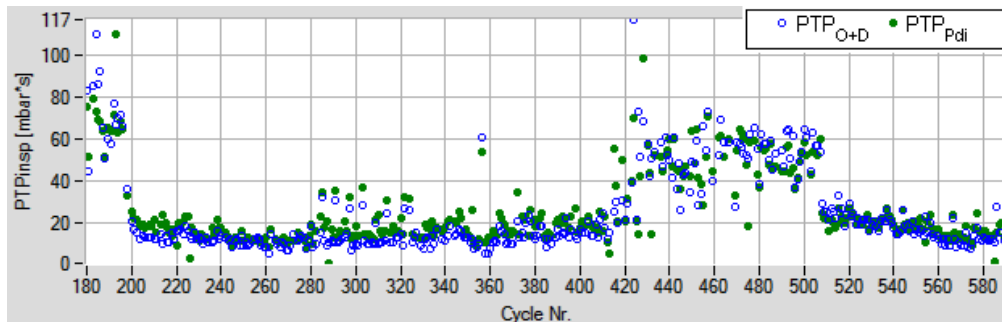


Figure 4-4: Effect of a constant Pdi offset in PTP_{insp} and correction

PTP_{insp} : inspiratory pressure-time product. PTP_{Pdi} : PTP_{insp} from the simulated pressure. PTP_{O+D} : PTP_{insp} from the pressure reconstructed with the O+D method.

If the test subject is fully relaxed, the muscular pressure at the end of the expirations is expected to be zero or the value that it had at the beginning of the cycle. However, slow

displacement of the catheter and/or slow change in the FRC (see 1.2.1.1) can produce a variable offset in the recorded pressure. Figure 4-5 shows a Pdi signal whose baseline varies with time. This offset can be removed if assuming that Pdi during quiet breathing is in fact equal at the beginning and the end of the cycles.

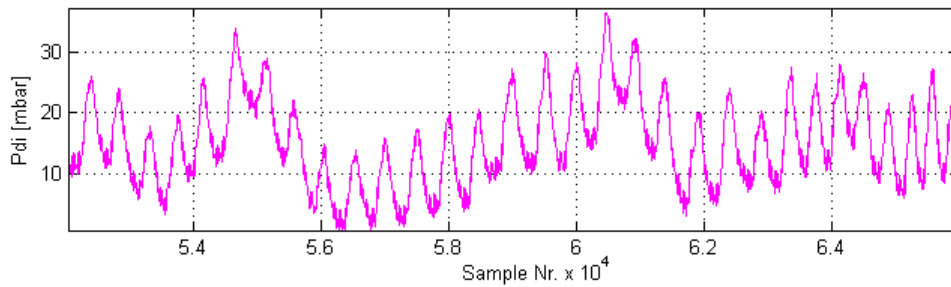


Figure 4-5: Changing offset in transdiaphragmatic pressure (Pdi)

Some considerations were necessary to correctly determine the offset. First, this determination is possible only for cycles with normal Pdi. Second, proper selection of the minima requires smoothing⁶ the signal. This was done by fitting the line to a 6th degree polynomial. Third, in cycles with slow increment of flow at inspiration begin it is possible that initial samples of Pdi (and thus the first minima) are missing. For this reason the baseline was not determined inside single cycles as the line connecting the minima of Pdi in the inspiration and expiration, but as the minima of the expiratory Pdi in adjacent cycles. The results of the baseline determination and offset correction were shown in 3.1.2.1.

In [65] the data from subject 7 and subject 9 were used to show that the differences in the results before and after using the filter and subtracting the varying offset are small. However their implementation permitted a more exact definition of the real Pdi, and with it, of the pressure actually being generated by the diaphragm for breathing. In both cases, linear regression and correlation analysis showed high agreement between methods ($R^2 > 0.85$).

4.1.1.4 Abnormal pressure signals

The exclusion of Pdi signals that do not correspond to quiet breathing (for example coughs or speaking) was highly relevant for the verification of the O+D method and was done by software. The rules described in 2.5.1 for recognizing cycles with abnormal⁷ Pdi were specified for this work, based on the knowledge of the system as modelled by the linear single compartment model. In the subjects 20 and 21 over 30% of all recorded cycles were deemed to have an abnormal Pdi. In the data from subject 16 this value was almost 60%. A reason for the differences between subjects is not obvious, neither from the data nor from the subjective answers from the subjects (to questions like whether they had to swallow more often than usual).

To give a clearer idea about what was defined as normal and abnormal Figure 4-6 shows in A) and B) two plots of normal and in C) and D) two plots of abnormal Pdi. Note that this classification is not valid for ASB where Pdi is expected to be close to zero during the entire cycle.

⁶ Note that the smoothed Pdi is only used to determine its baseline. The MLR is done with the raw signal.

⁷ *Abnormal* refers here only to the fact that the measured Pdi may not represent quiet breathing

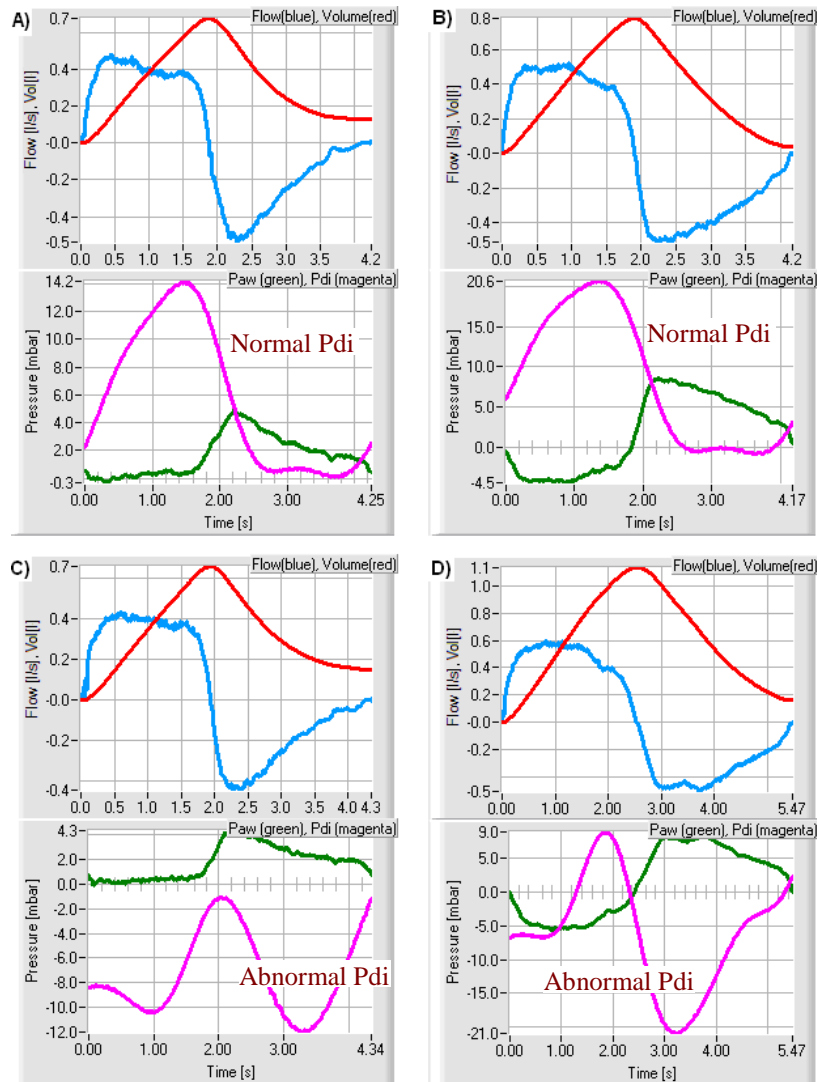


Figure 4-6: Cycles with normal and abnormal Pdi.
Paw: airway pressure. Pdi: transdiaphragmatic pressure.

4.1.2 Measurement of flow

4.1.2.1 Real expiratory flow

The technique called *the shutter method*, introduced in section 1.3.1.1 and early tested and documented in [26], was initially implemented in this work, using the breathing cycles that contained expiratory occlusions. No problems appeared in the determination of resistance, but only few breathing cycles showed the assumed exponential decrease of expiratory flow on which this technique bases for the determination of compliance. In the cases where the assumption seems strong (like in Figure 4-7) the flow-volume relationship can be described by a line with slope proportional to the time constant. This permits to calculate C .

In contrast, in more than 85% of the cases the decrease of the expiratory flow was not exponential (like in Figure 4-8) because the muscle relaxation is not complete or happens slowly. The flow-volume relationship is not linear and the time constant can not be reliably determined from its slope. If this is still done the values of C present large variance and a not negligible amount of results are far outside the range of real expectations.

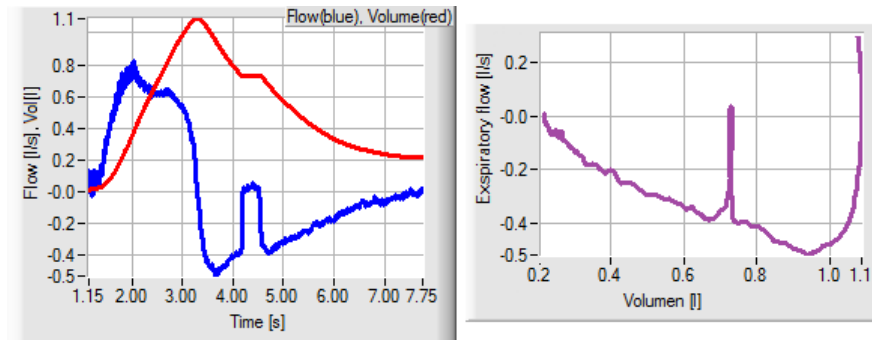


Figure 4-7: Exponential decrease of expiratory flow and FV-loop. Whole cycle (left) and expiratory flow volume loop (right).

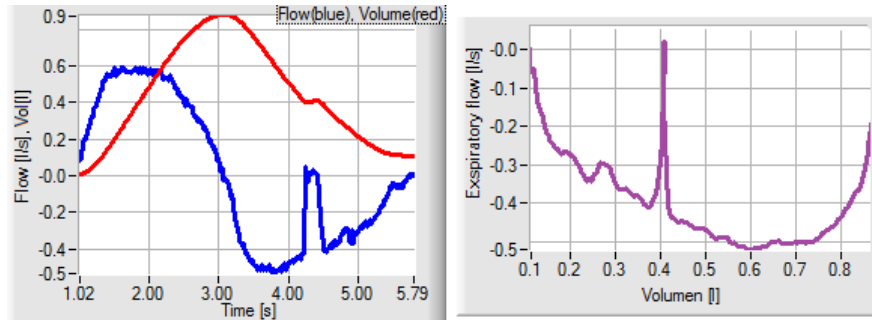


Figure 4-8: Non-exponential decrease of expiratory flow and FV-loop. Whole cycle (left) and expiratory flow volume loop (right).

4.1.2.2 Volume compensation and flow offset

Previous to the execution of the study with volunteers, data from an old study was available for the functional verification of the algorithms of the O+D method. These data had been modified, such that the flow was shifted up or down to compensate the volumes over a few cycles, i.e. to make the end-expiratory volume close to zero. That modification makes the data closer to a model of regular quiet breathing without hyperinflation, but was not adequate for being used in the MLR method. The appearance of a shift in flow becomes obvious in occluded cycles without leaks, where the flow during occlusion is constant but not zero. An example of this is shown in Figure 4-9.

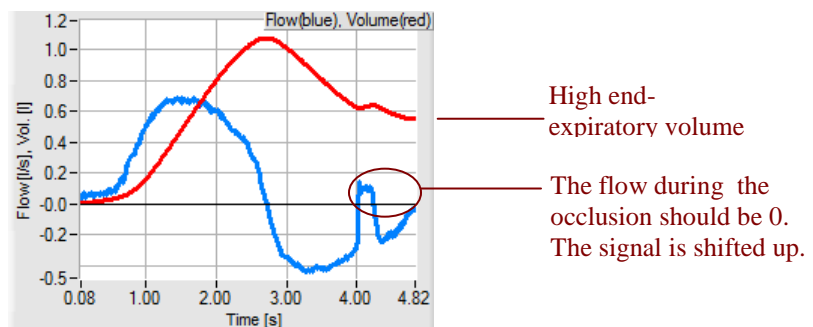


Figure 4-9: Offset in the flow signal

Even if it is done to compensate volume residuals, it is not a good idea to have an offset in the recorded flow. Whether introduced during the measurement due to lacking calibration of the sensors or entered in the offline analysis to compensate constant leakages trying to make the end volume zero, a shifting of the flow tends to produce a false volume and the variables entering the MLR method would return erroneous parameters.

The O+D method provides a solution to that problem because the occlusion, given that there are no leakages, shows where the real zero flow signal is located. On one hand, when an occlusion is found in a cycle with shifted flow, that occlusion can be used to correct the error. The following cycles can be then used to calculate R and C using MLR. On the other hand, the O+D method only uses the differences between signals, which means that if the selected pair of cycles have the same offset in the flow, the determination of R and C is still useful.

In the software written for O+D (see [Annex B](#)) the user can activate in the user interface the function “auto offset flow”. This will check the mean flow during the occlusion to shift the flow back to the real zero.

4.1.2.3 Quality of the occlusions

The occlusions were identified according to the waveform of the expiratory flow: a sudden decrease of flow towards zero, about 200ms of zero flow and a sudden return to a value close to that before occlusion. This identification method, here very simplified, may overlook occlusions with a very slow valve closure time. The occlusion shown in Figure 4-10 belongs to data from an old study and was done with an external magnetic shutter and recorded with a system of 100Hz sampling rate. Such slow onset of the occlusion may not only cause that the occlusion is not recognized but may also adulterate the values of C. By building a fast shutter (see [Annex C](#)) and using a measuring system with 5ms sampling rate this problem was avoided.

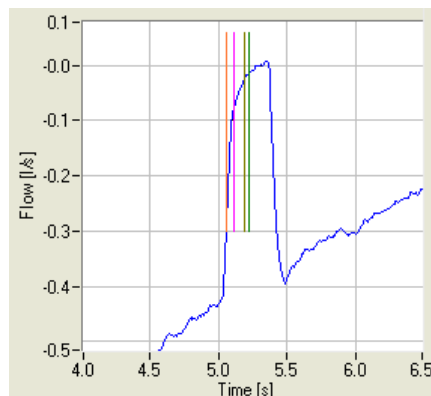


Figure 4-10: Flow signal from slow valve closure in an old study

4.2 The Occlusion+Delta method: Comparison to the state of the art

Mandatory ventilation is disadvantageous for patients that are able to breath spontaneously due to its inherent risks of causing lung damage, muscular atrophy and other consequences of adapting the patient to the ventilator, for example by sedation. The basis for the adaptation of assisted ventilation is the knowledge of the characteristics of the individual patient.

But the estimation of the parameters during assistance is more complicated than in controlled ventilation with sedated patients because: a) manoeuvres like long occlusions may be uncomfortable for the awake patient and are therefore hardly feasible, b) the varying muscular pressure must be constantly supervised making techniques that require quasi-static conditions not viable and creating results that are not reliable and c) the fact that the measurement must be done continuously, so that variable conditions are opportunely recognized, makes a robust but simple technique necessary.

The continuous assessment of muscular effort through invasive techniques, like measuring transdiaphragmatic pressure with balloon catheters or recording electromyography signals with electrodes inside the body, offers a good point of reference for assisted ventilation. But it also brings disadvantages, that already begin with the difficult positioning of the sensing elements and the increased risks of injury and infection. So, when measurements of muscular pressure are not feasible or acceptable, as for continuous monitoring, alternative non-invasive methods become necessary.

There are of course some similarities between the proposed method and the existing ones. The use of occlusions is one of them. A prominent method that bases on airway occlusions is the interrupter technique, previously summarized in 1.3.1.1.

This technique has been studied by numerous authors, for example in [19], [20], [21], [22], [23], [24], [25], who notably varied its implementation. For that reason, despite of its theoretical simplicity for the calculation of resistance, it lacked standardization over years [66]: Pesenti et al. [20] investigated first its application in partial ventilatory support by PSV and used dedicated valves to stop the inspiratory flow during 2 to 3 seconds in several breaths at different times and volumes. Bridge et al. [66] discussed in detail the conditions and calculations required by this method, whose application had been partially restricted to the determination of resistance and included inspiratory and expiratory interruptions. Bellani et al. [29] implemented the technique in a commercial ventilator arguing that slower valves do not impede the estimation of mechanics and would rather help to widespread the use of the technique. Its validation has mostly been done with oesophageal pressure measurements.

The assessment of muscular pressure by this technique is gained with flow interruptions (=occlusions) performed at different times and volumes to cover the whole tidal volume. Between interruptions at least 20 undisturbed cycles are allowed. In the O+D method proposed in this work, the occlusion is applied at any time from 300ms after the start of the expiration, in order to have enough measurement samples to establish the similarity of the cycles. For the validation study the occlusions were done after 3 to 7 undisturbed cycles, but in a future implementation this number can be greater.

Since the duration of the occlusions in the interrupter technique goes up to several seconds, it may disturb the patients and alter quiet breathing. The occlusions of the O+D only last about 200ms expecting less burden and reactions. Additionally, obtaining an assessment of the compliance directly from the equation of motion instead of from static manoeuvres is an advantage of the O+D, because it allows a thorough continuous assessment of respiratory mechanics. The implementation in a commercial ventilator is feasible with either method, but the speed of the valves must be contemplated.

Both methods serve also to calculate the muscular pressure but the approaches differ. The interrupter technique derives its values from the subtraction of a plateau pressure and the pressure right after the start of the interruption (see 1.3.1.1), whereas the O+D uses the estimated R and C for the calculation (see 2.1.4). In this sense, finding a plateau pressure that indicates relaxation is not an issue for the O+D. Furthermore, the assessment of the muscular pressure as the calculated muscular pressure P_{cmus} is obtained for each cycle instead of using several cycles to make one single estimation. This facilitates continuous assessment too.

Another well-known procedure to assess breathing effort with occlusions is the measurement of the P0.1 occlusion pressure, also introduced in 1.3.1.1, which is measured as an indication of the inspiratory force in the first 0.1 seconds of the inspiration [67]. Like all other variations of the manoeuvre where the flow is stopped by less than 300ms, the P0.1 does not generate physiological reactions since a muscular response would take longer [68]. Also the P0.1 occlusions are theoretically adequate to implement the O+D method. However this approach was not followed because:

- a) assuming smaller variations between cycles in the expiratory pressure seems more reasonable than assuming them in the inspiratory pressure. The reason is that the expiration is during quiet breathing a periodic passive process.
- b) it is not possible to make a comparison between cycles previous to a P0.1 occlusion, whereas a comparison of signals before an expiratory occlusion is indeed feasible.
- c) the amount of samples gained during an occlusion of 100 to 140ms is not advantageous over the amount of samples gained from an occlusion of twice its length.

The time inside the respiratory cycle at which the occlusion starts has also been subject of study. In the interrupter technique for instance, no crucial differences were found between the R found with interruptions done in the inspiration and with interruptions done in the expiration [66]. But for methods assuming the course or behaviour of P_{mus}, expiratory occlusions may be advantageous if the expiration is passive and therefore the effect of the muscular pressure is reduced [69]. The O+D method takes advantage of the passive behaviour of the expiratory phase to reduce the influence of the muscular force in the determination of R and C.

The study of O+D has been restricted in this very first stage to the evaluation of data from healthy volunteers, but future investigation could include patients with different pathologies. Further subjects of study for the novel method could be the effect of the volume in the transdiaphragmatic pressure or the expansion of models, for example, for the separation of R in lung- and airway resistance. Finally, the study of the O+D included the measurement of gastric pressure instead of the oesophageal pressure alone which provides useful information as documented in 3.1.2.1 and 4.1.1.1.

It has been shown that occlusion manoeuvres are a rather common procedure with great variation in its application. However, long interruptions may alter quiet breathing, particularly if periodically repeated. The Delta-Inst method, introduced in 2.1.2, avoids therefore entirely the use of occlusions. Nevertheless, it requires variations of pressure support which must be so clear that they and their effect on flow and pressure can be reliably measured. With that knowledge the proposed method O+D takes advantage of both, the interrupter technique and the Delta-Inst.

Resembling the principle of the Delta-Inst method variations are caused in one of the main variables to use multiple linear regression in a posterior step to obtain the parameters R and E. The main difference to the O+D consists on the selected variable. Instead of changing the support in a cycle, the proposed method uses an occlusion that generates direct changes in flow, volume and airway pressure. By interrupting the flow during only 200ms approximately, physiological reactions to the occlusion are virtually avoided. This implies a limitation in the amount of information available for the regression algorithms in comparison to the Delta-Inst method, but a wider background of measurements for the calculations in comparison to the interrupted technique. While the Delta-Inst method required P_{mus} to be constant over the complete breathing cycle, the O+D method has the advantage to require its similarity during only 200ms, which is more probable in the reality.

Advantageous for the implementation of the novel method is also the low requirement of additional devices. Except for the shutter, which can be installed inside the ventilator, no further hardware is required, minimizing implementation costs. If the expiratory valve of the ventilator is already able to produce occlusions, not even a shutter is required. All other features are covered by the software, which is written in the standard programming language C, facilitating its installation and test.

Direct comparison of the results from the different methods would be possible with a further study where a single population is studied with the relevant methods under fixed conditions.

4.3 Agreement between methods

The agreement between the invasive method and the non-invasive O+D was analyzed according to their values of R, C and PTP_{insp}. This subsection is dedicated to observations related to those data.

4.3.1 Resistance and Compliance

- R and C from the simulations

The O+D method was first verified using simulations. The values selected for R (2.5 and 5 mbar/l/s) describe a range of values usual for healthy adults. The values selected for C (25, 50 and 75 ml/mbar) rather represent stiff lungs, whereby the highest C is already close to the normal values of respiratory compliance. Considerations on temperature, air humidity and gas expansion were disregarded because all conditions were kept constant.

Nevertheless, there is some error between the calculations from the examined methods (R_{fit}, C_{fit}, R_{occ}, C_{occ}) and the real values of R and C used for simulation (see 2.2.2.2). The differences are reported in Table 4-1). This may occur because the mechanical elements used, similarly to the real anatomical system, are not completely linear; i.e. the values of R may change with the flow and the values of C may change with the volume. Interestingly, the resistance was in most cases underestimated, either by the control method or by O+D, whereas O+D tended to return slightly higher values for C.

Case	R _{occ} -R _{sim} [mbar/l/s]	C _{occ} -C _{sim} [ml/mbar]	R _{fit} -R _{sim} [mbar/l/s]	C _{fit} -C _{sim} [ml/mbar]
25--2	-0.56	2.50	-0.58	-1.09
25--4	-0.46	1.82	-0.18	-0.45
50--2	-0.26	2.28	-0.58	-0.48
50--4	-0.18	0.17	0.04	-1.44
75--2	-0.01	5.95	-0.45	-1.26
75--4	-0.31	-5.30	-0.29	-3.88
Min	-0.56	-5.30	-0.58	-3.88
Max	-0.01	5.95	0.04	-0.45

Table 4-1: Differences between mean resulting and simulated values of R and C.

R: Resistance. C: Compliance. R_{sim}, C_{sim}: simulated R and C.

R_{fit}, C_{fit}: R and C obtained with the simulated muscular pressure.

R_{occ}, C_{occ}: R and C obtained with the Occlusion+Delta method.

o R and C from real data

In the analysis of real data from the study with volunteers other factors as for example temperature and humidity play a role. Both conditions were kept constant in the room while the measurement took place.

Section 3.3.2.1 showed the mean resistances and compliances obtained for each volunteer. Both R and C present large variation independently of the method used to get them:

Their standard deviations go up to 2.94 and 3.94 mbar/l/s (i.e. 57.6 and 69.5% of the corresponding mean) for Rocc and Rfit respectively, and up to 33.3 and 41.0 ml/mbar (i.e. 37.1 to 36.4% of the corresponding mean) for Cocc and Cfit respectively (see Table 3-11). The average standard deviation for all volunteers are 1.44 mbar/l/s for Rocc, 2.38 mbar/l/s for Rfit, 25.6 ml/mbar for Cocc and 23.1ml/mbar for Cfit. As percentage of the corresponding means these values are 30.2, 30.4, 29.9 and 24.6%.

Such large variability of the parameters was not expected, but could be explained by a natural overall variation between the single cycles and by small differences in the signals that have large effect on the fitting algorithms.

Afterwards, section 3.3.2.2 (and [Annex F](#), Table F-2) showed the results classified in the three phases or levels of respiratory effort. Considerable variations could be seen in R and C between phases with either method. Figure 4-11 shows the results for subject 7 as example. In these plots both aspects can be seen: large dispersion of the results, particularly of Cfit (C from the invasive method), and clear variation of all resistances and compliances over time.

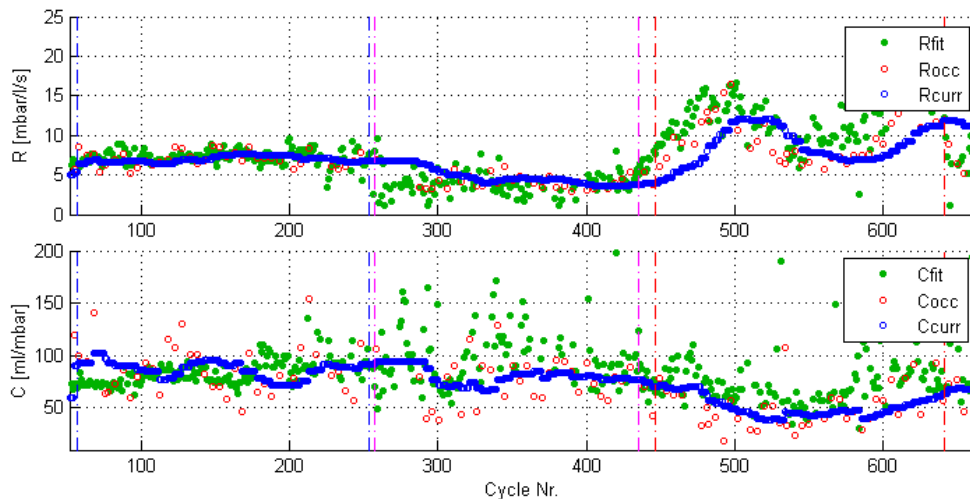


Figure 4-11: Example of large variation of R and C from real data
R: Resistance. C: Compliance. Rfit, Cfit: R and C obtained with the simulated muscular pressure. Rocc, Cocc: R and C obtained with the Occlusion+Delta method. Rcurr, Ccurr: moving averages from Rocc and Cocc.

Figure 4-12 offers a graphical overview on the mean values of R and C per volunteer per phase. Like in subject 7, a trend in the mean R of the other subjects can be recognized, according to which Rfit and Rocc tend to increase in phase 3 (pressure support by ASB) and to decrease in phase 2 (increased effort through added dead space). The differences in C are not that evident from the graphics.

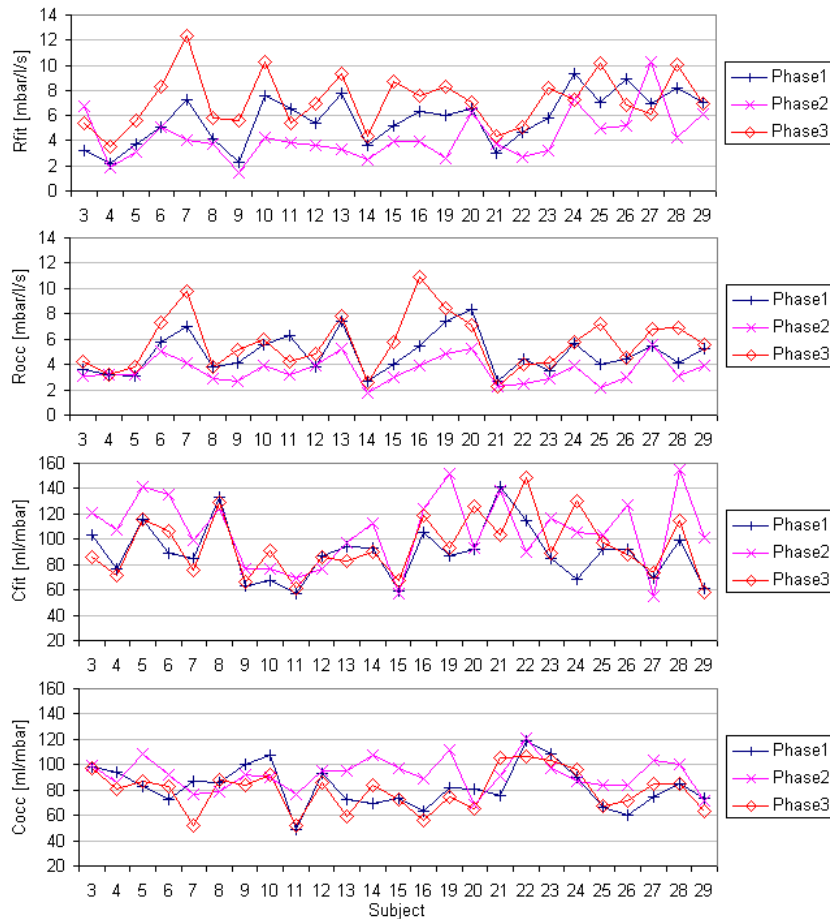


Figure 4-12: Mean R and C per volunteer per phase
 R: Resistance. C: Compliance. Rfit, Cfit: R and C obtained with the simulated muscular pressure. Rocc, Cocc: R and C obtained with the Occlusion+Delta method.
 Phase 1: quiet breathing; Phase 2: increased effort; Phase 3: pressure support.

The box plots in Figure 4-13 summarize all means, making clear that the mean resistances are significantly different between phases ($p < 0.05$). Cfit does not significantly differ between phases ($p = 0.054$) but Cocc does ($p < 0.05$).

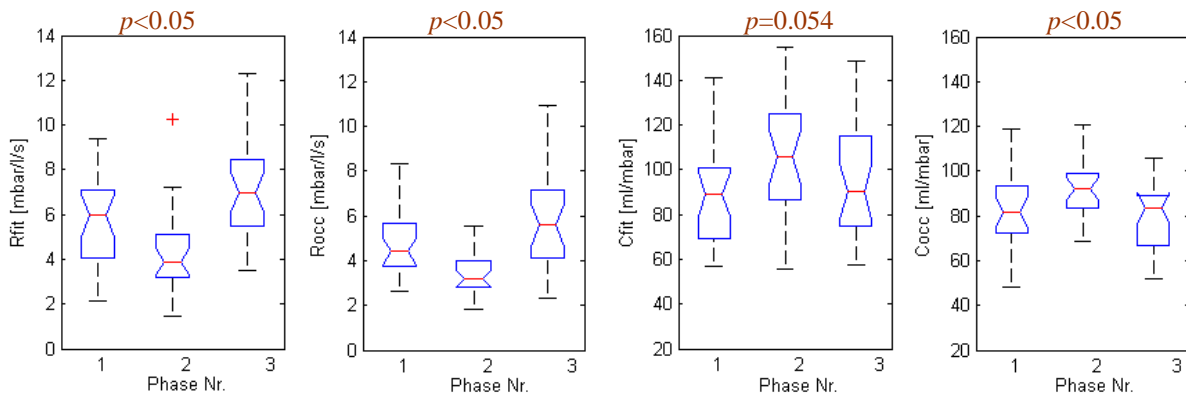


Figure 4-13: Mean R and C per volunteer per phase – Box plots
 R: Resistance. C: Compliance. Rfit, Cfit: R and C obtained with the simulated muscular pressure. Rocc, Cocc: R and C obtained with the Occlusion+Delta method.
 Phase 1: quiet breathing; Phase 2: increased effort; Phase 3: pressure support.

As well as the large variability of the parameters, their variation over time was not expected, but could be explained as a natural reaction to the amount of volume delivered to the lungs and the inspiratory flow: when the respiratory system is partially non-linear, R is flow dependent and C is volume dependent. In phase 2 the effort increases but is unconsciously compensated by the subjects, who start breathing slower (lower flow) and deeper (higher tidal volume). This may result in smaller R and bigger C.

Conversely, in phase 3 the support delivered by the Evita4 is given with a rapid change in pressure from 0 to the desired constant level (10 mbar) which is then sustained during the whole inspiration. The initial fast increase of pressure causes high positive flow; the sudden termination of pressure support at inspiration end causes high negative flow. Due to the fact that the subjects are not used to let the ventilator do the work of breathing their breaths are not as deep as in phase 2. Particularly the duration of the inspiratory phase is strongly influenced by the ventilation mode, causing a reduction in tidal volume. In a non-linear system, higher flows and smaller volumes may result in bigger R and smaller C.

The correlation between Rfit and Rocc was acceptable ($R_{occ} = 0.69 \cdot R_{fit} + 0.47$, $R^2 = 0.54$, $r = 0.73$) and much higher than the correlation between Cfit and Cocc ($C_{occ} = 0.17 \cdot C_{fit} + 68.87$, $R^2 = 0.07$, $r = 0.26$). Besides neglecting non-linear effects, a common problem determining C is the additional compliance that may appear in regions of the respiratory system outside the lungs, for example in the oro-pharynx and in the cheeks. The extra-thoracic compliance is not considered, neither by the reference method nor by the O+D method. Both are based on the linear single-compartment model. Finding an appropriate method to robustly evaluate extended models with data from O+D may bring substantial information about detailed real lung mechanics. In a practical sense, the relevance of the compliance of the cheeks is usually reduced by pressing the cheeks with the fingers or with the mask itself during ventilation to avoid their inflation.

4.3.2 Agreement of PTP_{insp}

The agreement between methods with respect to the determination of PTP_{insp} was measured by linear regression and Bland-Altman analysis. The agreement of PTP_{insp} in the simulations (see 3.3.1) varied between cases. Those with the lowest compliance (25 ml/mbar) had greater mean differences of PTP_{insp} than those with higher values of C (50 and 75 ml/mbar): -4.56 and -3.50 mbar*s against -1.35, -0.53, -0.8 and 0.34 mbar*s. Such differences may be a product of the error in C, the error in R, the combined error in R and C, an error in the calculation of the simulated muscular pressure, a neglected offset in the reconstructed pressure, or a combination of factors. Despite the increased error in the cases with low C all the differences were acceptable when compared to the absolute values of PTP_{insp}.

In section 3.3.2.3 the agreement was measured for the data from volunteers. Linear regression showed the correlation for the PTP_{insp} values of the single volunteers ($0.65 < R^2 < 0.98$, $0.806 < r < 0.989$) and for the overall analysis ($PTP_{O+D} = 1.13 \cdot PTP_{Pdi} - 0.85$, $R^2 = 0.84$, $r = 0.916$). This means that the estimation of respiratory effort made by the O+D method effectively follows the respiratory effort that one would get with the invasive measurement.

The mean differences in PTP_{insp} lay between -4.22 and 7.57 mbar*s with standard deviations between 0.7 and 8.62 mbar*s. The mean differences depend partially on the

determination of the baseline of the invasively measured Pdi and on the PEEP level used⁸ which makes part of the calculated reconstruction of the muscular pressure (Pcmus).

Whether the differences in PTPinsp are acceptable is rather a clinical issue, but in this work they have been observed under a “critical” value of 5 mbar*s for the mean and 5 mbar*s for the standard deviations, because the maximum difference obtained with the simulator in ideal conditions was -4.56 mbar*s. To this respect there are two further important aspects to consider: 1) the absolute values of PTPinsp, and 2) the adequacy of the RC model.

The discussion on the first point is shorter: Dependency between the variances and the means, as can be observed in the presented Bland-Altman diagrams, is a common fact in the analysis of biological data, and is usually treated using logarithmic or squared root transformations [60], [69]. In this study however, there is a considerable amount of small values for PTPinsp (desired and expected when giving support ventilation) and even negative values (when the volunteer breathes against the ventilator or just through inaccuracies in the measurement). This makes the logarithmic or squared root transformations not applicable and a percentual transformation of little sense.

The second point is also interesting: Is the divergence in PTPinsp only a result of the differences in the estimated R and C, or are there other factors apart from the determination of R and C that also cause such differences? In other words: Is the linear single-compartment model with parameters R and C adequate enough to make a satisfactory reconstruction of the transdiaphragmatic pressure? This question is discussed in detail in subsection 4.3.3.

o Differences between phases

Linear regression analysis would be misleading to evaluate single phases because the ranges of the variables of PTPinsp (PTP_{Pdi} and PTP_{O+D}) are restricted to the group of values more or less distributed around a single mean. But separated analysis of the effort levels is appropriate by Bland-Altman analysis as presented in 3.3.2.2 and 3.3.2.4.

A closer look to the single phases of measurement shows that the largest differences appear during increased effort (phase 2). This may occur because of several reasons. First, the natural breathing is disturbed such that the volunteers do not only need to put more effort but also tend to breath slower: a longer inspiratory time means also a higher PTPinsp. Second, a constant elevated effort can not be sustained over long time by the volunteers, causing higher variability between breaths.

The determination of the model parameters R and C by the O+D method is of course crucial for the non-invasive assessment of PTPinsp being close or not to the real effort. The definition of PTPinsp as the product from pressure (Pdi or Pcmus) and inspiratory time implies that its values, and so their differences, are proportional to the duration of the inspiration. The error between the invasively measured Pdi and its non-invasive assessment Pcmus, can be expressed according to the equation of motion of the single compartment RC model as

$$|P_{di}-P_{cmus}| = V'(dR+(1/dC)t)$$

⁸ for all subjects during the whole measurement PEEP was set to 1mbar

showing that their difference is not only influenced by the estimation errors in R and C (dR and dC), but also partly by the time t .

Errors in R or C , even if small, are thus reflected by P_{cmus} being (graphically) over or under P_{di} , so that the difference in the areas under the curve, i.e. in PTP_{insp} , will always increase for longer inspiratory times as the simplified scheme in the Figure 4-14 shows. The expected difference in PTP_{insp} for cycles with short inspiratory time t_1 is represented by $A1$, whereas for longer cycles with inspiratory time t_2 the expected difference in areas is given by $A1+A2$.

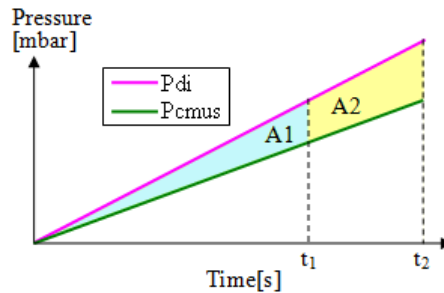


Figure 4-14: Scheme of expected differences in PTP_{insp}
 P_{di} : the simulated pressure, P_{cmus} : the calculated muscular pressure.
 The expected difference for cycles with short inspiratory time t_1 is represented by $A1$, whereas for longer cycles with inspiratory time t_2 the expected difference in areas is given by $A1+A2$.

4.3.3 Suitability of the RC model

Assuming that the proposed non-invasive O+D method would be capable of giving the same values of R and C that the MLR with invasive measurement of P_{di} gives, the reconstruction of P_{cmus} and thus the assessment of PTP_{insp} should be much closer to the reality.

The O+D method, which does not know P_{di} , returns R_{occ} and C_{occ} and uses them to make the reconstruction (P_{cmus}) and its area under the curve (PTP_{O+D}). This area is compared to $PTP_{P_{di}}$ which is the area under the invasively measured P_{di} . Now, if knowledge of P_{di} is an advantage, using R_{fit} and C_{fit} , i.e. the values of the parameters calculated by MLR with invasively measured P_{di} , to make the reconstruction of P_{di} and the calculation of the area under the curve would return values of PTP_{insp} (PTP_{MLR}) closer to $PTP_{P_{di}}$.

This hypothesis was tested by using R_{fit} and C_{fit} to make P_{cmus} and comparing its area to $PTP_{P_{di}}$. The results are shown in Table 4-2. From these data one can conclude that knowledge of P_{di} does not assure a perfect determination of R and C because these are just parameters of a simplified model. Note that the standard deviations lay between 0.94 and 6.96 mbar*s. Separate analysis of the three phases shows again increased differences for increased means, i.e. for phase 2 (see the results of subject 15 as an extreme example in Figure 4-15). This analysis demonstrates that not only R and C must be accurately determined, but also that the suitability of such a simplified model is limited.

A drawback of using R_{fit} and C_{fit} for the reconstruction is that, although the differences in PTP_{insp} are smaller, the amount of cycles ($n_{P_{di}}$) with normal P_{di} , undisturbed flow and airway pressure and values of R and C inside the physiological range greatly reduces (between 54 and 301 cycles less!). That means that the estimation is more accurate but also

infrequent. The difference in the amount of such cycles is shown in the last column of Table 4-2.

Subject	nPdi	m	b	R ²	BA [mbar*s]		Diff. in nPdi
					mean	sd	
3	257	0.99	0.24	1	-0.03	0.95	-160
4	192	0.97	-0.85	0.99	-1.11	1.09	-301
5	167	0.94	-0.19	0.97	-1.16	1.63	-154
6	198	0.88	2.63	0.97	0.13	2.09	-88
7	417	1.07	0.13	0.95	1.04	1.77	-124
8	216	0.97	-2.25	0.98	-2.99	1.94	-114
9	238	0.92	1.65	0.96	0.77	1.17	-257
10	189	0.92	3.50	0.94	1.92	2.09	-91
11	334	1.10	-0.02	1	1.89	1.85	-122
12	98	1.21	-0.76	0.98	5.97	6.96	-78
13	250	1.02	0.87	0.97	1.16	1.80	-93
14	198	0.88	3.81	0.97	1.29	2.13	-134
15	283	1.25	-0.41	0.94	2.98	2.98	-163
16	80	0.86	3.53	0.95	1.54	1.24	-89
19	189	1.02	-2.88	0.96	-2.40	2.46	-129
20	136	0.99	-0.63	0.98	-0.77	2.13	-56
21	77	1.09	-2.92	0.97	-0.48	2.46	-54
22	458	1.14	0.26	1	1.55	0.94	-112
23	179	0.84	3.78	0.96	1.08	1.52	-92
24	277	0.98	0.54	0.98	0.16	1.77	-79
25	187	1.03	0.71	0.99	1.62	1.89	-62
26	214	1.00	1.25	0.99	1.33	1.32	-74
27	304	1.15	-2.19	0.97	0.79	3.51	-93
28	175	0.98	2.13	0.98	1.79	1.43	-98
29	325	1.03	-0.79	0.99	-0.14	1.55	-96

Table 4-2: Agreement of PTP_{insp} using values of MLR for the reconstruction of muscular pressure. The last column shows the reduction in the amount of normal cycles that result in R and C inside the physiological range.

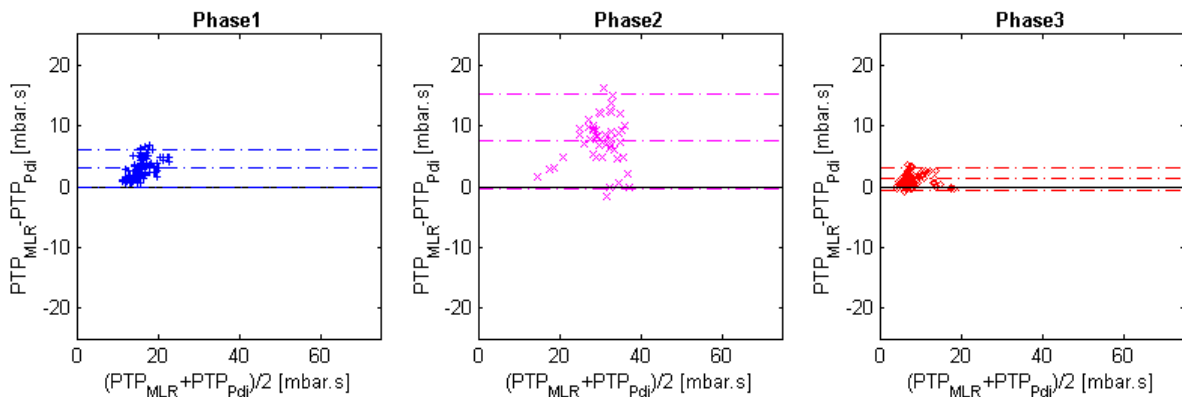


Figure 4-15: Example of agreement per phase using PTP_{MLR}

PTP_{insp}: inspiratory pressure-time product. PTP_{Pdi}: PTP_{insp} from the invasively measured pressure. PTP_{MLR}: PTP_{insp} from the reconstruction using parameters from MLR. Phase 1: quiet breathing; Phase 2: increased effort; Phase 3: pressure support.

5 Conclusions and Outlook

Goal of this work was the development and verification of a method to estimate continuously and non-invasively respiratory mechanics described by the single compartment RC model and respiratory effort quantified by the inspiratory Pressure-Time-Product (PTP_{insp}). The verification setup consisted of dedicated hardware (shutter, measurement box) and dedicated software and was implemented to analyse data gained from simulations with the lung simulator LS4000 and from a study with 25 healthy volunteers.

The control variable (PTP_{Pdi}) is the PTP_{insp} calculated from the transdiaphragmatic pressure (Pdi), which was first simulated and later, in the study, invasively measured using double-balloon catheters. The method developed here is called Occlusion+Delta (O+D) and was implemented to continuously give estimations (R_{occ}, C_{occ}) of respiratory resistance R and compliance C, and to use them to make a reconstruction (P_{cmus}) of the muscular pressure and a non-invasive estimation of the respiratory effort (PTP_{O+D}). The O+D requires expiratory occlusions of about 200ms and bases on the similarity of the muscular pressure between cycles of quiet breathing to eliminate the need for knowledge of Pdi.

The estimation of parameters in O+D was solved with base on the equation of motion of the linear RC model. The implementation of hardware was successful and did not present any problems during its utilisation. All measurement systems as well as the specific software performed as planned and expected. After thorough analysis with simulated cases, the study with volunteers followed. The study included 10 smokers and 15 non-smokers, all male and healthy. They breathed in three levels of spontaneous breathing: normal quiet, with increased effort by augmented dead-space and with reduced effort as supported by 10mbar of support ventilation. The short occlusions required by the O+D method were executed by the shutter and did not disturb any of the subjects involved in the study.

The suitability of the O+D method to replace the invasive measurement of Pdi was measured according to the agreement in the mean estimated parameters (R_{occ}, C_{occ}) to the mean parameters obtained with the invasive method (R_{fit}, C_{fit}) and the level of agreement between assessed and measured respiratory effort revealed by correlation, confidence intervals, mean differences and standard deviations of the differences.

In the simulations with the LS4000 linear regression and Bland-Altman analysis demonstrate high agreement between R and C (R_{occ} = 0.85*R_{fit} + 0.55, R²= 0.99; C_{occ} = 1.00*C_{fit} + 2.48, R²= 0.98; differences in R = 0.04±0.57 mbar/l/s; differences in C= 2.67±5.62 ml/mbar) and also between the PTP_{insp} calculated from both methods (PTP_{O+D} = 0.83*PTP_{Pdi} + 2.85; mean±2SD of the differences = -1.73±3.58 mbar*s; n=552).

The data gained from the study with volunteers required deeper analysis and processing. This begun with the identification of abnormal cycles, the correct identification of occlusions, the recognition of effort levels, the elimination of artefacts from heart and peristaltic movements on Pdi and the recognition of leaks.

The estimation of R by O+D tended to be lower than the R calculated with the invasive method, whereas the differences in C varied largely. Linear regression analysis showed

5 Conclusions and Outlook

low correlation, especially for C ($R_{occ} = 0.69 \cdot R_{fit} + 0.47$, $R^2 = 0.54$; $C_{occ} = 0.17 \cdot C_{fit} + 68.67$, $R^2 = 0.07$; differences in R = -1.39 ± 2.07 mbar/l/s; differences in C = -8.33 ± 40.66 ml/mbar). According to these results, the O+D method can help to identify R but the determination of C is not precise enough. Besides this, R and C considerably varied independently of the method used: the average standard deviations of all volunteers were 1.44 mbar/l/s for R_{occ} , 2.38 mbar/l/s for R_{fit} , 25.6 ml/mbar for C_{occ} and 23.1 ml/mbar for C_{fit} . The results of one subject were considered as outliers.

In the subjects analyzed separately linear regression showed positive agreement of PTP_{insp} ($0.65 < R^2 < 0.98$), whereas the Bland-Altman analysis showed acceptable agreement (mean differences between -4.22 and 7.57 mbar*s with standard deviations of the differences between 0.77 and 8.52 mbar*s) with large differences between subjects. Additionally, the overall analysis of the study with volunteers revealed positive agreement between the PTP_{insp} calculated from both methods ($PTP_{O+D} = 1.13 \cdot PTP_{Pdi} - 0.85$, $R^2 = 0.84$; mean $\pm 2SD$ of the differences = -1.78 ± 7.18 mbar*s; $n=2500$).

Interestingly R and C changed during the different phases classifying the levels of effort. A separate analysis of phases revealed higher differences and deviations during the phase of augmented effort. Those were related to the fact that the subjects tended to breath slower than usual, which directly influences PTP_{insp}, and to the increased variability of signals between breaths. The logarithmic or percentual transformation typically used to diminish the dependence of variance and mean in the Bland-Altman analysis was not appropriate, due to the presence of small and negative PTP_{insp} values during support ventilation. All in all, the measurement of Pdi and its non-invasive assessment by the O+D method delivered similar values of PTP_{insp} as expression of breathing effort.

In conclusion, the results obtained here demonstrate the potential of the Occlusion+Delta method to assess non-invasively Pdi and PTP_{insp}. Its easy implementation makes the O+D method suitable for analysis in a clinical study including patients with restrictive and obstructive pathologies. The determination of R and C can still be improved to offer a more exact estimation of the muscular pressure, as far as the respiratory system of the patient can be modelled as an RC compartment and the muscular effort is done by the diaphragm.

The Occlusion+Delta method offers a non-invasive alternative to continuously assess respiratory effort during spontaneous breathing and support ventilation, oriented to guide a fast and adequate adaptation of ventilation parameters to the patient's demands.

6 Literature

- [1] A. Esteban, N. D. Ferguson, M. O. Meade, F. Frutos-Vivar, C. Apezteguia, L. Brochard, K. Raymondos, N. Nin, J. Hurtado, V. Tomicic, M. González, J. Elizalde, P. Nightingale, F. Abroug, P. Pelosi, Y. Arabi, R. Moreno, M. Jibaja, G. D’Empaire, F. Sandi, D. Matamis, A. M. Montañez, and A. Anzueto, “Evolution of mechanical ventilation in response to clinical research,” *Am. J. Respir. Crit. Care Med.*, vol. 177, no. 2, pp. 170–177, Jan. 2008.
- [2] C. Putensen, R. Hering, T. Muders, and H. Wrigge, “Assisted breathing is better in acute respiratory failure,” *Curr. Opin. Crit. Care*, vol. 11, no. 1, pp. 63–68, Feb. 2005.
- [3] A. Despopoulos, *Color atlas of physiology*, 4th ed. Stuttgart, New York: Thieme Medical Publishers, 1991.
- [4] Wikibooks, “Human Physiology/The respiratory system.” [Online]. Available: http://en.wikibooks.org/wiki/Human_Physiology/The_respiratory_system.
- [5] J. H. T. Bates, *Lung Mechanics. An Inverse Modelling Approach*. Leiden: Cambridge University Press, 2009.
- [6] E. Voigt and J. Pelikan, *CO₂-Messung in der Beatmung*. Städt. Krankenhaus Süd Anästhesieabteilung.
- [7] J. O. Benditt, “Esophageal and gastric pressure measurements,” *Respir. Care*, vol. 50, no. 1, pp. 68–75; discussion 75–77, Jan. 2005.
- [8] G. A. Iotti and A. Braschi, *Measurement of respiratory mechanics during mechanical ventilation*. Rhäzüns, Switzerland, 2001.
- [9] M. Heck and M. Fresenius, *Repetitorium Anästhesiologie für die Facharztprüfung und das Europäische Diplom*. Heidelberg: Springer, 2007.
- [10] J. Rathgeber and J. Baum, *Grundlagen der maschinellen Beatmung. Einführung in die Beatmung für Ärzte und Pflegekräfte*. Stuttgart, New York: Thieme, 2010.
- [11] A. Esteban, A. Anzueto, I. Alía, F. Gordo, C. Apezteguía, F. Pálizas, D. Cide, R. Goldwaser, L. Soto, G. Bugedo, C. Rodrigo, J. Pimentel, G. Raimondi, and M. J. Tobin, “How is mechanical ventilation employed in the intensive care unit? An international utilization review,” *Am. J. Respir. Crit. Care Med.*, vol. 161, no. 5, pp. 1450–1458, May 2000.
- [12] M. Younes, “Proportional assist ventilation, a new approach to ventilatory support. Theory,” *Am. Rev. Respir. Dis.*, vol. 145, no. 1, pp. 114–120, Jan. 1992.
- [13] M. Younes, A. Puddy, D. Roberts, R. B. Light, A. Quesada, K. Taylor, L. Oppenheimer, and H. Cramp, “Proportional assist ventilation: Results of an initial clinical trial,” *Am. Rev. Respir. Dis.*, vol. 145, no. 1, pp. 121–129, Jan. 1992.
- [14] R. Byrd and Z. Mosenifar, “Mechanical Ventilation. Complications of Mechanical Ventilation.” *Medscape*. [Online]. Available: <http://emedicine.medscape.com/article/304068-overview#aw2aab6b7>. [Accessed: 12-Jun-2013].
- [15] J. Milic-Emili, J. Mead, J. M. Turner, and E. M. Glauser, “Improved Technique For Estimating Pleural Pressure From Esophageal Balloons,” *J. Appl. Physiol.*, vol. 19, pp. 207–211, Mar. 1964.
- [16] C. S. Sassoon, T. T. Te, C. K. Mahutte, and R. W. Light, “Airway occlusion pressure. An important indicator for successful weaning in patients with chronic obstructive pulmonary disease,” *Am. Rev. Respir. Dis.*, vol. 135, no. 1, pp. 107–113, Jan. 1987.
- [17] G. A. Iotti, J. X. Brunner, A. Braschi, T. Laubscher, M. C. Olivei, A. Palo, C. Galbusera, and A. Comelli, “Closed-loop control of airway occlusion pressure at 0.1 second (P0.1) applied to pressure-support ventilation: algorithm and application in intubated patients,” *Crit. Care Med.*, vol. 24, no. 5, pp. 771–779, May 1996.

- [18] M. Ranieri, C. Micelli, and L. Appendini, "Method for determining the resistance of the respiratory system of a patient," 2008.
- [19] W. Zapol, *Adult respiratory distress syndrome. Chapter 7: Measurement of Respiratory Elastance and Resistance in Mechanically Ventilated Patients*. New York: M. Dekker, 1991.
- [20] A. Pesenti, P. Pelosi, G. Foti, L. D'Andrea, and N. Rossi, "An interrupter technique for measuring respiratory mechanics and the pressure generated by respiratory muscles during partial ventilatory support," *Chest*, vol. 102, no. 3, pp. 918–923, Sep. 1992.
- [21] E. R. Carter, A. A. Stecenko, B. H. Pollock, and M. J. Jaeger, "Evaluation of the interrupter technique for the use of assessing airway obstruction in children," *Pediatr. Pulmonol.*, vol. 17, no. 4, pp. 211–217, Apr. 1994.
- [22] P. D. Bridge, S. Ranganathan, and S. A. McKenzie, "Measurement of airway resistance using the interrupter technique in preschool children in the ambulatory setting," *Eur. Respir. J. Off. J. Eur. Soc. Clin. Respir. Physiol.*, vol. 13, no. 4, pp. 792–796, Apr. 1999.
- [23] G. L. Hall, J. H. Wildhaber, M. Cernelc, and U. Frey, "Evaluation of the interrupter technique in healthy, unsedated infants," *Eur. Respir. J.*, vol. 18, no. 6, pp. 982–988, Dec. 2001.
- [24] C. Delacourt, H. Lorino, C. Fuhrman, M. Herve-Guillot, P. Reinert, A. Harf, and B. Housset, "Comparison of the forced oscillation technique and the interrupter technique for assessing airway obstruction and its reversibility in children," *Am. J. Respir. Crit. Care Med.*, vol. 164, no. 6, pp. 965–972, Sep. 2001.
- [25] C. S. Pao, M. J. R. Healy, and S. A. McKenzie, "Airway resistance by the interrupter technique: Which algorithm for measuring pressure?," *Pediatr. Pulmonol.*, vol. 37, no. 1, pp. 31–36, Jan. 2004.
- [26] L. Roeder, "Ein Algorithmus zur adaptiven Steuerung eines Beatmungsgerätes," Fachhochschule Lübeck, Lübeck, 2002.
- [27] G. A. Iotti, A. Braschi, J. X. Brunner, T. Smits, M. Olivei, A. Palo, and R. Veronesi, "Respiratory mechanics by least squares fitting in mechanically ventilated patients: applications during paralysis and during pressure support ventilation," *Intensive Care Med.*, vol. 21, no. 5, pp. 406–413, 1995.
- [28] D. Navajas, J. Alcaraz, R. Peslin, J. Roca, and R. Farré, "Evaluation of a method for assessing respiratory mechanics during noninvasive ventilation," *Eur. Respir. J. Off. J. Eur. Soc. Clin. Respir. Physiol.*, vol. 16, no. 4, pp. 704–709, Oct. 2000.
- [29] G. Bellani, N. Patroniti, D. Weismann, L. Galbiati, F. Curto, G. Foti, and A. Pesenti, "Measurement of pressure-time product during spontaneous assisted breathing by rapid interrupter technique," *Anesthesiology*, vol. 106, no. 3, pp. 484–490, Mar. 2007.
- [30] U. Lucangelo, F. Bernabé, and L. Blanch, "Respiratory mechanics derived from signals in the ventilator circuit," *Respir. Care*, vol. 50, no. 1, pp. 55–65; discussion 65–67, Jan. 2005.
- [31] F. Dietz, *Flowregelung für die nicht-invasive Beatmung unter Berücksichtigung von Maskenleckage und Spontanatmung*. Düsseldorf: VDI-Verl., 2004.
- [32] S. B. Phagoo, R. A. Watson, M. Silverman, and N. B. Pride, "Comparison of four methods of assessing airflow resistance before and after induced airway narrowing in normal subjects," *J. Appl. Physiol. Bethesda Md 1985*, vol. 79, no. 2, pp. 518–525, Aug. 1995.
- [33] H. Arets, "Measurements of airway mechanics in spontaneously breathing young children," *Paediatr. Respir. Rev.*, vol. 5, no. 1, pp. 77–84, Mar. 2004.
- [34] J. X. Brunner and G. A. Iotti, "Adaptive Support Ventilation (ASV)," *Minerva Anesthesiol.*, vol. 68, no. 5, pp. 365–368, May 2002.

- [35] D. Tassaux, E. Dalmas, P. Gratadour, and P. Jolliet, "Patient-ventilator interactions during partial ventilatory support: a preliminary study comparing the effects of adaptive support ventilation with synchronized intermittent mandatory ventilation plus inspiratory pressure support," *Crit. Care Med.*, vol. 30, no. 4, pp. 801–807, Apr. 2002.
- [36] M. Wysocki, C. Cracco, A. Teixeira, A. Mercat, J.-L. Diehl, Y. Lefort, J.-P. Derenne, and T. Similowski, "Reduced breathing variability as a predictor of unsuccessful patient separation from mechanical ventilation," *Crit. Care Med.*, vol. 34, no. 8, pp. 2076–2083, Aug. 2006.
- [37] Dräger medical, *EvitaXL. Intensive Care Ventilator Software 6.n Instructions for Use*. Germany, 2004.
- [38] L. Appendini, A. Purro, M. Gudjonsdottir, P. Baderna, A. Patessio, S. Zanaboni, C. F. Donner, and A. Rossi, "Physiologic response of ventilator-dependent patients with chronic obstructive pulmonary disease to proportional assist ventilation and continuous positive airway pressure," *Am. J. Respir. Crit. Care Med.*, vol. 159, no. 5 Pt 1, pp. 1510–1517, May 1999.
- [39] E. Kondili, G. Prinianakis, C. Alexopoulou, E. Vakouti, M. Klimathianaki, and D. Georgopoulos, "Respiratory load compensation during mechanical ventilation—proportional assist ventilation with load-adjustable gain factors versus pressure support," *Intensive Care Med.*, vol. 32, no. 5, pp. 692–699, Mar. 2006.
- [40] M. Sydow, H. Burchardi, J. Zinserling, H. Ische, T. A. Crozier, and W. Weyland, "Improved determination of static compliance by automated single volume steps in ventilated patients," *Intensive Care Med.*, vol. 17, no. 2, pp. 108–114, Feb. 1991.
- [41] R. Peslin, J. F. da Silva, F. Chabot, and C. Duvivier, "Respiratory mechanics studied by multiple linear regression in unsedated ventilated patients," *Eur. Respir. J. Off. J. Eur. Soc. Clin. Respir. Physiol.*, vol. 5, no. 7, pp. 871–878, Jul. 1992.
- [42] E. Rother, "Vergleich von Modellen des respiratorischen Systems zur Entwicklung von Algorithmen für die adaptive nicht-invasive Beatmung," Fachhochschule Lübeck, Lübeck, 2011.
- [43] G. R. Washko, C. R. O'Donnell, and S. H. Loring, "Volume-related and volume-independent effects of posture on esophageal and transpulmonary pressures in healthy subjects," *J. Appl. Physiol. Bethesda Md 1985*, vol. 100, no. 3, pp. 753–758, Mar. 2006.
- [44] D. Talmor, T. Sarge, C. R. O'Donnell, R. Ritz, A. Malhotra, A. Lisbon, and S. H. Loring, "Esophageal and transpulmonary pressures in acute respiratory failure," *Crit. Care Med.*, vol. 34, no. 5, pp. 1389–1394, May 2006.
- [45] D. Talmor, T. Sarge, A. Malhotra, C. R. O'Donnell, R. Ritz, A. Lisbon, V. Novack, and S. H. Loring, "Mechanical Ventilation Guided by Esophageal Pressure in Acute Lung Injury," *N. Engl. J. Med.*, vol. 359, no. 20, pp. 2095–2104, Nov. 2008.
- [46] Q. Hamid, J. Shannon, and J. Martin, *Physiologic basis of respiratory disease. Chapter 55: Esophageal Pressure Measurement*. Hamilton, Ontario, Canada: BC Decker Inc., 2005.
- [47] J. Marini, *Critical care medicine: the essentials*, 3rd ed. Philadelphia: Lippincott Williams & Wilkins, 2006.
- [48] M. Pinsky, *Applied physiology in intensive care medicine*. Dordrecht; New York: Springer, 2009.
- [49] J. Martínez Llorens, "3r curs d'insuficiència respiratòria i ventilació mecànica hospitalària i domiciliària. Avaluació funcional del pacient candidat a ventilació mecànica domiciliària.," Barcelona.
- [50] P. D. Hughes, M. I. Polkey, D. Kyroussis, C. H. Hamnegard, J. Moxham, and M. Green, "Measurement of sniff nasal and diaphragm twitch mouth pressure in patients," *Thorax*, vol. 53, no. 2, pp. 96–100, Feb. 1998.

- [51] K. Toussaint, "Atemmechanik unter Atmung mit PSV und BIPAP," Universitäts-Krankenhaus Eppendorf Hamburg, 2000.
- [52] G. Dimitriou, A. Greenough, G. F. Rafferty, and J. Moxham, "Effect of maturity on maximal transdiaphragmatic pressure in infants during crying," *Am. J. Respir. Crit. Care Med.*, vol. 164, no. 3, pp. 433–436, Aug. 2001.
- [53] A. Aliverti, E. Carlesso, R. Dellacà, P. Pelosi, D. Chiumello, A. Pedotti, and L. Gattinoni, "Chest wall mechanics during pressure support ventilation," *Crit. Care Lond. Engl.*, vol. 10, no. 2, p. R54, 2006.
- [54] X.-J. Zhang, G. Yu, X.-H. Wen, Z.-C. Lin, F.-Q. Yang, Z.-G. Zheng, R.-C. Chen, and N.-S. Zhong, "Effect of propofol on twitch diaphragmatic pressure evoked by cervical magnetic stimulation in patients," *Br. J. Anaesth.*, vol. 102, no. 1, pp. 61–64, Jan. 2009.
- [55] D. J. Walker, "Prädiktion des Oesophagusdruckes durch den Mundverschlussdruck nach Magnetstimulation des Nervus phrenicus," Albert-Ludwigs-Universität Freiburg im Breisgau, 2006.
- [56] H. Motulsky, *Analyzing Data with GraphPad Prism*. www.graphpad.com, 1999.
- [57] J. M. Bland and D. G. Altman, "Statistical methods for assessing agreement between two methods of clinical measurement," *Lancet*, vol. 1, no. 8476, pp. 307–310, Feb. 1986.
- [58] J. M. Bland and D. G. Altman, "Applying the right statistics: analyses of measurement studies," *Ultrasound Obstet. Gynecol.*, vol. 22, no. 1, pp. 85–93, Jul. 2003.
- [59] D. G. Altman and J. M. Bland, "Measurement in Medicine: The Analysis of Method Comparison Studies," *The Statistician*, vol. 32, no. 3, p. 307, Sep. 1983.
- [60] J. M. Bland and D. G. Altman, "The use of transformation when comparing two means," *BMJ*, vol. 312, no. 7039, p. 1153, May 1996.
- [61] J. M. Bland and D. G. Altman, "Agreement between methods of measurement with multiple observations per individual," *J. Biopharm. Stat.*, vol. 17, no. 4, pp. 571–582, 2007.
- [62] M. Strutz, "Vergleich dreier Atemmodelle bei assistierter Spontanatmung zur Entwicklung der adaptiven, nicht-invasiven Beatmung," Fachhochschule Lübeck, Lübeck, 2012.
- [63] A. Zanella, G. Bellani, and A. Pesenti, "Airway pressure and flow monitoring," *Curr. Opin. Crit. Care*, vol. 16, no. 3, pp. 255–260, Jun. 2010.
- [64] H. Motulsky and A. Christopoulos, *Fitting models to biological data using linear and nonlinear regression: a practical guide to curve fitting*. Oxford; New York: Oxford University Press, 2004.
- [65] K. Lopez-Navas, S. Brandt, M. Strutz, H. Gehring, and U. Wenkebach, "Comparison of two methods to assess transdiaphragmatic pressure at different levels of work of breathing," *Biomed. Tech. Eng.*, Sep. 2012.
- [66] P. D. Bridge and S. A. McKenzie, "Airway resistance measured by the interrupter technique: expiration or inspiration, mean or median?," *Eur. Respir. J. Off. J. Eur. Soc. Clin. Respir. Physiol.*, vol. 17, no. 3, pp. 495–498, Mar. 2001.
- [67] J. Milic-Emili, W. A. Whitelaw, and J. P. Derenne, "New tests to assess lung function: occlusion pressure - a simple measure of the respiratory center's output," *N. Engl. J. Med.*, vol. 293, no. 20, pp. 1029–1030, Nov. 1975.
- [68] J. N. Davis and T. A. Sears, "The effects of sudden alterations in load on human intercostal muscles during voluntary activation," *J. Physiol.*, vol. 190, no. 2, p. 36P–38P, May 1967.
- [69] S. B. Phagoo, N. M. Wilson, and M. Silverman, "Evaluation of a new interrupter device for measuring bronchial responsiveness and the response to bronchodilator in

- 3 year old children,” *Eur. Respir. J. Off. J. Eur. Soc. Clin. Respir. Physiol.*, vol. 9, no. 7, pp. 1374–1380, Jul. 1996.
- [70] J. M. Bland and D. G. Altman, “Transforming data,” *BMJ*, vol. 312, no. 7033, p. 770, Mar. 1996.

7 List of publications

Parts of this work are contained in the following publications:

- Lopez-Navas K., Gehring H., Wenkebach U. Validation design for a method to determine respiratory resistance and compliance in non-sedated patients. *Eur Respir J.* 2011; 38: Suppl.55. *Abstract and Poster*. Annual congress of the European Respiratory Society ERS2011; Sep 24-28, 2011 in Amsterdam, The Netherlands.
- Lopez-Navas K., Gehring H., Wenkebach U. A test setup for the validation of a method to determine respiratory mechanics in spontaneously breathing patients. *Biomed Tech* 2011; 56: Suppl.1. *Abstract and Poster*. Annual meeting of the DGBMT-BMT2011; Sep 27-30, 2011 in Freiburg, Germany.
- Lopez-Navas K., Brandt S., Gehring H., Strutz M., Wenkebach U. A method for continuous non-invasive assessment of respiratory mechanics during spontaneous breathing. *Crit Care* 2012; 16: Suppl.1: P117 (DOI: 10.1186/cc10724). *Abstract and Poster*. 32nd International Symposium on Intensive Care and Emergency Medicine ISICEM 2012; Mar 20-23, 2012 in Brussels, Belgium.
- Lopez-Navas K., Rother E., Strutz M., Wenkebach U. Vergleich von drei parametrischen Atemmodellen basierend auf der Rekonstruktionsgüte des transdiaphragmalen Drucks. In: Automatisierungstechnische Verfahren für die Medizin (ISBN 978-3-18-328614-1). *Peer-reviewed article and Oral presentation*. Annual workshop AUTOMED; Mar 29-30, 2012 in Aachen, Germany.
- Strutz M., Lopez-Navas K., Wenkebach U. Filtering cardiac artefacts from transdiaphragmatic pressure for the validation of a non-invasive method to assess work of breathing. In: Proceedings of Studierendentagung 2012 Medizintechnik in Lübeck. *Article and Oral presentation*. Studierendentagung 2012 in Lübeck, Germany.
- Brandt S., Lopez-Navas K., Strutz M., Gehring H., Wenkebach U. Non-invasive assessment of transdiaphragmatic pressure in smoking and non-smoking volunteers. *Abstract and Poster*. Proceedings of IAMPOV 2012 in Yale, USA.
- Lopez-Navas K., Brandt S., Strutz M., Gehring H., Wenkebach U. Validation of a method for non-invasive assessment of transdiaphragmatic pressure during support ventilation. *Eur Respir J.* 2012; 40: Suppl.56; *Abstract and Oral presentation*. Annual congress of the European Respiratory Society ERS2012; Sep 1-5, 2012 in Vienna, Austria.
- Lopez-Navas K., Rother E., Wenkebach U. Comparison of six models of the respiratory system based on parametric estimates from three identification models. *Biomed Tech* 2012; 57: Suppl.1 (DOI: 10.1515/bmt-2012-4011). *Peer-reviewed Conference proceeding and Oral presentation*. Annual meeting of the DGBMT-BMT2012; Sep 16-19, 2012 in Jena, Germany.
- Lopez-Navas K., Brandt S., Strutz M., Gehring H., Wenkebach U. Comparison of two methods to assess transdiaphragmatic pressure at different levels of work of breathing. *Biomed Tech* 2012; 57: Suppl.1 (DOI: 10.1515/bmt-2012-4124). *Peer-reviewed*

Conference proceeding and Oral presentation. Annual meeting of the DGBMT-BMT2012; Sep 16-19, 2012 in Jena, Germany.

- Lopez-Navas K., Brandt S., Strutz M., Gehring H., Wenkebach U. Non-invasive determination of respiratory effort in spontaneous breathing and support ventilation: a validation study with healthy volunteers. *Journal Paper to be published.*
- Lopez-Navas K., Strutz M., Rother E., Wenkebach U. Analysis of extended models of the respiratory system for the non-invasive determination of respiratory effort during support ventilation. *Journal Paper in preparation.*

Investigations related to this work were published in three theses:

- Steffner M. Rechnergestützte Messwerterfassung und Kalibrierung eines Lungensimulators. Technische Akademie Nord, Fachschule für Technik Kiel. Kiel, 2011
- Rother E. Vergleich von Modellen des respiratorischen Systems zur Entwicklung von Algorithmen für die adaptive nicht-invasive Beatmung. Fachhochschule Lübeck, Lübeck 2011
- Strutz M. Vergleich dreier Atemmodelle bei assistierter Spontanatmung zur Entwicklung der adaptiven nicht-invasiven Beatmung. Fachhochschule Lübeck, Lübeck 2012

Annex A1. Poster

The image below shows the poster that hung on the wall during the examinations with volunteers. This gave all participants a clear overview on the steps of the procedure.



TANDEM
Centre of Excellence for
Technology and Engineering in Medicine

Messung der Atemmechanik durch kurze Okklusionen der Atemwege bei assistierender Beatmung



UNIVERSITÄT ZU LÜBECK
FACH HOCHSCHULE LÜBECK
University of Applied Sciences

Vorbereitung

- Lagerung mit 30°-Elevation des Oberkörpers
- EKG, SpO2 und Blutdruckmessung, venöse Verweilkanüle
- Topische Anästhesie der Nasenhöhlen und Epipharynx
- Katheter einführen, Maske anlegen

Phase	Ziel	Aufbau	Evita 4 Einstellungen	Dauer ca.	
1	Gewöhnung	Proband kann wie gewohnt atmen	Proband atmet mit Katheter und Maske	ASB 0 - 5 mbar (max. 15mbar)	3 min
2	Spontanatmung	<i>Messung</i>		10 min	
3	Umstellung und Gewöhnung	Erhöhte Atemarbeit	Erhöhung des Totraums (2 bis 4 zusätzliche Filter zwischen Sensoren und Beatmungsgerät)	ASB 0mbar	3 min
4	Spontanatmung mit erhöhter Atemarbeit	<i>Messung</i>		10 min	
5	Umstellung und Gewöhnung	Verminderte Atemarbeit	Der zugefügte Totraum wird entfernt	ASB 10 - 20 mbar	3 min
6	Spontanatmung mit verminderter Atemarbeit	<i>Messung</i>		10 min	
7	Normalisierung	Proband kann wieder wie gewohnt atmen	Proband atmet mit Katheter und Maske	ASB 0 - 5 mbar (max. 15mbar)	3 min

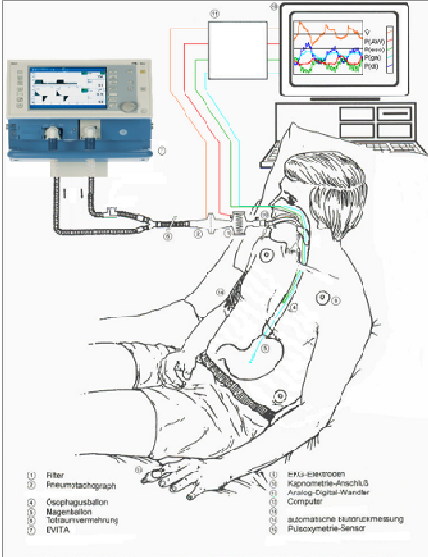
Nachbereitung

- Entfernung der Maske
- Weiterer Durchlauf möglich?
- Entfernen des Katheters
- Beschwerden?

Wie anstrengend ist es zu atmen?

0 Finger „ganz leicht“

10 Finger „abgerst“ „anstrengend“



Alles in Ordnung?

Rechter Fuß: Alles ok!
Linker Fuß: Problem!



ZUKUNFTSprogramm
Wirtschaft
Investition in Ihre Zukunft
financed by the European Union,
European Regional Development Fund (ERDF)

Annex A2. Letter from the commission of ethics



UNIVERSITÄT ZU LÜBECK

Universität zu Lübeck · Ratzeburger Allee 160 · 23538 Lübeck

Herrn
Prof. Dr. med. Hartmut Gehring
Klinik für Anaesthesiologie

im Hause

nachrichtlich:

Herrn Prof. Dr. med. Schmucker
Direktor der Klinik für Anaesthesiologie

Ethik-Kommission

Vorsitzender:

Herr Prof. Dr. med. Dr. phil. H. Raspe
Universität zu Lübeck
Stellv. Vorsitzender:
Herr Prof. Dr. med. F. Gieseler
Ratzeburger Allee 160
23538 Lübeck

Sachbearbeitung: Frau Janine Erdmann
Tel.: +49 451 500 4639
Fax: +49 451 500 3026
janine.erdmann@medizin.uni-luebeck.de

Aktenzeichen: 11-074

Datum: 17. Juni 2011

Sitzung der Ethik-Kommission am 14. Juni 2011

Antragsteller: Herr Prof. Gehring / Herr Prof. Schmucker

Titel: Messung der Atemmechanik durch kurze Okklusionen der Atemwege bei assistierender Beatmung (PADVENT)

Sehr geehrter Herr Prof. Gehring,

der Antrag wurde unter berufsethischen, medizinisch-wissenschaftlichen und berufsrechtlichen Gesichtspunkten geprüft.

Die Kommission hat nach der Berücksichtigung folgender **Hinweise** keine Bedenken: Die Kommission wundert sich über die Vorlage des Hamburger Votums aus dem Jahr 1996. Sie empfiehlt, in das Protokoll einen Absatz über die Berichterstattung unerwünschter Ereignisse aufzunehmen.

Bei Änderung des Studiendesigns sollte der Antrag erneut vorgelegt werden. Über alle schwerwiegenden oder unerwarteten und unerwünschten Ereignisse, die während der Studie auftreten, muss die Kommission umgehend benachrichtigt werden. Nach Abschluss des Projektes bitte ich um Übersendung eines knappen Schlussberichtes (unter Angabe unseres Aktenzeichens), aus dem der Erfolg/Misserfolg der Studie sowie Angaben darüber, ob die Studie abgebrochen oder geändert bzw. ob Regressansprüche geltend gemacht wurden, ersichtlich sind.

Die ärztliche und juristische Verantwortung des Leiters der klinischen Studie und der an der Studie teilnehmenden Ärzte bleibt entsprechend der Beratungsfunktion der Ethikkommission durch unsere Stellungnahme unberührt.

Mit freundlichem Gruß bin ich
Ihr

Prof. Dr. med. Dr. phil. H. Raspe
Vorsitzender

anwesende Kommissionsmitglieder:

Prof. Dr. Dr. H.-H. Raspe
(Sozialmedizin, Vorsitzender der EK)
 Prof. Dr. Schweiger
(Psychiatrie)
 Prof. Dr. Handels
(Medizinische Informatik)
 Frau Prof. E. Stubbe
(Theologin)
Prof. Dr. Borck
(Medizin- und Wissenschaftsgeschichte)

Frau H. Müller
(Pflege)
 Dr. Kaiser
(Kinderchirurgie)
 Herr Dr. Fieber
(Richter am Amtsgericht Ahrensburg)
Prof. Schwinger
(Humangenetik)
 Dr. R. Vonthein
(Zentrum für Klin. Studien)

Herr Prof. Dr. Giesler
(Med. Klinik I, Stellv. Vorsitzender)
 Frau Prof. Dr. M. Schrader
(Plastische Chirurgie)
Herr PD Lauten
(Kinder- und Jugendmedizin)
 Frau A. Farries
(Richterin am Amtsgericht Lübeck)

Annex B. Dedicated software

This section presents the software program written for the implementation and validation of the Occlusion+Delta method. The software is also available in the attached CD.

Program for the Occlusion+Delta method

For the online⁹ assessment of resistance, compliance and respiratory effort by the O+D method a computer program was written. The development environment was LabWindows CVI 8.5.1 and the programming language was C. The program reads flow, airway pressure and transdiaphragmatic pressure (if available) as input and delivers, while reading, respiratory resistance and compliance as output. The reconstruction of the muscular pressure is then possible. The program performs the functions explained below.

1. Acquire data

Once the program is started a window appears where the user can select the source of data. Data can be obtained whether from the hardware while performing measurements or by reading an existing file.



Figure B-1: Window for source selection

- a) Acquiring from hardware: The software uses the USB interface to read flow and pressure data. It receives through the data acquisition card the measured gastric and oesophageal pressures if available and controls the shutter to produce short occlusions in the expiratory valve of the ventilator during the exhalation. The sampling rate is 200Hz. The signals can be acquired from a patient or a simulator.
- b) Reading a file: The software can read files in ASCII format (typically .csv) or in netCDF format (usually .nc). The .csv files must contain lines of five float values separated by commas as “flow, Paw, Pes, Pga, Pdi” where flow is given in l/s and the pressures in mbar, one line for each recorded sample. The .nc files must contain the variables time, flow, Paw and Pdi in double format.

After selecting the source the graphical interface shown in Figure B-2 appears. There the user can:

- Select whether data is being measured from a patient or simulator. If simulator is selected, the slope and the offset for calibration are required; default values are available.
- Select whether Pdi data is available. If so, MLR is performed to calculate R and C. Otherwise only the non-invasive Occlusion+Delta method determines the parameters.

⁹ analysis and results already available while measuring

- Enter the parameters for occlusion, i.e. the number of desired breaths between occlusions and the time after begin of expiration to initiate an occlusion.
- Select the file extension .csv or .nc if reading data from files

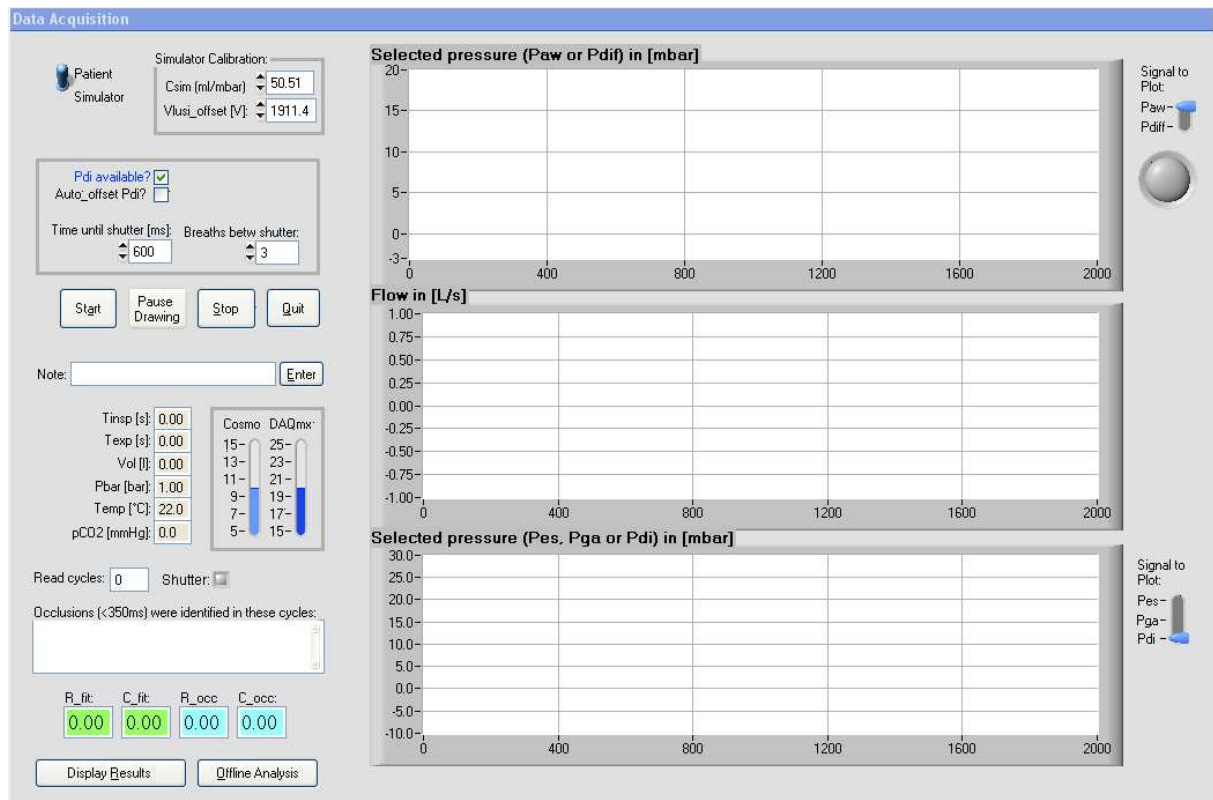


Figure B-2: User interface

2. Analyze and save data

The software receives the measured samples and does following tasks:

- Phase identification and cycle check: the program identifies the respiratory phase (inspiration, expiration or transition) for the current sample. The identification of phases is done with the flow signal and its points of reversal. Once an inspiration followed by an expiration is identified the program checks the values to confirm if the cycle is normal for quiet breathing (no cough, sighs, speaking, etc.), counts complete respiratory cycles and saves them separately for immediate or posterior analysis.
- Multiple linear regression: for each complete cycle with available Pdi, MLR is used to find R and C, which are used as reference for the validation of O+D and appear in the user interface as Rfit and Cfit. The PTP_{insp} of Pdi (PTP_{Pdi}) is calculated as the area under the inspiratory part of Pdi.
- Identification of occlusions: the software looks for an expiratory occlusion in each completed cycle. If no occlusion is found, the program continues reading and analysing the next cycle. If an occlusion is found, the cycle is compared to the previous ten to fifteen breaths, usually around one minute before occlusion. For all similar pairs of cycles the O+D method is applied to obtain R and C, which appear in the user interface as R_{occ} and C_{occ}. A moving average of the last ten values is calculated making R_{curr} and C_{curr}, which are used to obtain the calculated muscular pressure (P_{mus}) and to calculate its PTP_{insp} as the area of its inspiratory part (PTP_{O+D}), later compared against PTP_{Pdi}.

- d) Evaluation of results: Values outside the established physiological range are discarded. All data is saved in arrays for immediate or posterior analysis.

During online analysis the program outputs the amount of samples read from the acquisition hardware, the cycle number, the numbers of the occluded cycles, a led light indicating when the shutter is active and the Rfit and Cfit after each complete cycle as well as the Rocc and Cocc after each successful occlusion. Three stripcharts show the flow, airway pressure and transdiaphragmatic pressure read. The inspiratory and expiratory times (T_{insp}, T_{exp}), tidal volume, barometric pressure, temperature and CO₂ concentration in the exhaled air are displayed after each cycle helping to supervise the ventilatory activity of the subject. All data acquired from the hardware is saved in a netCDF file. These files can be used later as input for the program. An example of how the user interface looks like while the program is running is shown below.

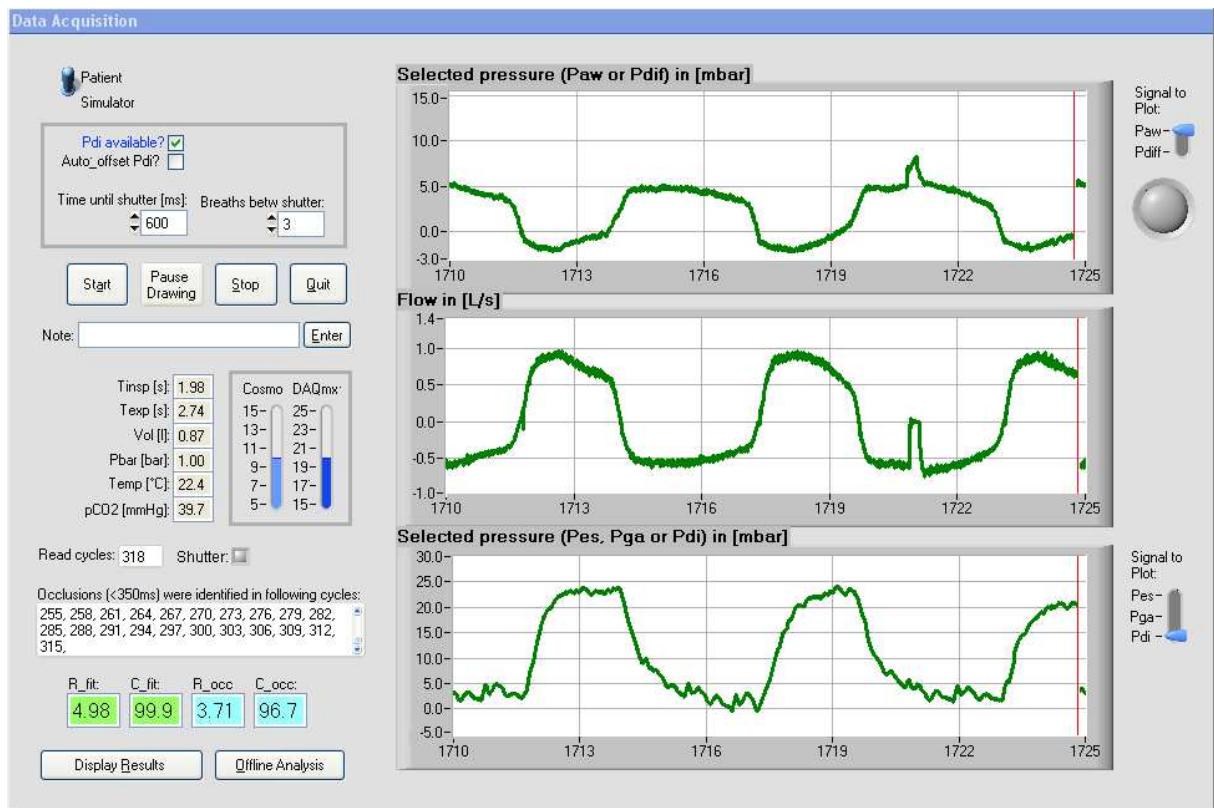


Figure B-3: Example of outputs while the program is running

The tasks of the program designed for the non-invasive method, up to this point, can be summarized in the flow chart shown in Figure B-4.

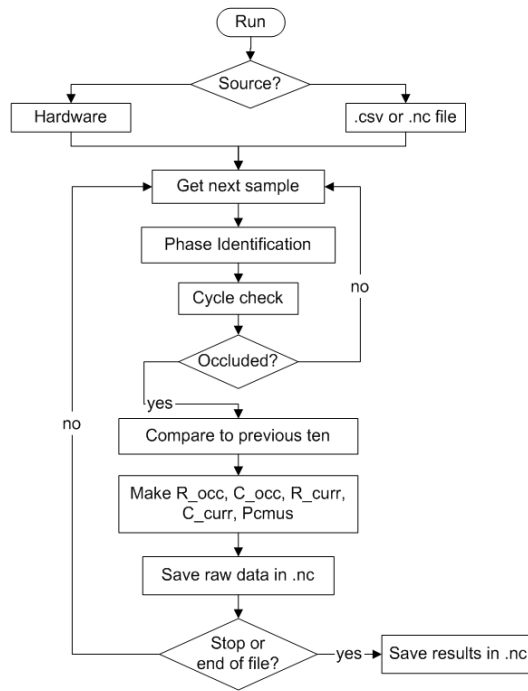


Figure B-4: Flow chart of the program for O+D

3. Display results

Once the program has finished reading the selected file or the stop button has been pressed, the function “Display results” becomes available. The window shown below appears.

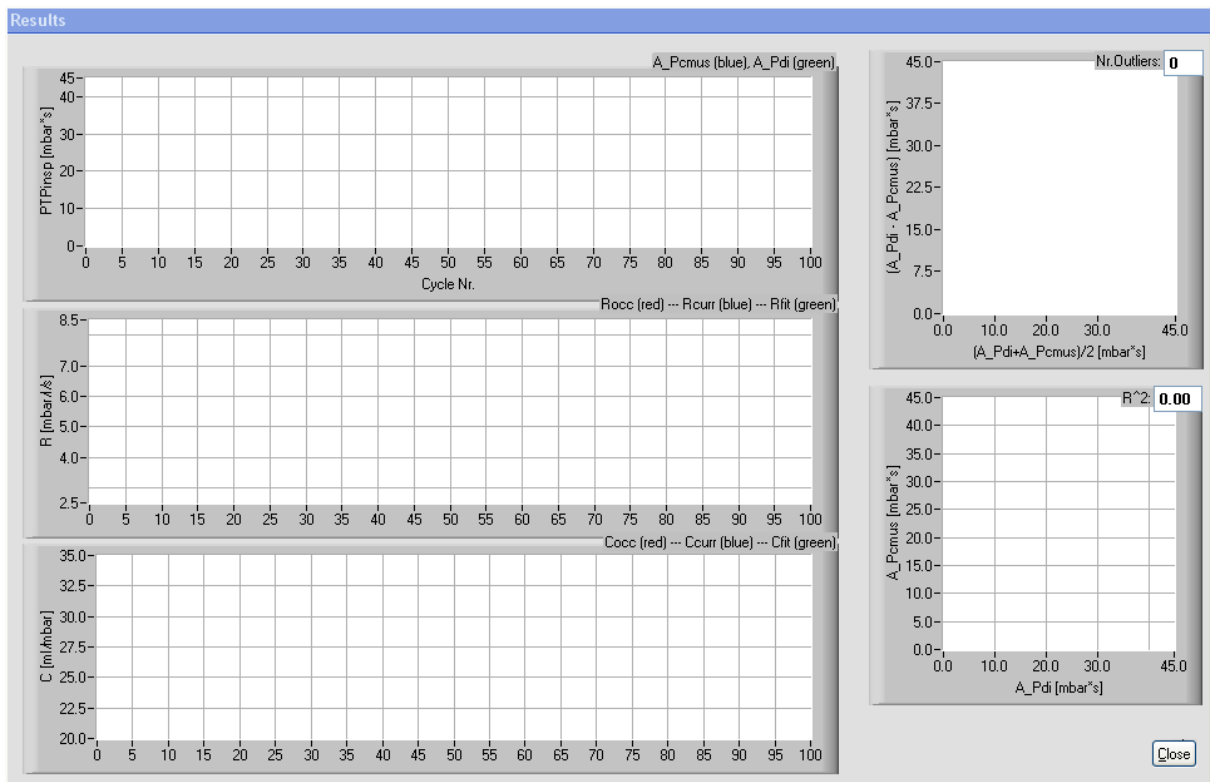


Figure B-5: Window for results

The function “Display Results” summarizes all results in the window shown in Figure B-5. For each cycle, starting with the first occlusion, the values obtained for PTP_{Pdi} and PTP_{O+D} (A_{Pdi} and A_{Pcmus} in the window), R_{fit} , C_{fit} , R_{occ} , C_{occ} , R_{curr} and C_{curr} are

displayed. Additionally, a Bland-Altman diagram, linear regression and R^2 for the PTPinsp values are shown on the right side. For deeper understanding of the acquired data, the program additionally offers a window for offline analysis.

4. Offline analysis

In this window the user can enter the number of a selected cycle and the corresponding signals are displayed. A second cycle can be selected and its signals are displayed too. If the second cycle is occluded the Occlusion+Delta method is performed using both selected cycles. The charts on the right side display the expiratory flow-volume loops and the differences (deltas) of the variables.

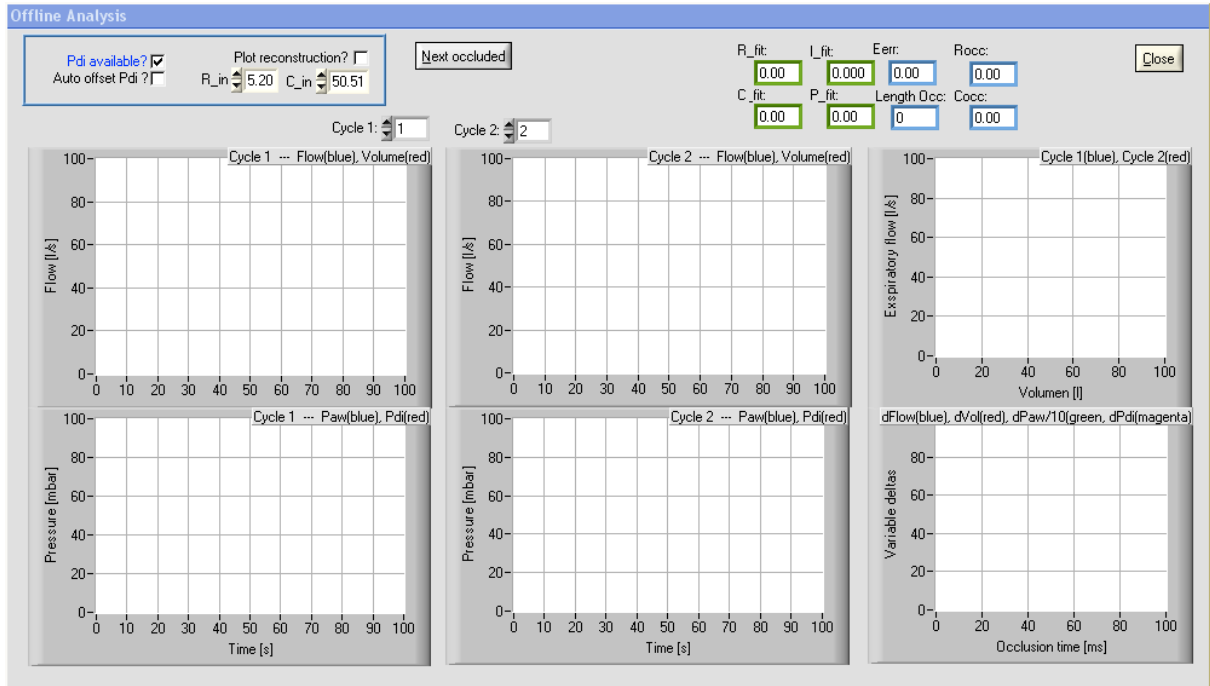


Figure B-6: Window for offline analysis

Annex C. Dedicated hardware

For the Occlusion+Delta method a device called *shutter* was built to control the expiratory valve of a commercial ventilator to generate expiratory occlusions. Principal component of the shutter is a current source that closes the expiratory valve of the ventilator during approximately 200ms.

The current source requires a digital signal from the computer to provide a current capable of shutting the expiratory valve. For this, the shutter also contains a data acquisition card DAQ (USB-6009, National Instruments Germany GmbH, München, Germany). One of its digital outputs is controlled by software to generate a rising edge (low to high level transition) each time that an occlusion is wanted. This output drives a monoflop to give temporarily a positive voltage to the base of a transistor which controls a double-pole double-throw relay to break the default circuit and connect the load for the desired time to the current source instead. A power supply (SNP-Z061, Günter Dienstleistungen GmbH, Neuenbürg, Germany) with certification EN60601-1 energizes the circuit.

Figure C-1 shows the circuitry of the shutter. V_{in} represents the digital control signal. The load R_L is in the real application the expiratory valve, which is otherwise connected to the internal circuitry of the Evita4.

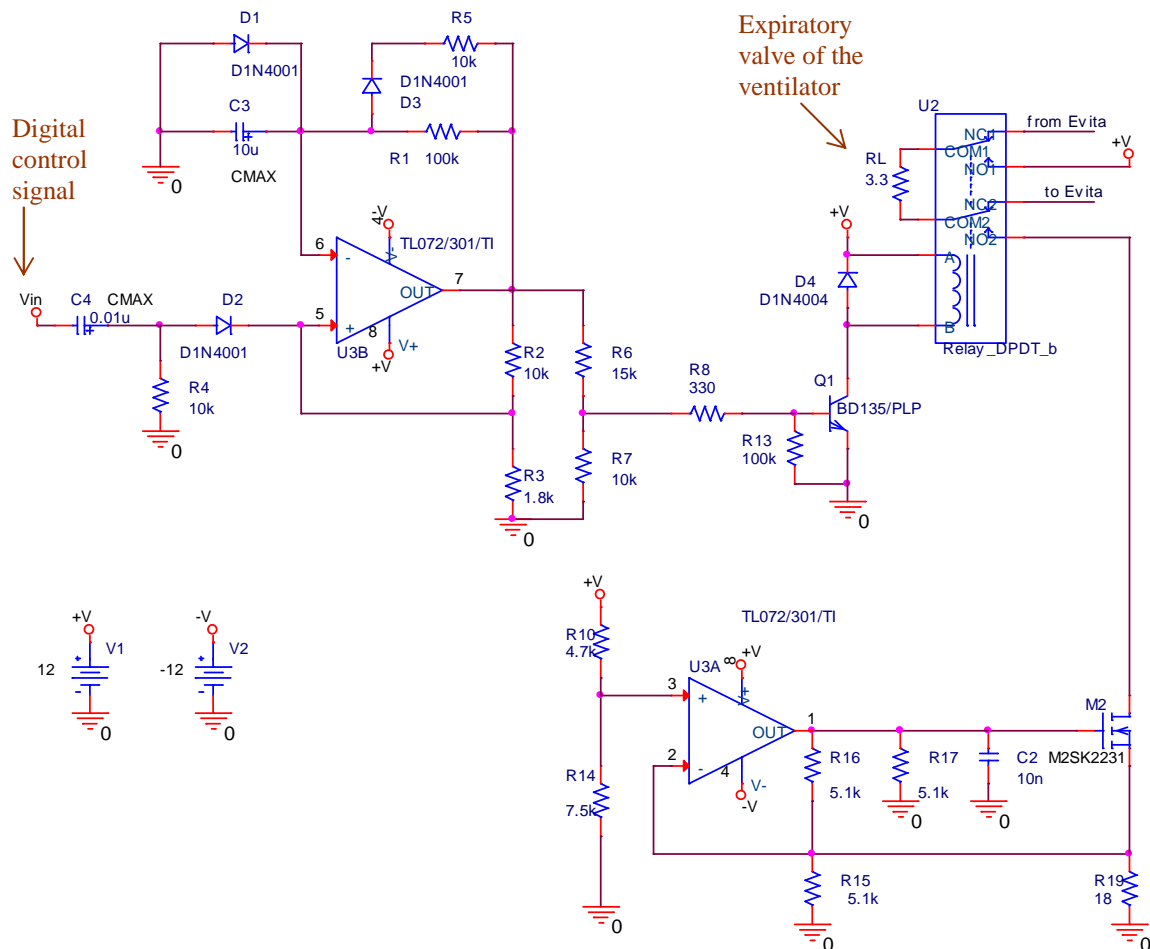


Figure C-1: Shutter circuitry

Annex D. Electronic data

The attached CDs contains the acquired electronic data and the software developed for this investigation. The data is organised in the following folders:

Folder	Description
Software_OD\Include	- Include files for the dedicated software for the O+D
Software_OD\NetCDF	- Installation files to manipulate data in NetCDF format as required by the dedicated software for O+D - The file Installation.txt explains how to use the other files.
Software_OD\OD	- Dedicated O+D software: Program for the O+D method. - The file ReadMe.txt explains how to use the software. - See full description in Annex B .
LS	- Source data, results and plots (.fig and .png files) of the analysis of simulations with the LS4000. - It includes the MATLAB scripts to create the plots and the statistical analysis.
PADVENT	- Source data, results and plots of the analysis of the study with volunteers. The plots include: baseline plots (.png), plots from statistical analysis (.fig and .png) and plots of results per subject (.fig and .png). - It includes the MATLAB scripts to create the plots and the statistic analysis.

Electronic data contained in the attached CD

Annex E. Smokers vs. Non-smokers

In the study with volunteers 15 young non-smokers and 10 older smokers were included to examine whether there were differences in their lung mechanics.

The mean values of resistance and compliance of both groups were compared with a t-test for independent samples of unequal sizes and unequal variance using $p=0.05$. According to the results shown in the next table the differences are not statistically significant.

	Rfit		Cfit		Rocc		Cocc	
	S	NS	S	NS	S	NS	S	NS
Mean	6.56	5.74	93.97	92.74	5	4.46	88	82.83
Variance	2.127	1.969	412	389.9	1.541	2.116	195.2	144.8
Observations	10	15	10	15	10	15	10	15
Hypothesized mean difference	0		0		0		0	
Degrees of freedom	19		19		21		17	
t Statistic	1.407		0.15		1.002		0.956	
P(T<=t) two-tail	0.176		0.883		0.328		0.353	
t Critical two-tail	2.093		2.093		2.08		2.11	

S= smokers, NS= non-smokers

Figure E-1: t-test for comparison of R and C of smokers and non-smokers

The absence of significant differences can be explained by the fact that even after years of active smoking all volunteers were healthy. But of course many other factors like air pollution, nutrition or sport activities influence the state of health of different people. In the complete sample of volunteers no significant differences in R and C were found between the groups, as they could be found in a future study comparing healthy volunteers against patients suffering from COPD, ARDS or similar.

Annex F. Detailed results of the analysis of phases

The parameters R and C measured with the lung simulator did not considerably change with the simulated level of respiratory effort. In contrast, the values from the study with volunteers presented visible variations.

The means and standard deviations of the parameters obtained with the invasive method (Rfit, Cfit) and the non-invasive method (Rocc, Cocc), calculated for each phase separately, are shown in the next tables.

The total amount of cycles inside a phase is given in the column “cycles”. The column nPdi indicates the amount of cycles with normal Pdi, undisturbed flow and airway pressure and values of R and C inside the physiological range. The means and standard deviations (sd) were calculated for all recorded cycles. The results of Bland-Altman (BA) analysis (mean and standard deviation of the differences) refer to the comparison of the PTPinsp values from both methods.

o Simulations

	Phase	cycles	nr. Occls	Rfit		Cfit		Rocc		Cocc		nPdi	BA	
				[mbar/l/s]		[ml/mbar]		[mbar/l/s]		[ml/mbar]			[mbar*s]	
				mean	sd	mean	sd	mean	sd	mean	sd		mean	sd
25--2	1	27	9	1.92	0.57	23.9	0.51	2.03	0.3	26.0	1.91	27	-4.89	0.84
	2	34	12	1.93	0.49	23.9	0.44	1.97	0.69	28.5	1.76	34	-4.40	0.62
	3	29	9	1.87	0.65	24.0	0.58	1.85	0.36	27.4	1.27	29	-4.44	0.31
25--4	1	33	12	4.98	0.4	24.6	0.27	4.72	0.23	26.7	1.36	28	-3.95	0.22
	2	33	11	4.72	0.37	24.7	0.21	4.44	0.23	27.3	1.59	33	-3.70	0.49
	3	28	10	4.76	0.52	24.4	0.4	4.44	0.25	26.5	0.9	28	-2.82	0.33
50--2	1	33	12	2.01	0.32	49.7	0.75	2.14	0.14	52.6	3.84	28	-1.48	0.42
	2	33	11	1.87	0.2	49.5	0.77	2.21	0.2	54.0	4.96	33	-1.66	0.25
	3	28	10	1.88	0.27	49.4	0.91	2.40	0.19	50.0	4.07	28	-0.88	0.41
50--4	1	33	12	5.22	0.24	48.7	0.75	4.92	0.39	50.5	3.12	28	-0.51	0.28
	2	33	11	4.97	0.24	48.6	0.52	4.78	0.24	50.3	2.95	33	-0.68	0.13
	3	28	10	4.91	0.18	48.4	0.69	4.75	0.13	49.6	1.86	28	-0.37	0.20
75--2	1	27	9	2.16	0.08	74.0	0.47	2.58	0.13	83.8	7.56	27	-0.96	0.13
	2	34	12	2.04	0.09	73.8	0.65	2.50	0.1	80.8	6.12	34	-0.85	0.10
	3	28	10	1.92	0.05	73.4	0.38	2.41	0.1	79.0	3.43	28	-0.61	0.12
75--4	1	27	9	4.84	0.15	71.3	0.94	4.64	0.22	63.9	7.31	27	0.15	0.56
	2	34	12	4.71	0.13	71.2	0.91	4.67	0.14	70.9	5.01	34	0.64	0.25
	3	28	10	4.57	0.12	70.8	0.8	4.70	0.26	71.0	12.9	28	0.17	0.26

Table F-1: Results of simulated cases per phase.

○ Study with volunteers

Phase	cycles	nr. Occls	Rfit [mbar/l/s]		Cfit [ml/mbar]		Rocc [mbar/l/s]		Cocc [ml/mbar]		nPdi	BA [mbar*s]		
			mean	sd	mean	sd	mean	sd	mean	sd		mean	sd	
3	1	138	45	3.18	1.13	103.4	19.6	3.57	0.45	98.52	20.4	127	1.44	1.72
	2	115	37	6.76	1.7	121	21.1	3.1	0.61	98.78	23.0	115	-1.32	2.96
	3	135	44	5.36	0.85	85.52	10.7	4.2	0.47	97.48	19.2	135	-2.53	0.78
4	1	194	30	2.13	0.92	76.4	27.4	3.19	0.59	93.94	20.6	151	0.53	2.55
	2	125	31	1.84	0.73	107.4	21.3	3.24	0.8	86.07	16.9	93	4.01	2.44
	3	216	56	3.5	1.26	71.28	10.4	3.22	0.57	80.81	14.5	198	-2.53	1.05
5	1	107	28	3.71	3.27	115.8	22.1	3.13	0.59	82.68	19.2	90	3.50	3.04
	2	122	35	3.08	1.97	141.4	41.8	3.17	0.6	108.7	23.7	81	3.11	5.31
	3	140	44	5.6	0.84	115.6	20.4	3.85	0.71	87.21	31.7	138	-0.28	3.11
6	1	97	26	5.11	1.48	89.05	14.4	5.73	1.66	72.04	29.8	85	4.53	2.96
	2	81	20	5.11	1.61	135	28.7	5.06	0.76	92.32	20.4	68	8.45	3.52
	3	107	29	8.34	1.43	106.5	21.7	7.26	1.44	82.9	27.7	98	1.70	2.99
7	1	197	38	7.23	0.9	84.5	11.8	7.04	0.94	86.92	23.6	191	0.48	1.57
	2	178	31	4	1.52	98.89	28.1	4.16	0.97	76.84	21.5	152	4.82	2.69
	3	195	38	12.31	3.06	75.46	23.9	9.78	3.05	51.55	20.4	168	0.56	1.91
8	1	133	33	4.18	1.5	133.8	29.5	3.79	0.94	85.71	21.5	112	3.54	4.30
	2	103	18	3.69	1.95	124.1	35.7	2.84	0.93	78.25	30.1	70	4.77	3.95
	3	141	40	5.83	1.19	129.5	31.9	3.81	0.92	87.65	24.7	116	0.14	3.20
9	1	152	44	2.33	0.89	63.74	7.9	4.09	0.74	100.8	30.8	137	-2.08	0.98
	2	140	42	1.45	0.39	76.17	10.4	2.66	0.79	92.37	27.9	127	3.74	2.25
	3	218	48	5.55	1.35	66.58	12.2	5.16	1.61	83.59	24.7	204	-1.68	1.87
10	1	232	46	7.56	4.23	67.18	21.1	5.51	1.02	107.3	26.9	175	-3.62	2.82
	2	63	18	4.26	2	76.57	13.1	3.96	1.92	89.55	24.3	40	-3.93	5.76
	3	23	5	10.28	2.28	90.84	8.6	5.94	1.26	92.16	16.2	19	-1.48	1.00
11	1	137	36	6.56	1.47	56.69	6.5	6.23	1.03	48.43	7.3	124	3.41	1.45
	2	150	33	3.8	2.82	69.34	11.6	3.15	0.78	77.08	27.3	143	3.86	7.61
	3	163	36	5.37	1.05	60.67	8.4	4.22	0.8	51.61	9.3	160	0.01	1.32
12	1	50	13	5.41	1.96	87.04	16.6	3.83	0.85	93.57	35.1	34	0.48	6.77
	2	47	13	3.66	1.71	76.33	7.0	3.96	0.77	95.03	39.6	38	1.82	9.02
	3	105	29	6.99	1.08	85.98	9.1	4.79	0.95	85.62	25.8	90	-0.27	3.22
13	1	126	30	7.74	1.55	93.87	10.3	7.44	0.85	72.36	25.3	110	5.87	1.99
	2	101	19	3.3	1.34	96.7	13.6	5.28	1.11	94.82	23.7	79	5.31	2.85
	3	152	28	9.36	1.79	82.93	14.0	7.78	1.16	58.65	15.8	126	0.69	3.43
14	1	105	30	3.65	1.61	93.02	12.9	2.68	0.54	69.57	19.1	93	5.10	3.66
	2	134	24	2.46	2.57	112.8	20.7	1.8	0.34	107.6	25.4	111	3.03	6.97
	3	121	27	4.38	1.2	90.21	12.1	2.56	0.4	83.98	13.7	101	-1.90	3.12
15	1	168	25	5.19	2.52	59.23	19.9	4.04	0.84	73.6	22.2	138	-0.98	1.96
	2	199	33	3.9	2.45	57.14	14.8	3.03	0.72	96.83	28.9	147	1.59	3.91
	3	172	34	8.7	2.09	67.75	21.5	5.75	1.11	72.82	19.0	138	-2.53	2.98
16	1	155	28	6.32	1.87	105.9	42.7	5.46	1.39	63.67	13.4	73	5.47	3.11
	2	199	46	3.93	1.36	123.6	35.4	3.87	1.2	89.08	27.7	56	7.41	4.00
	3	28	8	7.6	2.13	119.3	33.0	10.91	5.81	55.53	23.1	27	6.71	4.53
19	1	97	24	5.97	2.37	86.57	23.1	7.41	1.4	81.49	27.4	73	4.03	5.64
	2	118	27	2.63	1.57	151.3	34.2	4.8	1.92	111.6	33.3	88	14.04	7.09
	3	151	32	8.34	1.45	93.37	13.3	8.43	1.65	74.19	17.8	132	-2.46	2.62
20	1	71	9	6.58	2.57	91.7	25.6	8.36	1.51	80.5	31.7	41	3.70	2.30
	2	74	16	6.21	1.99	93.35	20.8	5.2	1.31	68.42	18.7	41	3.76	2.97
	3	124	25	7.08	1.65	125.8	33.2	7.1	1.65	65.23	14.7	101	4.25	3.20

Continues in next page...

...continues from previous page

	1	14	6	2.97	0.91	141.3	24.1	2.64	0.46	75.84	26.3	5	2.76	3.01
21	2	47	9	3.73	2.07	138.2	15.8	2.24	0.69	91.01	33.0	30	41.70	9.62
	3	118	30	4.32	3.03	103.3	23.6	2.3	0.43	105.5	22.9	91	-4.94	10.07
	1	174	29	4.64	0.53	114.9	9.0	4.4	0.52	118.9	22.8	171	1.48	0.46
22	2	187	26	2.74	0.78	89.69	6.4	2.52	0.56	120.8	31.6	188	0.41	0.38
	3	191	35	5.1	0.47	148.4	14.6	4.04	0.64	106	36.0	183	1.24	0.89
	1	123	29	5.81	1.57	84.69	15.8	3.46	0.92	108.6	31.4	101	-2.52	1.77
23	2	72	20	3.22	1.48	117	35.1	2.85	0.83	96.96	27.4	52	2.32	4.20
	3	121	34	8.23	1.3	89.35	14.6	4.11	1.32	103	25.3	113	-5.53	2.33
	1	159	29	9.37	2.97	67.97	17.0	5.67	1.41	90.27	24.6	114	-3.98	4.68
24	2	130	22	7.23	2.18	105.7	25.6	3.89	0.98	86.45	27.6	91	-0.26	2.32
	3	155	41	7.25	0.9	130.6	18.8	5.77	1.52	95.88	25.8	139	1.39	1.81
	1	88	19	7.04	2.08	92.08	16.4	4.01	1.07	65.83	18.2	69	9.05	3.85
25	2	91	18	4.96	1.85	102.9	22.9	2.15	0.48	83.46	25.5	74	5.40	9.71
	3	96	24	10.17	3.08	97.63	14.5	7.25	1.49	67.43	19.5	89	4.65	9.09
	1	100	26	8.97	1.86	92.09	14.8	4.4	0.93	59.88	17.8	90	6.41	3.25
26	2	94	22	5.18	1.63	127.3	18.8	2.96	0.86	83.51	20.4	86	17.71	6.47
	3	108	27	6.83	1.09	88.45	10.6	4.57	0.72	71.48	9.6	106	0.38	3.00
	1	143	29	6.95	3.16	69.58	10.3	5.41	1.22	74.6	21.8	124	-1.54	2.45
27	2	112	22	10.28	4.27	55.44	13.3	5.56	1.61	103	34.0	85	-11.0	6.08
	3	181	40	6.14	1.38	73.89	10.2	6.78	1.11	85.26	20.5	164	-2.89	1.64
	1	112	21	8.19	2.81	99.61	27.5	4.11	1.5	84.53	29.3	85	-1.10	3.89
28	2	153	33	4.24	1.65	154.5	31.8	3.08	0.61	99.97	20.6	99	7.69	3.31
	3	90	20	10.04	1.62	115	21.6	6.85	1.22	84.99	26.3	84	0.94	2.74
	1	126	28	7.07	1.2	60.8	7.5	5.23	0.78	73.72	14.0	126	-4.22	1.63
29	2	117	23	6.08	1.61	101.7	26.7	3.96	1.39	71.13	12.1	112	7.58	5.56
	3	168	38	6.99	1.73	57.7	7.9	5.58	0.67	63.56	16.7	167	-4.43	1.83

Table F-2: Results of measurement with volunteers per phase.
The agreement in respiratory effort between methods is higher
in phase 1 (quiet breathing) and phase 3 (pressure support)
than in phase 2 (increased effort)

Acknowledges

My thanks go to Prof. Dr. Ullrich Wenkebach for his technical advice, to Prof. Dr. Hartmut Gehring and Dr. Sebastian Brandt from the UKSH for their valuable contribution to the medical component of this work and to all the colleagues who somehow participated in the development of this project.

Many thanks to Mrs. Marianne Löhndorf, Mrs. Gabriele Ramien and Mrs. Rita Milinski for their excellent organisational support; to my students Matthias Steffner, Eva Rother and Merle Strutz for their committed participation and fulfilment of their tasks and to Mr. Harald Steden and Mr. Willi Mertins for their collaboration in the laboratory.

The support of Dr. Dieter Weismann and PD Dr. Hajo Reissmann is also gratefully acknowledged. To my family and friends the greatest thanks for making life easy.

This project was financially supported by the European Union and the state Schleswig-Holstein (Program for the Future-Economy 122-09-024).

Curriculum vitae



Personal data

Name: Kristel Lopez-Navas
Address: Fischergrube 69/71, 23552 Lübeck
Place and date of birth: Bogotá, Colombia, 12.03.1983

Education and Experience

- Nov. 2009 – Oct. 2012 Research associate in the project “Adaptive regulation of ventilation parameters” – Dissertation/**PhD**
Fachhochschule Lübeck Forschungs-GmbH - Project TANDEM, Lübeck, Germany
- Sep. 2007 – Oct. 2009 **Master** (MSc.) in Biomedical Engineering
University of Lübeck and Lübeck University of Applied Science, Lübeck, Germany
Master’s thesis: “Verification and optimization of a method to determine respiratory resistance in spontaneously breathing patients” carried out at Drägerwerk AG & Co. KGAA, Research Unit, Lübeck, Germany
- Aug. 2008 – Jan. 2009 Internship in the department of Development and Construction, Electronic Systems of Dräger Medical GmbH, Lübeck, Germany
- Nov. 2006 – Jun. 2007 Certification of proficiency in English and German (TOEFL, GRE and TestDAF)
- Sep. 2005 – Sep. 2006 International exchange year for voluntary work in social institutions in Germany
- Feb. 2000 – Sep. 2005 **Diploma** in Electronics Engineering
Universidad Nacional de Colombia, Bogotá, Colombia
Thesis: Design of a simplified monitor of vital signs and implementation of a driver on a FPGA to display signals on a LCD display
- Feb. 1988 – Nov. 1999 High School Degree
Colegio San Jose, Bogotá, Colombia
Award “Andres Bello” to the best high-school graduates of the country



Kristel Lopez-Navas
November 2013